Available online at www.sciencedirect.com
SCIENCE DIRECT
ELSEVIER
Coordination Chemistry Reviews 250 (2006) 468–518
COORDINATION CHEMISTRY REVIEWS
www.elsevier.com/locate/ccr

Review

Recent developments in heteroporphyrins and their analogues

Iti Gupta, M. Ravikanth *

Department of Chemistry, Indian Institute of Technology, Powai, Mumbai 400076, India

Received 8 April 2005; accepted 12 October 2005
Available online 5 December 2005

Contents

Abstract

Monoheteroatom substituted porphyrins and diheteroatom substituted porhyrins resulting from the replacement of one and two nitrogen atoms, respectively, are very stable aromatic molecules possessing very interesting properties. Significant progress has been made in last 5–6 years by developing newer methods and also by modifying the existing synthetic methodologies. These have been used to synthesize several heteroanalogues of porphyrins and their derivatives including the synthesis of chlorins, corroles, confused porphyrins, covalent and non-covalent porphyrin assemblies. This article reviews the developments that have been occurred in heteroporphyrin chemistry during 1999–2005.

Keywords: Heteroporphyrins; Confused porphyrins; Corroles; Chlorins; Covalent and non-covalent porphyrin arrays

* Corresponding author. Tel.: +91 22 5767176; fax: +91 22 5723480.
E-mail address: ravikanth@chem.iitb.ac.in (M. Ravikanth).

0010-8545/$ – see front matter © 2005 Elsevier B.V. All rights reserved.
doi:10.1016/j.ccr.2005.10.010

1. Introduction

Porphyrins are a class of conjugated macrocyclic compounds in which four pyrrole rings are linked to each other in cyclic fashion through *meso*-carbon bridges. These represent one of the most widely studied of all known macrocyclic systems [1]. Replacement of pyrrole nitrogen(s) by other donor atoms, such as O, S, Se and Te in a porphyrin ring leads to new macrocyclic systems referred to as core-modified porphyrins or heteroatom substituted porphyrins [2]. Such core perturbation affects the electronic structure of the ring system thereby altering the physical and chemical characteristics of the porphyrin macrocyle while retaining the aromatic character. Thus, the modification of the porphyrin core led to very interesting properties which are quite different from regular porphyrins. Specifically, the heteroporphyrins have the ability to stabilize metals in unusual oxidation states, such as copper in +1 and nickel in +1 oxidation states which are not possible to attain with regular porphyrins [3–11]. The heteroatom substituted porphyrins were first synthesized in 1969 [12–15] and for the last 35 years some elegant methodologies have been developed which resulted in much research activity on these porphyrin systems. However, until the late 1990s, most of the work on heteroporphyrins was limited to the preparation of different metal derivatives and the exploration of their structural, spectroscopic and electrochemical properties [3,4,6,9–11,16,18–24]. Latos-Grażyński, who is one of the pioneers in developing the heteroporphyrin chemistry has reviewed recently all the work that appeared on heteroporphyrins until

Porphyrin

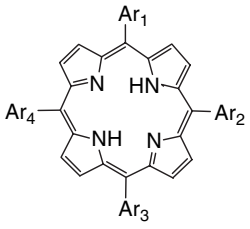

$Ar_1 = Ar_2 = Ar_3 = Ar_4 = Ph$: **N_4P 1**

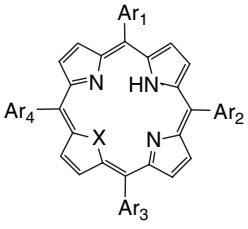

21-Monoheteroporphyrins

$Ar_1 = Ar_2 = Ar_3 = Ar_4 = Ph$; X = O : **21-$N_3$OP 2a**
$Ar_1 = Ar_2$ = Ph; $Ar_3 = Ar_4$ = *p*-Tol; X = O : **21-N_3OP 2b**
$Ar_1 = Ar_2$ = Mes; $Ar_3 = Ar_4$ = Ph; X = O : **21-N_3OP 2c**
$Ar_1 = Ar_2 = Ar_3 = Ar_4 = Ph$; X = S : **21-$N_3$SP 3a**
$Ar_1 = Ar_2$ = *p*-NO_2Ph; $Ar_3 = Ar_4$ = Ph; X = S : **21-N_3SP 3b**
$Ar_1 = Ar_2$ = Mes; $Ar_3 = Ar_4$ = Ph; X = S : **21-N_3SP 3c**
$Ar_1 = Ar_2 = Ar_3 = Ar_4 = Ph$; X = Se : **21-$N_3$SeP 4a**
$Ar_1 = Ar_2$ = Tol; $Ar_3 = Ar_4$ = Ph; X = Se : **21-N_3SeP 4b**
$Ar_1 = Ar_2 = Ar_3 = Ar_4 = Ph$; X = Te : **21-$N_3$TeP 5a**
$Ar_1 = Ar_2$ = Ph; $Ar_3 = Ar_4$ = *p*-Tol; X = Te : **21-N_3TeP 5b**
$Ar_1 = Ar_2$ = OMePh; $Ar_3 = Ar_4$ = Ph; X = Te : **21-N_3TeP 5c**

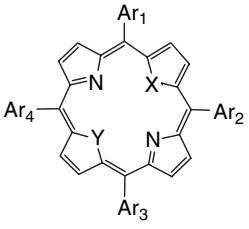

21,23-Diheteroporphyrins

$Ar_1 = Ar_2 = Ar_3 = Ar_4 = Ph$; X = Y = O : **21,23-$N_2O_2$P 6**
$Ar_1 = Ar_2 = Ar_3 = Ar_4 = Ph$; X = Y = S : **21,23-$N_2S_2$P 7a**
$Ar_1 = Ar_2 = Ar_3 = Ar_4$ = *p*-Tol; X = Y = S : **21,23-N_2S_2P 7b**
$Ar_1 = Ar_2 = Ar_3 = Ar_4 = Ph$; X = Y = Se : **21,23-$N_2Se_2$P 8**
$Ar_1 = Ar_2 = Ar_3 = Ar_4 = Ph$; X = S, Y = O : **21,23-N_2SOP 9**
$Ar_1 = Ar_2 = Ar_3 = Ar_4 = Ph$; X = S, Y = Se : **21,23-N_2SSeP 10**
$Ar_1 = Ar_2 = Ar_3 = Ar_4 = Ph$; X = S, Y = Te : **21,23-N2$_S$TeP 11**

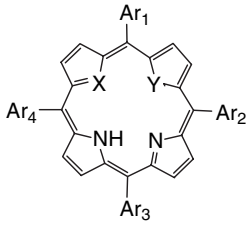

21,22-Diheteroporphyrins

$Ar_1 = Ar_2 = Ar_3 = Ar_4 = Ph$; X = Y = O : **21,22-$N_2O_2$P 12**
$Ar_1 = Ar_2 = Ar_3 = Ar_4 = Ph$; X = Y = S : **21,22-$N_2S_2$P 13**
$Ar_1 = Ar_2 = Ar_3 = Ar_4 = Ph$; X = S, Y = O : **21,22-N_2SOP 14**

Chart 1. The structures of 13 different mono- and diheteroporphyrins.

1998 in "The Porphyrin Handbook" [2]. To the best of our knowledge, this is the only review on heteroporphyrins covering the synthetic aspects and discussing in detail the metalation studies, crystal structures, ground and excited state properties. However, during the last 5–6 years, there has been rapid development in heteroporphyrin chemistry with main emphases on synthesis of novel analogues of porphyrins, such as chlorins, carbaporphyrins, corroles, N- or X-confused porphyrins, β- and *meso*-substituted porphyrins and different covalent and non-covalent porphyrins arrays containing heteroatom substituted porphyrin units. The main objective of the present review is to provide an update on what has been achieved in the area of monoheteroatom substituted (21-N_3X systems) and diheteroatom substituted porphyrin (21,23-N_2X_2 or 21,23-N_2XY and 21,22-N_2X_2 or 21,22-N_2XY systems) chemistry between 1999-Feburary and 2005. This review is restricted to the developments occurred on heteroporphyrins containing four five-membered heterocyclic rings and does not include any discussion on heteroatom substituted expanded porphyrins containing more than four or five-membered heterocyclic rings which had been reviewed very recently [25,26]. Until now 13 different mono- and diheteroatom substituted porphyrins with various core combinations have been synthesized by replacing one or two nitrogen atoms of regular porphyrin **1** (Chart 1)

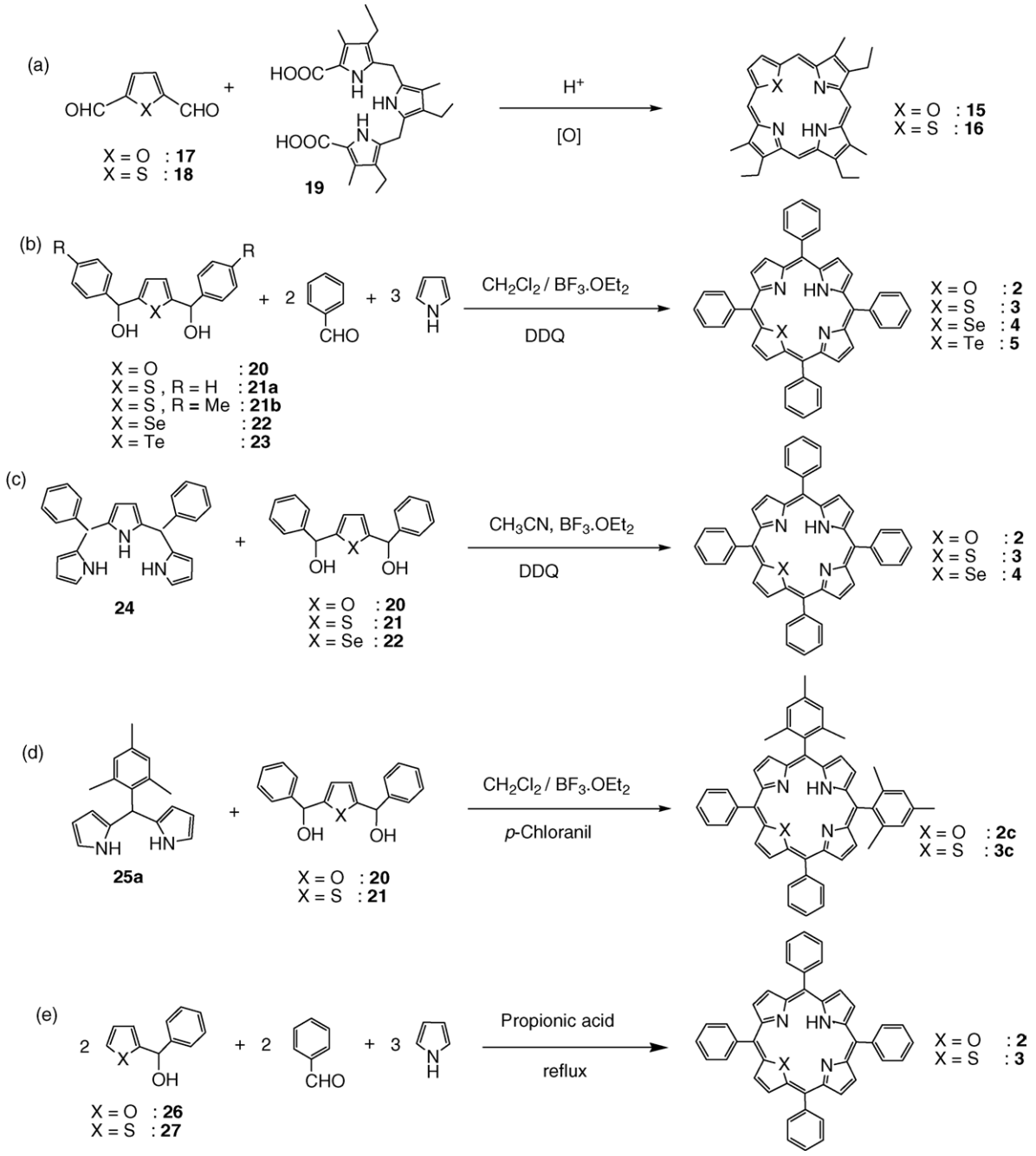

Scheme 1. Synthetic routes for 21-monoheteroatom substituted porphyrins.

and this review discusses the developments with these systems (Chart 1). For setting the platform for review, in the first following two sections, we discuss very briefly the various synthetic approaches to obtain 21-hetero, 21,22 or 21,23-diheteroa atom substituted porphyrins and their general properties. For detailed discussion on these two aspects, the interested reader is referred to Latos-Grażyński's article in "The Porphyrin Handbook" [2].

2. General synthetic strategies for mono- and diheteroatom substituted porphyrins

A few elegant methodologies have been developed over the years to synthesize mono- and diheteroatom substituted porphyrins which has been reviewed by Latos-Grażyński in "The Porphyrin Handbook" [2]. However, for continuity of the present review, we briefly summarize the various synthetic routes to synthesize the heteroatom substituted porphyrins containing one or two heteroatoms in the porphyrin core.

2.1. Synthetic routes for 21-monoheteroatom substituted porphyrins

To the best of our knowledge, there are five synthetic routes presently available to synthesize the 21-heteroatom substituted porphyrins as shown in Scheme 1. The first synthesis of 21-monoheteroatom substituted porphyrins was reported by Broadhurst et al. [12–15]. They adopted a [3 + 1] approach to synthesize β-pyrrole alkylated and *meso*-unsubstituted 21-oxa **15** and 21-thia **16** porphyrins (Scheme 1a). The reaction of 2,5-diformylfuran **17** or thiophene **18** with tripyrrane diacid **19** generated in situ in the presence of HBr resulted in the formation of 21-oxa (25%) **15** or 21-thiaporphyrin **16** (12%), respectively. The Broadhurst approach was not found to be suitable for the synthesis of *meso*-tetraphenyl derivatives hence alternate methods have been developed using 2,5-bis-(arylhydroxymethyl)heterocyclopentadienes **20**–**23** as precursors [17,21,27–35]. One mole of the corresponding diol, 2,5-bis(arylhydroxymethyl)heterocyclopentadiene **20**–**23** was condensed with two moles of arylaldehyde and three moles of pyrrole under Adler et al.'s [36] or Lindsey et al.'s [37] porphyrin forming conditions to give a mixture of three porphyrins and the required corresponding 21-heteroatom substituted porphyrins **2**–**5** which were separated from the mixture using column chromatography (Scheme 1b).

The 21-heteroatom substituted porphyrins **2**–**4** (X = S, O, Se) were also prepared by condensing the corresponding 2,5-bis(arylhydroxymethyl)heterocyclopentadiene **20**–**22** with regular tripyrrane **24** in CH_3CN under mild acidic conditions [31–33] (Scheme 1c). Recently, Chandrashekar and co-workers [34,35] have shown that the 21-oxa **2** or 21-thiaporphyrins **3** can also be prepared by condensing the corresponding heterocyclopentadiene diols **20** or **21**, respectively, with *meso*-aryl dipyrromethane **25** under mild acid catalyzed conditions (Scheme 1d). We recently developed a mono-ol method [38,39] to prepare 21-oxa and 21-thiaporphyrins (Scheme 1e). In this method, two equivalents of 2-(arylhydroxymethyl) furan **26** or thiophene **27** were condensed with two equivalents of aryl aldehyde and three equivalents of pyrrole under Adler et al.'s or

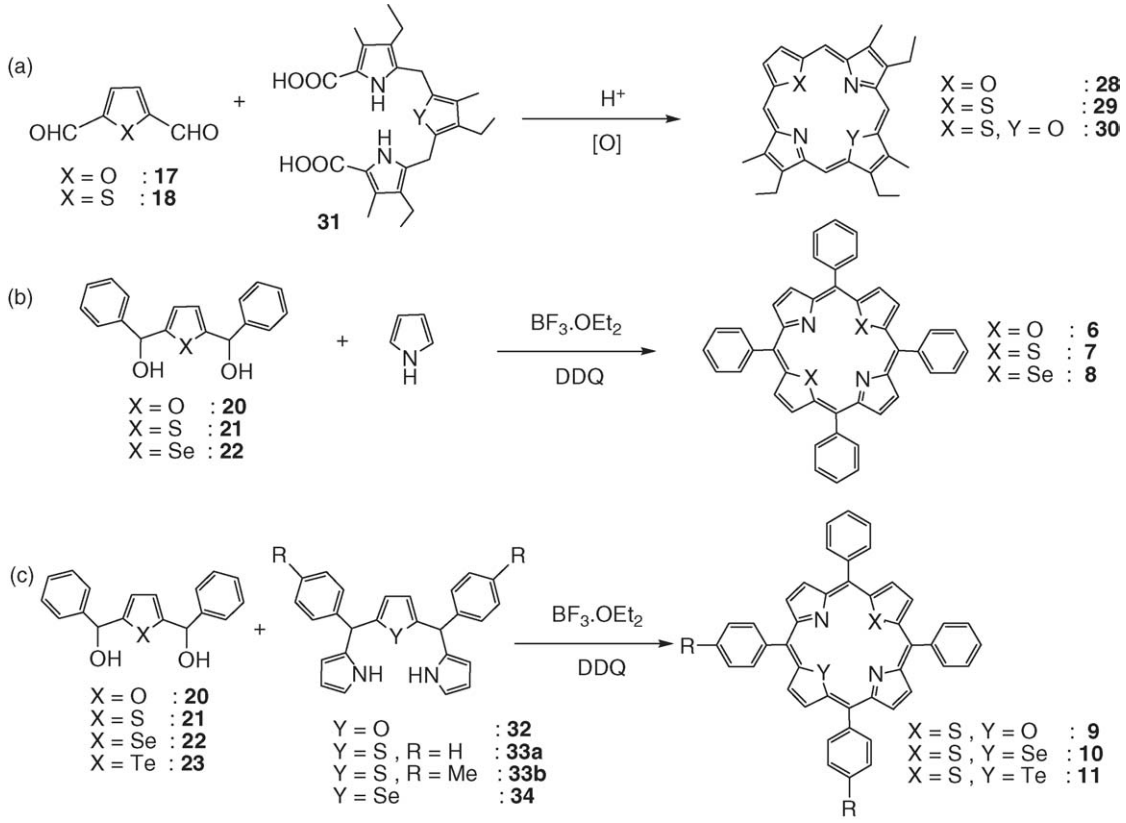

Scheme 2. Synthetic routes for 21,23-diheteroatom substituted porhyrins.

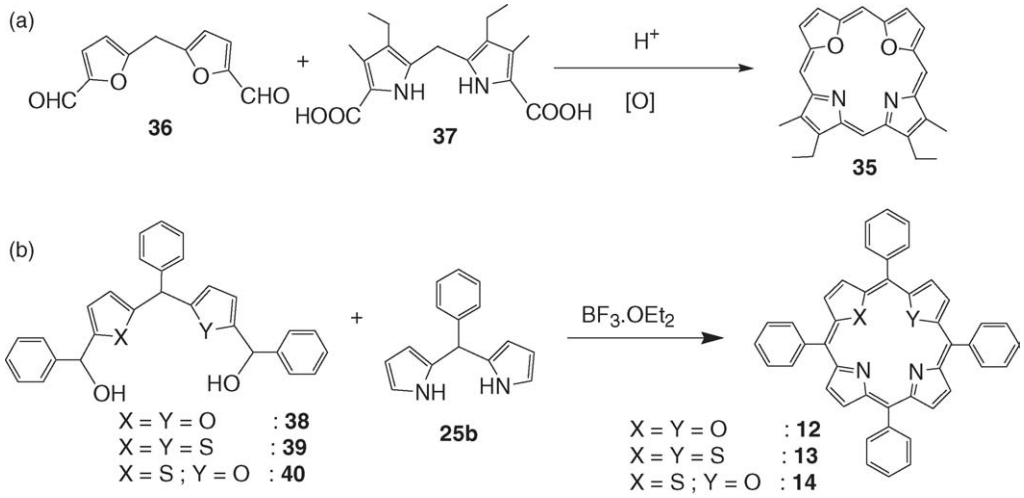

Scheme 3. Synthetic routes for 21,22-diheteroatom substituted porphyrins.

Lindsey et al.'s conditions [36,37] resulting in a mixture of two porphyrins and the 21-oxa **2** or 21-thiaporphyrins **3** which were separated easily by column chromatography.

2.2. Synthetic routes for 21,23-diheteroatom substituted porphyrins

21,23-Diheteroatom substituted porphyrins were synthesized by following three different strategies. Broadhurst et al. [12–15] prepared the 21,23-diheteroatom substituted porphyrins **28**–**30** by acid catalyzed condensation of the 2,5-diformylfuran **17** or thiophene **18** with modified tripyrrane diacid **31** generated in situ (Scheme 2a). This route gave access only to β-substituted *meso*-unsubstituted 21,23-diheteroatom substituted porphyrins **28**–**30**. Ulman and Manassen [27–30] developed two simple synthetic routes to prepare the *meso*-aryl substituted 21,23-diheteroporphyrins (Scheme 2b and c). One equivalent of the corresponding heterocycle diol **20**–**22** was condensed with one equivalents of pyrrole under mild acid conditions followed by DDQ oxidation and this afforded 21,23-diheteroporphyrins having two similar heteroatoms **6**–**8**. The mixed heteroatom substituted porphyrins **9**–**11** [28,29,31,32,35] were prepared by condensing one equivalent of the corresponding heterocyclopentadiene diols **20**–**23** with modified appropriate tripyrranes **32**–**34** under two step one flask room temperature conditions [37] (Scheme 2c).

2.3. Synthetic routes for 21,22-diheteroatom substituted porphyrins

There are very few synthetic methods available to synthesize 21,22-diheteroatom substituted porphyrins [15,40,41]. Broadhurst and Grigg [15] synthesized the first 21,22-dioxaporphyrin **35** by [2 + 2] acid catalyzed condensation of a 5,5′-diformyldifuryl **36** with a dipyrromethane diacid **37** (Scheme 3a). Lee and Cho [40,41] recently developed a novel synthetic strategy to prepare 21,22-diheteroporphyrins **12**–**14** containing sulfur and oxygen atoms (Scheme 3b). The acid catalyzed condensation of one equivalent of 1,9-bis(phenylhydroxymethyl)-5-phenyldifuryl **38** or dithienyl **39** or furylthienylmethane **40** with one equivalent of 5-phenylpyrromethane **25b** followed by oxidation with DDQ resulted in 21,22-diheteroporphyrins **12**–**14**.

3. General properties of heteroporphyrins

The spectroscopic properties of heteroporphyrins indicate that they are aromatic and obey $4n + 2$ π-electron Huckel rule [2]. The replacement of one or two nitrogen atoms with heteroatoms results in the alteration of π-delocalization, which in turn affects the electronic properties. Some of the salient features of the heteroporphyrins follow: (1) the alteration in π-delocalization due to heteroatoms results in considerable downfield shifts in ^{1}H NMR of the pyrrole and heterocyclopentadiene moieties (Table 1). The deshielding was more for monoheteroatom substituted porphyrins than for diheteroatom substituted porphyrins [42,43]. This is attributed to the distortion of the porphyrin macrocycle by the two large heteroatoms, which decreases the ring current effect arising from the π-delocalization. (2) Similar to N_4 porphyrins, the heteroporphyrins shows an intense Soret band and 3–4 *Q*-bands in 700–450 nm region. The introduction of a heteroatom in place of "N" results in large red shifts of both Soret and *Q*-bands (Table 1). The maximum red shifts were observed with "S", "Se" and "Te" containing heteroporphyrins and the shifts were minimum for "O" containing heteroporphyrins [35,44]. Furthermore, the red shifts of the absorption bands of diheteroatom substituted porphyrins were greater than those of the monoheteroatom [35,44] substituted porphyrins. (3) The emission bands of the heteroporphyrins [35,44–46] were also red shifted with reduction in quantum yields compared to N_4 porphyrins (Table 1). The lifetimes of singlet excited state were generally very low except for oxaporphyrins whose lifetimes are almost comparable to those of N_4 porphyrins [35]. (4) The heteroatom porphyrins are easy to reduce and difficult to oxidize compared to regular porphyrins [35,47] (Table 1). This is attributed to the inductive or electron withdrawing effect

Table 1
Selective data of general properties of *meso*-aryl heteroporphyrins with different heteroatom substituted cores

Compound	^{1}H NMR β-heterocycle proton (ppm)	Electronic spectra, λ_{abs} (nm)		Fluorescence			Electrochemical		X-ray distance (Å)	
		Soret	*Q*(*I*)	*Q* (0,0), λ_{em} (nm)	ϕ_f	τ_f (ns)	$E^{\circ\,oxd}_{1/2}$ (V)	$E^{\circ\,red}_{1/2}$ (V)	N(22)···N(24)	X(21)···X(23), X(21)···N(23)
N_4P	8.72	419	647	650	0.110	9.52	1.03	−1.23	4.06	4.20
21-N_3OP	9.13	422	672	678	0.037	8.43	–	−1.20	4.03	4.13
21-N_3SP	9.81	428	680	685	0.016	1.36	1.04	−1.07	4.40	3.54
21-N_3SeP	10.03	433	678	–	–	–	1.14	−0.88	4.49	3.36
21-N_3TeP	10.42	440	681	–	–	–	–	–	4.65	3.13
21,23-N_2O_2P	9.37	416	704	655	0.418	–	–	−0.92	4.00[a]	4.25[a]
21,23-N_2S_2P	9.63	435	699	706	0.007	1.25	1.18	−0.94	4.65	3.07
21,23-N_2Se_2P	9.86	447	694	–	–	–	1.14	−0.88	–	2.85
21,23-N_2SOP	9.78 (S), 9.19 (O)	428	707	713	0.005	–	–	−0.90	–	–
21,23-N_2SSeP	9.58 (S), 9.96 (Se)	441	692	–	–	–	1.17	−0.91	–	2.89
21,23-N_2STeP	9.05 (S), 10.14 (Te)	445	668	–	–	–	–	−0.82	–	2.65
21,22-N_2O_2P	9.68, 9.77	410	640	–	–	–	–	–	–	–
21,22-N_2S_2P	9.38, 9.42	441	698	–	–	–	–	–	–	–
21,22-N_2SOP	9.81, 9.91 (O) 9.94, 10.18 (S)	427	692	–	–	–	–	–	–	–

[a] X-ray data of porphyrin dication.

that the heteroatom has on the frontier orbital of the porphyrin. The heteroporphyrins also has a strong ability to stabilize metals in unusual oxidation states, which are not possible with regular porphyrins [2]. (5) The crystal structures solved for various heteroatom substituted porphyrins and metalloporphyrins [2] indicate that the presence of large heteroatoms shrinks the core of mono and diheteroporphyrins relative to those of regular porphyrins as revealed by the comparison of the diagonal of the tetragon formed by the donor atoms of the porphyrin core (Table 1). The variation of the structures of the heteroporphyrins compared to regular porphyrins alters the electronic properties considerably. However, the structures of oxaporphyrins are almost similar to those of regular porphyrins because of the similar sizes of the "N" and "O". Hence, the properties of oxaporphyrins are almost similar to that of N_4 porphyrins [35].

4. Latest developments in metal complexes of heteroporphyrins

It was well established that 21-monothia, 21-monooxa, 21-monoselena, 21,23-dioxa and 21-oxa-23-thiaporphyrins form metal complexes and the interesting features of the crystal structures solved for few of the metal complexes were discussed in detail in the Porphyrin Handbook [2]. Until recently, it was assumed that the 21,23-dithiaporphyrin did not form metal complexes which was attributed to the weaker co-ordinating ability of the thiophene moiety and also to its smaller core-size. However, Hung et al. [48] reported the synthesis and characterization of $Ru(S_2TPP)Cl_2$ **41**, the first metal complex of 21,23-dithiaporphyrin (Chart 2). The 21,23-dithiaporphyrin was treated with five equivalents of Ru(cyclooctadiene)Cl_2 $\{Ru(COD)Cl_2\}$ in *o*-dichlorobenzene at refluxing temperature

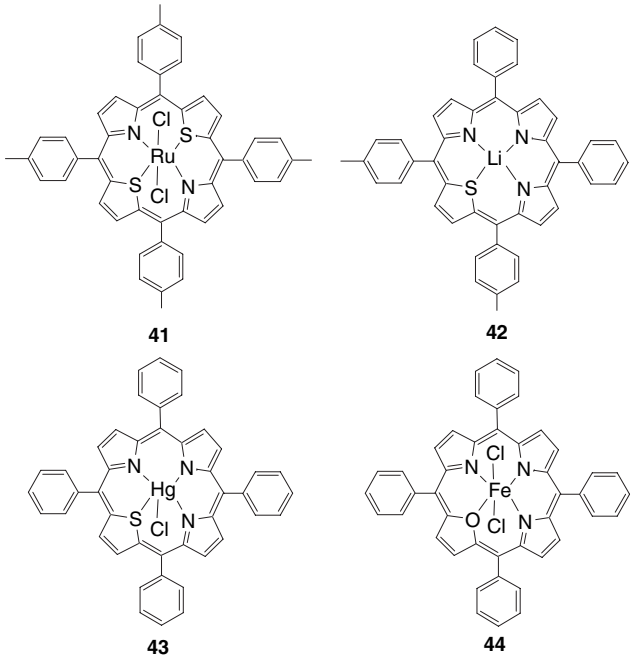

Chart 2. New metal complexes of heteroporphyrins.

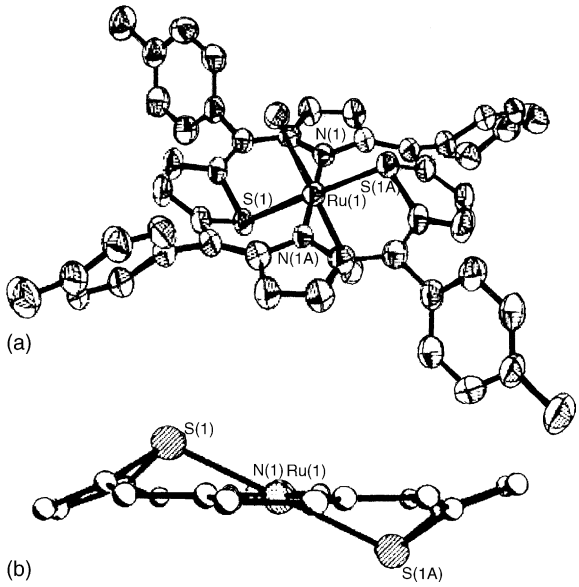

Fig. 1. X-ray structure of **41** (a) top view and (b) side view (reproduced with permission from Ref. [48]).

followed by recrystallization yielded $Ru(S_2TPP)Cl_2$ in 52% yield. When other ruthenium metal sources, such as $Ru_3(CO)_{12}$ were used, metalation did not occur indicating that $Ru(COD)Cl_2$ is essential for the reaction. The absorption spectrum of **41** exhibited bathochromically shifted Soret (468 nm) and three *Q*-bands (563, 594 and 810 nm) and the bathochromic shifts were attributed to the distortion of the porphyrin ring.

The X-ray structure solved for **41** showed that both thiophene rings coordinate to ruthenium in a pyramidal side-on fashion and the geometry of sulfur resembles those of the thiaporphyrin and η^1-thiophene complexes (Fig. 1). The dithiaporphyrin ring was tilted away from the mean porphyrin plane. The pyrrole rings were planar with mean deviation of 0.038 Å, which was much smaller than the mean deviation of 0.373 Å observed for the thiophene rings. The chloride ions were tilted 26° from the normal of the mean plane and provide a regular octahedral co-ordinating geometry around the Ru(II) metal ion. The bond distances and bond angles around the dithiaporphyrin in **41** match closely with those of free base 21,23-dithiaporphyrin and this indicates that the ring distortion resulting from the insertion of large Ru(II) metal ion into the porphyrin ring did not affect the π-delocalization of the dithiaporphyrin. An electrochemical study of **41** showed the first oxidation at 0.35 V and the first reduction at −0.71 V which were assigned to Ru(II)/Ru(III) and Ru(II)/Ru(I) couple, respectively; however, it is more likely that the reduction process involves porphyrin reduction and not reduction to Ru(I).

Recently, three more metal complexes of 21-heteroporphyrins were reported [49–52]. Arnold and co-workers [49] prepared a lithium complex of 21-monothiaporphyrin **42** in 90% yield by reacting the porphyrin with lithiumbis(trimethylsilyl)amide in THF at room temperature. The lithium complex **42** decomposes on exposure to even a slight trace of moisture. The absorption spectrum showed one strong Soret like absorption at 458 nm along with a weaker broad

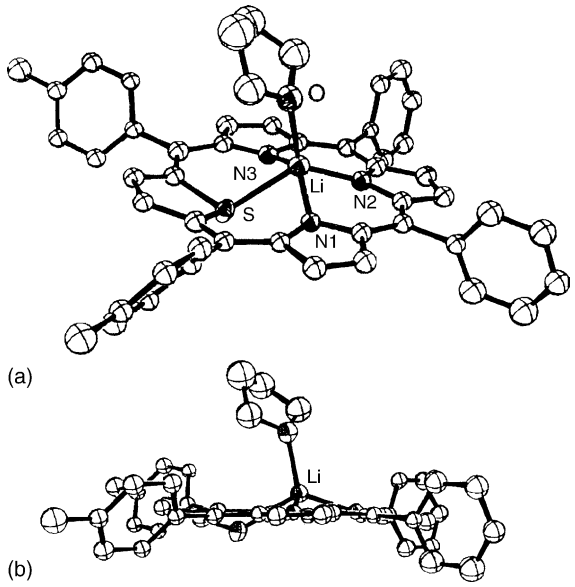

Fig. 2. X-ray structure of **42** (a) top view and (b) side view (reproduced with permission from Ref. [49]).

absorption at 346 nm and two *Q*-type absorption bands at 570 and 619 nm. The ^{7}Li NMR showed a single peak at −10.2 ppm, which was at higher field compared to the dilithiated tetraarylporphyrins and supported that the lithium cation is bound in the centre of the macrocycle [49]. The X-ray analysis of **42** indicated that the macrocycle was distorted from planarity (Fig. 2). The three pyrrolic subunits were almost planar and thiophene ring was out of plane with a dihedral angle of 12.5° to the plane defined by the tripyrrane unit. The dihedral angle in **42** was smaller than that found for nickel(I)-21-thiaporphyrin complex (14.6°) but larger than of iron(II)-21-thiaporphyrin complex (11.8°). The lithium cation was located 0.64 Å above the tripyrrane plane which was larger than that found for Ni(I)-21-thiaporphyrin complex (0.042 Å) and Fe(II)-21-thiaporphyrin complex (0.538 Å) [2]. The lithium ion in **42** was in a roughly square pyramidal arrangement with oxygen atom of the THF molecule occupying the fifth coordination site. The sulfur to lithium distance in **42** {2.33(2) Å} was comparable to those found in the corresponding Ni(I) {2.143(6) Å} and Fe(II) complexes {2.388(3) Å} of 21-thiaporphyrin [2] suggesting the presence of bonding interaction between these atoms.

The diamagnetic Hg^{II}(STPP)Cl **43** was prepared in 75% yield by treating the 21-thiaporphyrin with $Hg(OAc)_2$ in CH_2Cl_2/CH_3OH at refluxing temperature followed by recrystallization [50]. Interestingly, unlike the other five co-ordinated complexes of M(STPP)Cl {M = Fe(II), Ni(II) and Cu(II)} which were square pyramidal [2], **43** is a five co-ordinated distorted trigonal bipyramid with Cl^{-} and N(2) occupying the two apical sites (Fig. 3). The five co-ordinated mercury(II) bonds three pyrrole nitrogen atoms [Hg(I)–N(1) = 2.626(4) Å], [Hg(I)–N(2) = 2.104(4) Å], [Hg(I)–N(3) = 2.640(4) Å], one thiophene sulfur [Hg(I)–S = 2.801(1) Å] and one axial chloride ligand [Hg(I)–Cl(1) = 2.318(1) Å]. The porphyrin macrocycle in **43** is non-planar and the thiophene moiety was bent out of the 3*N* plane and the dihedral angle (23°) was smaller than that

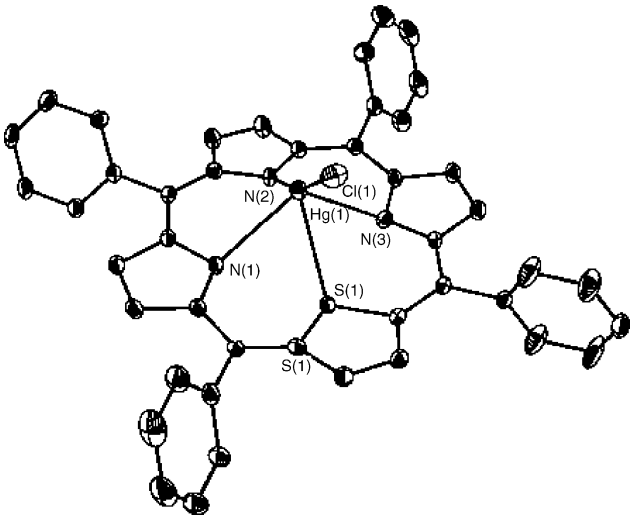

Fig. 3. X-ray structure of **43** (reproduced with permission from Ref. [50]).

of Fe(STPP)Cl (40.0°), Ni(STPP)Cl (38.1°) and Cu(STPP)Cl (38.4°). The three pyrrole nitrogen atoms were only slightly tipped away from the 3*N* plane and the thiophene ring was slightly folded. The bending and slight folding of the thiophene ring in **43** helps the sulfur to co-ordinate to the mercury in the usual η^{1}(S) fashion.

Pawlicki and Latos-Grażyński synthesized the iron complexes of 21-oxaporphyrin [51,52]. The high spin six co-ordinate (OTPP)$Fe^{III}Cl_2$ **44** was obtained in 63% yield by treating 21-oxaporphyrin with $FeCl_2$ in $CHCl_3/CH_3OH$ followed by one electron oxidation with dioxygen [51]. The compound **44** was characterized by ^{1}H NMR and single crystal X-ray analysis. The structure of **44** presented in Fig. 4 indicates that iron(III) ion is co-planar with the furan ring which coordinates the metal ion in η^{1} fashion. The Fe^{III}–Cl(1) [2.302(1) Å] and Fe^{III}–Cl(2) [2.301(1) Å] distances in **44** were the longest found among the

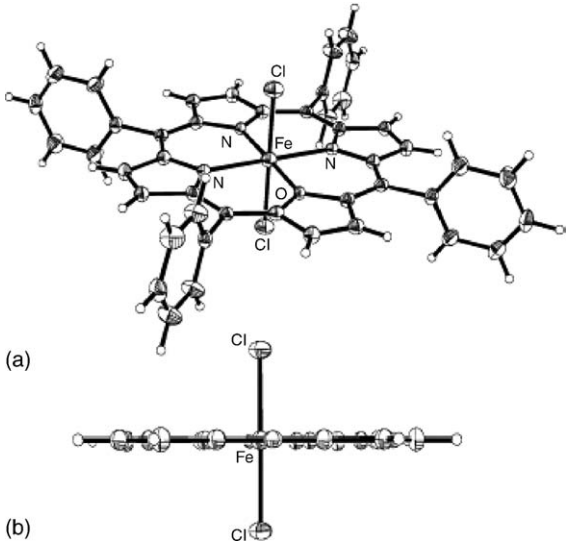

Fig. 4. X-ray structure of **44** (a) top view and (b) side view (reproduced with permission from Ref. [51]).

high-spin iron(III) porphyrins indicating the mutual *trans* interaction of axial chloride ligands.

The complex **44** was subjected to various reactions. When **44** was treated with mild reducing agents, such as sodium dithionite, this resulted in the formation of the one electron reduced product (OTPP)$Fe^{II}Cl$. When excess potassium cyanide was added to **44** in methanol, it resulted in the formation of low spin complex [(OTPP)$Fe^{III}(CN)_2$]. However, when this reaction was carried out under anaerobic conditions, the cyanide acts as a one electron reducing agent and produced the diamagnetic $[(OTPP)Fe(CN)_2]^-$. The (OTPP)$Fe^{II}(CH_2CH_2CH_2CH_3)$ was obtained by reacting **44** or (OTPP)$Fe^{II}Cl$ with *n*-BuLi in *n*-hexane at 205 K. The (OTPP)$Fe^{II}(CH_2CH_2CH_2CH_3)$ decomposed at 250 °C via homolytic cleavage of the iron–carbon bond and produced the low spin paramagnetic (OTPP)Fe^{I}. Recently, the reactivity of chloroiron(II) derivative of 5,20-ditolyl-10,15-diphenyl-21-oxaporphyrins [(ODTDPP)$Fe^{II}Cl$] was tested with various aryl Grignard reagents [52]. (ODTDPP)$Fe^{II}Cl$ when treated with $(C_6F_5)MgBr$ in toluene resulted in the formation of high-spin σ-aryl complex (ODTDPP)$Fe^{II}(C_6F_5)$. (ODTDPP)$Fe^{II}Cl$ reacts with $(C_6H_5)MgBr$, to give a rare six-coordinate $[(ODTDPP)Fe^{II}(C_6H_5)_2]^-$ which on further warming above 270 K yielded the mono-σ-phenyl complex (ODTDPP)$Fe^{II}(C_6H_5)$. The controlled oxidation of $[(ODTDPP)Fe^{II}(C_6H_5)_2]^-$ with Br_2 afforded (ODTDPP) $Fe^{III}(C_6H_5)Br$.

5. Heteroporphyrin building blocks and covalent and non-covalent porphyrin systems

Although the general synthetic methods for heteroporphyrins have been well established, no attempts have been made to synthesize heteroporphyrins having functional groups at *meso*-positions. These could be useful to synthesize complex heteroporphyrin systems. Recently, a series of heteroporphyrin building blocks with porphyrin cores, such as N_2S_2, N_3S, N_3O and N_2SO having 1–4 functional groups, such as iodo-, ethynyl-, hydroxy, aldehyde etc on *meso*-phenyls or pyridyl groups at *meso*-positions were synthesized [33,38,39,53–62]. These building blocks were used further to construct energy donor appended heteroporphyrin systems [56,58,63,64] and covalent [38,39,54,55,62] and non-covalent [59–61] unsymmetrical porphyrin arrays containing two dissimilar porphyrin cores.

5.1. Heteroporphyrin building blocks with four functional groups

The 21,23-dithiaporphyrin building blocks having four ethynyl, iodo and bromo functional groups on *meso*-phenyls **45a–d** were reported recently [54,55,64]. The thiophene diols **46a–c** were synthesized by reacting 2,5-dilithiothiophene with 4-bromobenzaldehyde, 4-iodobenzaldehyde and 4-trimethylsilylethynylbenzaldehyde, respectively, in THF (Scheme 4) under Ulman and Manassen conditions [30]. The porphyrins **45a–c** were synthesized in 13–19% yields by condensing the respective diol **46a–c** with pyrrole under mild acid porphyrin forming conditions (Scheme 5). The 21,23-dithiaporphyrin with four ethynyl groups at *para*-position of *meso*-phenyls **45d** was prepared in 80% yield by deprotecting the porphyrin **45c** using K_2CO_3 in THF/CH_3OH at room temperature.

The tetra-functionalized 21,23-dithiaporphyrin building blocks have been used to synthesize the covalently linked diaryl ethyne bridged boron-dipyrrin (BDPY) appended 21,23-dithiaporphyrin [55,63] $(BDPY)_4S_2TPP$ **47** using copper free palladium(0) coupling conditions [65]. Coupling of **45d** with

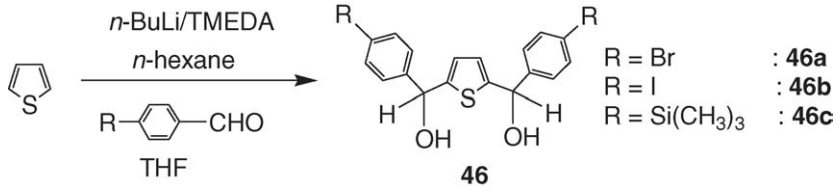

Scheme 4. Synthesis of thiophene diols **46a–c**.

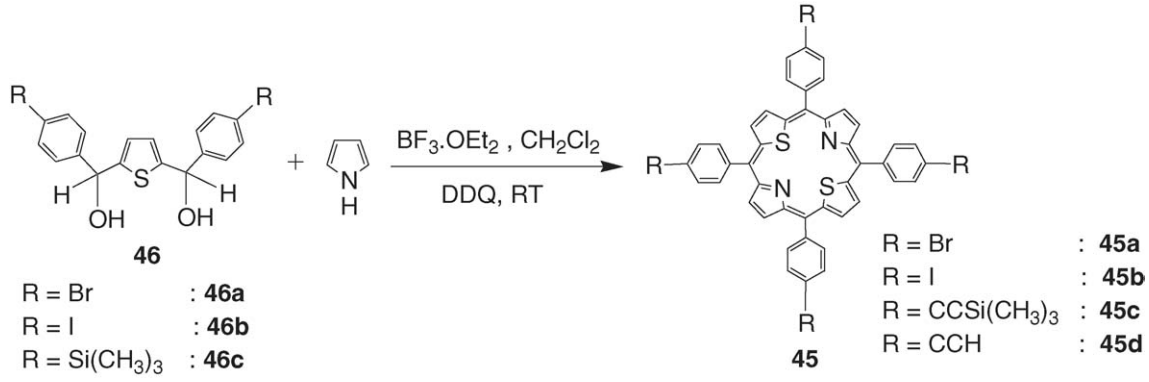

Scheme 5. Synthesis of tetra-functionalized 21,23-dithiaporphyrins.

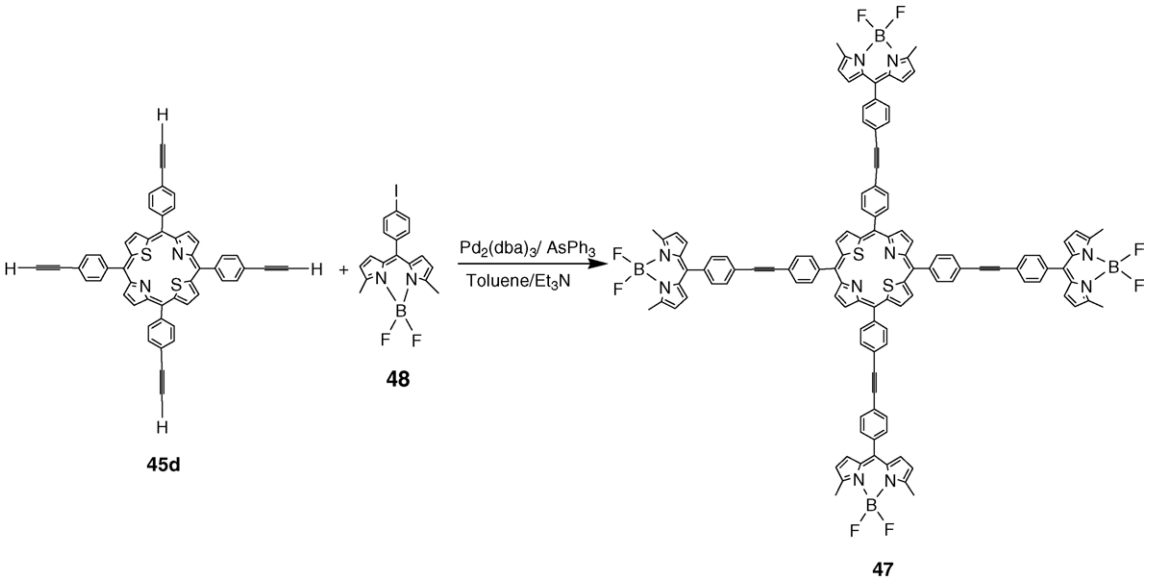

Scheme 6. Synthesis of N_2S_2 porphyrin appended with four boron-dipyrrin appended units.

N,*N*-difluoroboryl-1,9-dimethyl-5-(4-iodophenyl)dipyrrin **48** at 35 °C in the presence of a catalytic amount of $Pd_2(dba)_3$ and $AsPh_3$ followed by column chromatographic purification resulted **47** in 20% yield (Scheme 6).

The ^{1}H NMR spectrum of **47** showed peaks corresponding to both porphyrin and boron-dipyrrin units with negligible changes in chemical shifts indicating little interaction between the units. The absorption spectrum of **47** showed one strong Soret and three *Q*-bands with almost no shifts in peak maxima confirming the weak interaction between the units. The photophysical properties of **47** were studied using both steady state and time-resolved fluorescence techniques [55,64,66]. The steady state fluorescence study carried out at 485 nm excitation wavelength where boron-dipyrrin units predominantly absorb, showed major emission from boron-dipyrrin units, indicated a very inefficient energy transfer from boron-dipyrrin units to 21,23-dithiaporphyrin unit (Fig. 5). The time resolved fluorescence study indicated that the rate of energy transfer in **47** from boron-dipyrrin unit to N_2S_2 porphyrin unit was slow [66]. The slow rate of energy transfer in **47** was attributed to the presence of two sulfur atoms in the porphyrin core, which increased the contribution of non-radiative decay channels. However, the similar boron-dipyrrin appended systems with regular porphyrin $(BDPY)_4H_2TPP$ (the structure is not shown) reported earlier showed an efficient energy transfer (Fig. 5) from boron-dipyrrin unit to N_4 porphyrin unit [67].

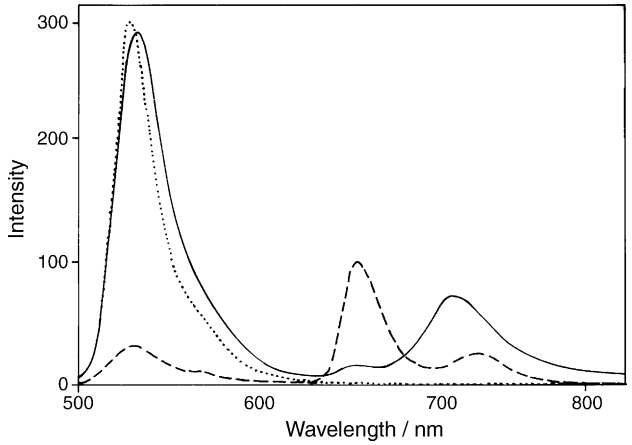

Fig. 5. Emission spectra of $(BDPY)_4S_2TPP$ **47** (—), $(BDPY)_4H_2TPP$ (- - -) and free boron dipyrrin (BDPY) (. . .) recorded in toluene at λ_{ex} = 485 nm.

The 21,23-dithiaporphyrin building block with four ethynylphenyl groups **45d** was also used to synthesize the unsymmetrical porphyrin pentamer **49** containing one N_2S_2 unit and four N_4 units in 37% yield by coupling **45d** with 5,10,15-tri(3,5-di-tert-butylphenyl)-20-(4-iodophenyl)porphyrin under similar copper free palladium coupling conditions (Chart 3) [54,55]. The Zn(II) derivative $(ZnTPP)_4S_2TPP$ **Zn49** (Chart 3) was prepared in 90% yield by treating **49** with $Zn(OAc)_2$ in CH_2Cl_2/CH_3OH under standard conditions [55]. The ^{1}H NMR and absorption studies indicated a weak interaction between the central N_2S_2 porphyrin unit and peripheral N_4 porphyrin units. The photophysical studies carried out at 420 nm for **49** where N_4 units absorbs strongly and at 550 nm for **Zn49** where the zinc(II) derivative of N_4 unit is the dominant absorber indicated an efficient energy transfer from the peripheral N_4 or ZnN_4 porphyrin units to the central N_2S_2 porphyrin unit [54,55,64,66].

5.2. Heteroporphyrin building blocks with three functional groups

There are no reports available to synthesize the tri-functionalized heteroporphyrins prior to the recent mono-ol method developed by Gupta and Ravikanth, which gave access to the tri-functionalized 21-thia and 21-oxaporphyrin building blocks [38,39]. Condensation of two equivalents of 2-(α-aryl-α-hydroxymethyl) thiophene **27** or furan **26** (thiophene or furan

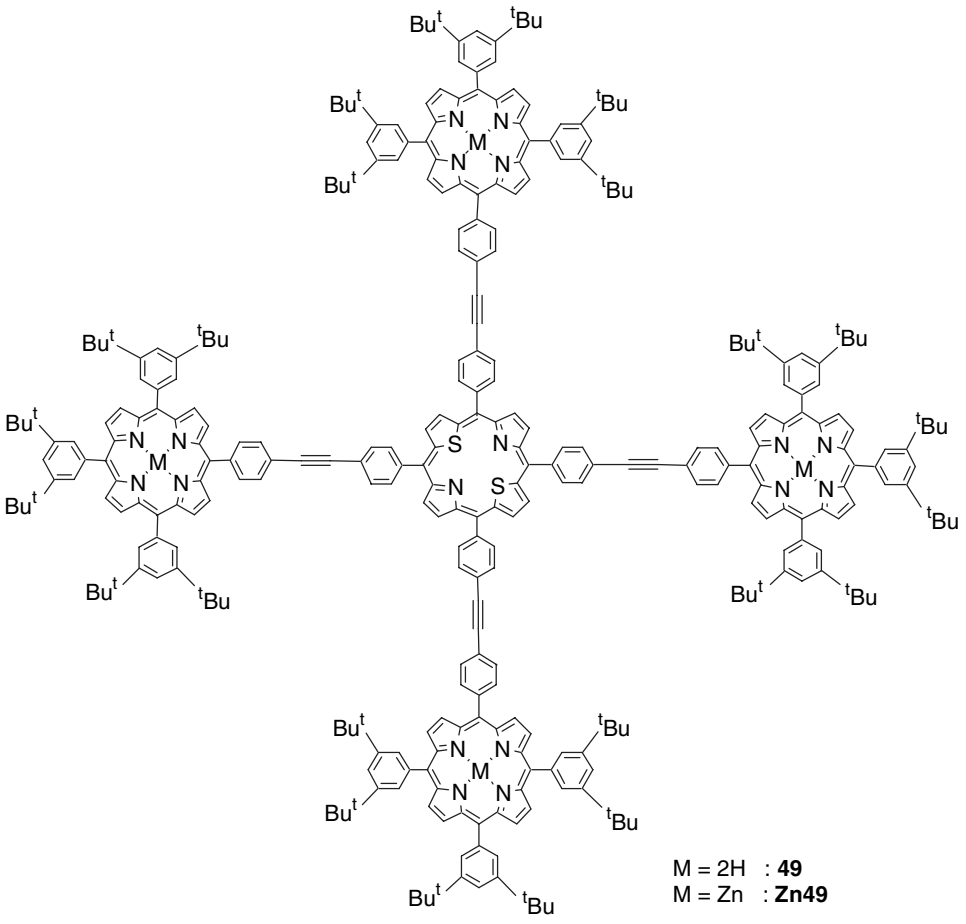

Chart 3. Diaryl ethyne bridged unsymmetrical covalent pentamers.

mono-ol) with two equivalents of functionalized aryl aldehyde and three equivalents of pyrrole under acid catalyzed conditions followed by column chromatography gave the desired tri-functionalized 21-thia or 21-oxaporphyrins (Scheme 7). By following this route, 21-thia **50a–d** and 21-oxaporphyrins **51a–c** containing three iodophenyl and pyridyl groups at the *meso*-positions were synthesized. Although this method gave low yields (2–6%), the trifunctionalized 21-thia and 21-oxaporphyrins can be prepared in good quantity using easily available precursors.

The use of the trifunctionalized heteroporphyrin building blocks was demonstrated by synthesizing two non-covalent unsymmetrical tetramers **52** and **53** containing one N_3S and three N_4 porphyrin units (Chart 4) [39]. The non-covalent porphyrin

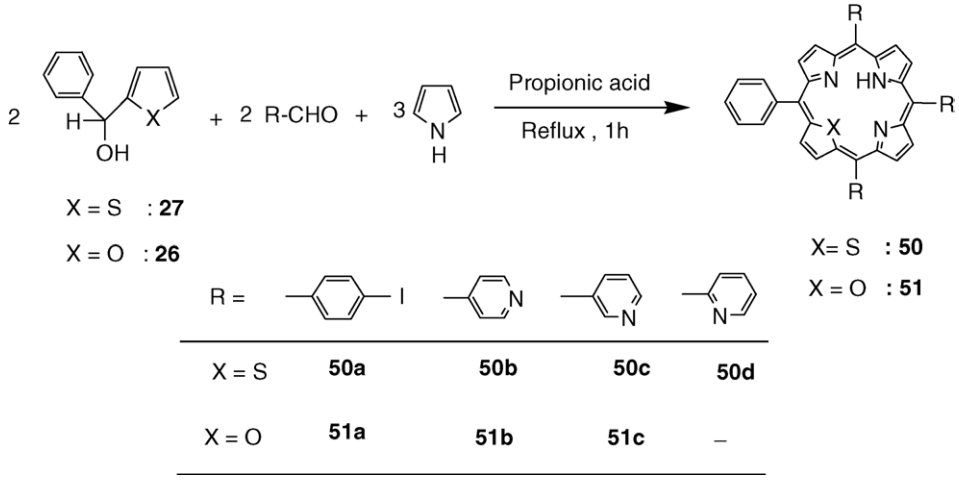

Scheme 7. Synthesis of tri-functionalized 21-thia and 21-oxaporphyrins.

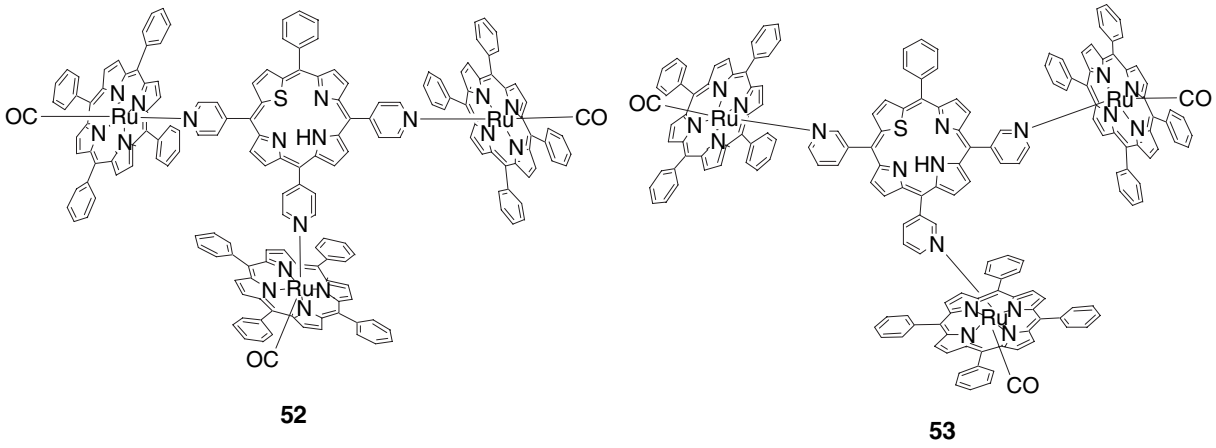

52 **53**

Chart 4. Unsymmetrical non-covalent porphyrin tetramers.

arrays **52** and **53** were synthesized by treating porphyrin **50b** and **50c**, respectively, with RuTPP(CO)(EtOH) in toluene at refluxing temperature. Similar unsymmetrical tetramers were not formed when N_3O porphyrin **51b** or **51c** were treated with RuTPP(CO)(EtOH) under identical reaction conditions.

The tetramer formation resulted in the large ^{1}H NMR upfield shifts of inner NH, β-pyrrole and pyridyl protons of 21-thiaporphyrin sub-unit in tetramers compared to the corresponding monomers (Table 2). The inner NH proton of the thiaporphyrin unit in **52** and **53** experienced about a ∼2 ppm upfield shift compared to their corresponding monomers. Similarly the pyridyl protons which were adjacent to RuTPP(CO) unit and β-pyrrole protons of thiaporphyrin unit in **52** and **53** also shifted upfield by ∼6 and ∼2 ppm, respectively, compared to their corresponding monomers.

5.3. Heteroporphyrin building blocks with two functional groups

Lindsey and co-workers [53] have developed a novel efficient method to prepare *trans* substituted 21-thia **54** and 21-oxaporphyrin **55** building blocks. Condensation of the functionalized thienylpyrromethane diol **56** or furylpyrromethane diol **57** with a functionalized dipyrromethane **58** under acid catalyzed conditions followed by column chromatography n yielded **54** or **55** (Scheme 8) having iodophenyl and trimethylsilylethynylphenyl groups at the *meso*-positions in trans fashion. However, these compounds were not used in any applications.

A series of 21-thia and 21-oxaporphyrins with two functional groups at the *meso*-positions in *cis* fashion **59a–f** and **60a–f**, respectively, were synthesized [56–58,60] by condensing 2,-bis(α-aryl-α-hydroxymethyl)thiophene **21** or furan **20** with two equivalents of funtionalized aryl aldehyde and three equivalents of pyrrole under porphyrin forming conditions (Scheme 9). This condensation resulted in the formation of a mixture of three porphyrins: a desired 21-thia **59** or 21-oxaporphyrin **60** along with 21,23-dithiaporphyrin **7** and regular porphyrin **1** which were separated by column chromatography. Using this approach the *cis*-porphyrin building blocks containing functional groups, such as iodophenyl, ethynylphenyl and pyridyl groups at the *meso*-positions were synthesized.

The 21-thia and 21-oxaporphyrin building blocks with two functional groups at the *meso*-positions in *cis* fashion were used to synthesize complex heteroporphyrin based systems. The covalently linked boron-dipyrrin appended 21-thia **61** and 21-oxaporphyrin **62** systems (Chart 5) were synthesized by coupling **59a** and **60b** respectively with **48** under copper free palladium coupling conditions [65]. The ^{1}H NMR and absorption spectroscopic studies of **61** and **62** suggested a weak interaction between the boron-dipyrrin and porphyrin units. The photophysical properties were studied for **61** and **62** using static and time-resolved fluorescence techniques. The study indicated that both in **61** and **62**, the energy transfer occurred from boron- dipyrrin units to 21-thia and 21-oxaporphyrin units, respectively. However, the rate of energy transfer in **62** was relatively faster than **61**, which was attributed to the proximity of donor and acceptor units in **62** [64,66].

The *cis*-heteroporphyrin building blocks having *meso*-pyridyl functional groups were used to synthesize the non-covalent heteroporphyrin systems [59,60]. The non-covalent unsymmetrical trimers **63** and **64** (Chart 6) containing one

Table 2
^{1}H NMR chemical shift (δ in ppm) of selected protons of tetramers and their corresponding monomers

Compound	Inner NH	2,6-Pyridyl	β-Pyrrole
50b	−2.84	9.09 (m), 9.05(m)	8.94 (d), 8.76 (d), 8.70 (d), 8.61 (d), 8.57(d)
52	−4.33	1.86 (d), 1.78 (t)	6.90 (m), 6.82 (m), 6.71 (d), 6.50 (d)
50c	−2.74	9.44 (m), 9.04 (br s)	8.94 (s), 8.76 (d), 8.69 (d), 8.60 (d), 8.53 (m)
53	−4.20	1.99 (m)	6.59 (m), 6.77 (m), 6.92 (m)

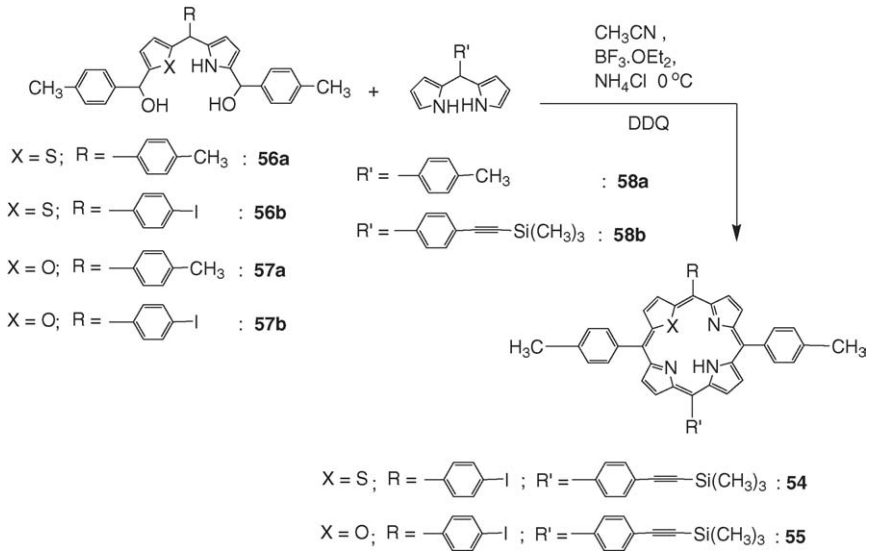

Scheme 8. Synthesis of *trans*-substituted 21-thia and 21-oxaporphyrins.

N_3S porphyrin core and two N_4 porphyrins cores were synthesized in 36–45% yields by treating *cis*-pyridyl porphyrins **59c** and **59d**, respectively, with RuTPP(CO)(EtOH) in toluene at refluxing temperature. The shifts of NH, β-pyrroles and pyridyl protons towards upfield compared to their corresponding *meso*-pyridyl porphyrin monomers in ^{1}H NMR confirmed the formation of trimers. The attempts to prepare the non-covalent trimers containing N_3O porphyrin **60c**–**d** were not successful. Latos-Grażyński and co-workers [59] used the *cis* pyridyl N_3S porphyrin **59c** to synthesize a self-assembled cyclic rhomboid dimer **65** (Chart 6) by treating **59c** with 1,3-bis(diphenylphosphino)platinum bistriflate complex.

5.4. Heteroporphyrin building blocks with one functional group

Lindsey and co-workers [53] extended the same synthetic strategy, which they have used for the synthesis of *trans*-substituted core-modified porphyrin building blocks (shown in Scheme 8) to synthesize 21-thia and 21-oxaporphyrins with one functional group **66** and **67** (Chart 7). Condensation of the dipyrromethane **58b** with thienylpyrromethane diol **56a** and furylpyrromethane diol **57a** resulted in the formation of mono-functionalized 21-thia **66** and 21-oxaporphyrin **67**, respectively. By this method, 21-thia and 21-oxaporphyrins

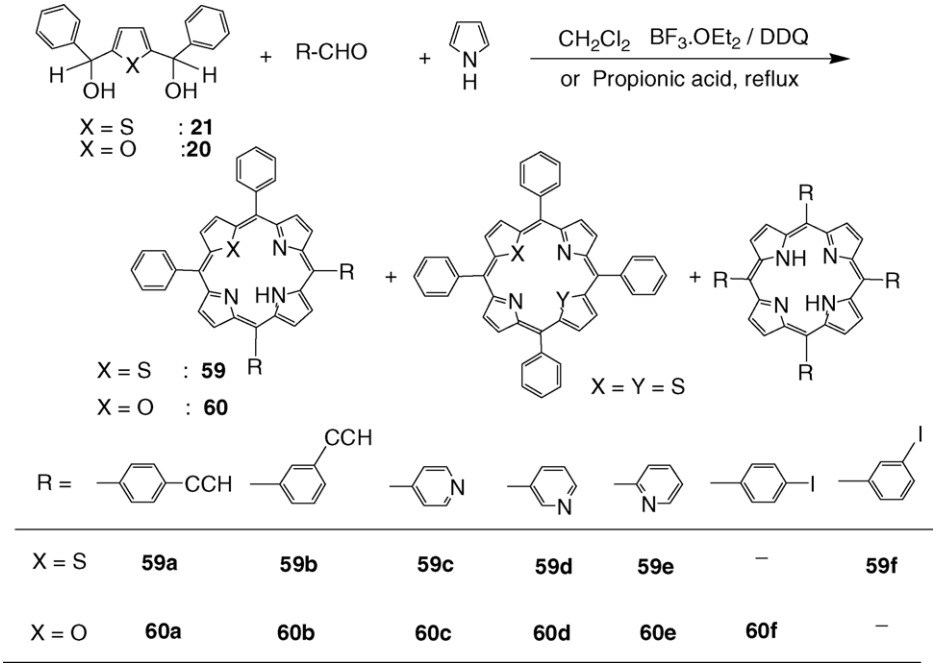

X = S	**59a**	**59b**	**59c**	**59d**	**59e**	–	**59f**
X = O	**60a**	**60b**	**60c**	**60d**	**60e**	**60f**	–

Scheme 9. Synthesis of *cis*-21-thia and 21-oxaporphyrin building blocks.

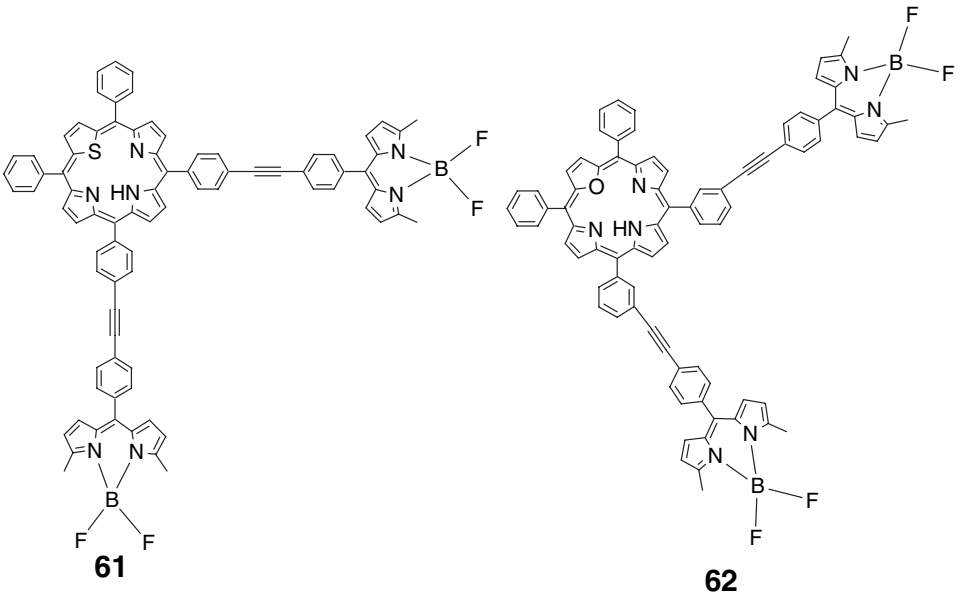

Chart 5. Boron-dipyrrin appended 21-thia and 21-oxaporphyrin systems.

containing a trimethylsilylethynylphenyl functional group at *meso*-position adjacent to pyrrole ring were synthesized; the applications of these building blocks have not been explored [53].

Lee et al. [33] also prepared the mono-functionalized 21-thiaporphyrin **68** and 21-oxaporphyrin **69** by condensing the functionalized unsymmetrical tripyrrane **70** with symmetrical thiophene **27** or furan diol **26** under Lindsey's conditions (Scheme 10). This condensation resulted in the formation of a mixture of three porphyrins and the required porphyrin **68** or **69** was separated by column chromatography. The method was used only to synthesize 21-thia and 21-oxaporphyrins containing an iodophenyl group at *meso*-position.

The mono-ol method which we have used to synthesize the tri-functionalized 21-thia and 21-oxaporphyrins was further extended to synthesize the mono-functionalized 21-thia **71a**–**d**

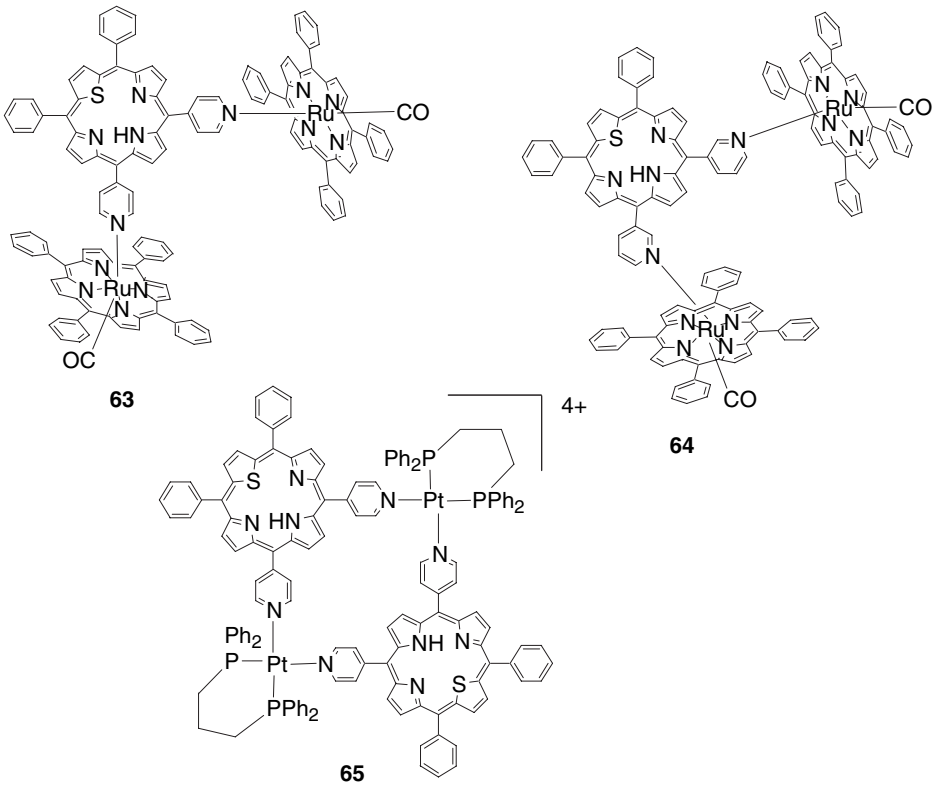

Chart 6. Unsymmetrical non-covalent heteroporphyrin systems.

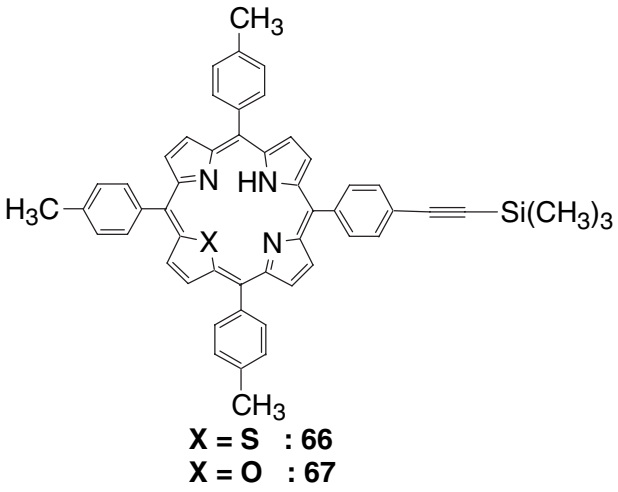

Chart 7. 21-Thia and 21-oxaporphyrins having trimethylsilylethynylphenyl functional group.

and 21-oxaporphyrins **72a**,**b**. To prepare 21-thia **71a**–**d** and 21-oxaporphyrins **72a**,**b** having one *meso*-functional group adjacent to heterocyclic ring, the functionalized thiophene **73** or furan **74** mono-ols were used [38,39]. The functionalized thiophene or furan mono-ol was condensed with aryl aldehyde and pyrrole under porphyrin forming conditions resulting in a mixture of two porphyrins. The desired **71** or **72** was separated by column chromatography (Scheme 11). The method was used to synthesize the mono-functionalized 21-thia and 21-oxaporphyrins containing iodophenyl, bromophenyl, hydroxyphenyl, ethynylphenyl functional groups at the *meso*-position.

We also developed an alternate method to synthesize the mono-functionalized 21-thia **71**, 21,23-dithia **75** and 21-thia-23-oxaporphyrins **76** using functionalized unsymmetrical thiophene diol **77** as a single common precursor [38,62] (Scheme 12).

To synthesize the monofunctionalized 21-thiaporphyrins, one equivalent of diol **77** was condensed with two equivalents of aryl aldehyde and three equivalents of pyrrole under Lindsey or Adler's conditions. This condensation gave a mixture of four porphyrins and the desired 21-thiaporphyrin **71** was separated by column chromatography. The mono-functionalized 21,23-dithiaporphyrins **75** were synthesized [62] by condensing the diol **77** with 16-thiatripyrrane **33** (Scheme 12). The condensation resulted in the formation of mono-functionalized 21,23-dithiaporphyrin as sole product in 10–12% yields. The mono-functionalized 21-thia-23-oxaporphyrins **76** were prepared [62] as a single product by condensing diol **77** with 16-oxatripyrrane **32** (Scheme 12).

The mono-functionalized porphyrin building blocks gave access for the first time to the unsymmetrical porphyrin dimers containing any two desired porphyrin units. We have explored the use of the mono-functionalized heteroporphyrins in the synthesis of a series of covalently linked unsymmetrical diaryl ethyne bridged porphyrin dimers **78**–**84** containing two different porphyrin cores [38,39,62]. The porphyrin dimers containing two different porphyrin cores were synthesized by coupling the appropriate porphyrin building block having the iodophenyl group with the porphyrin building block with ethynylphenyl group under Lindsey's copper free mild palladium coupling conditions [65] as illustrated in Scheme 13 for the synthesis of **78**. The dimer **78** was prepared by coupling of zinc(II) 5,10,15-tri(mesityl)20-(iodophenyl) **85** with the deprotected form of **71a** in the presence of $Pd_2(dba)_3/AsPh_3$ in toluene/triethylamine at 35 °C for 2 h (Scheme 13). Thus, a series of dimers containing different porphyrin cores (Chart 8), such as N_4–N_3S **78**,**79**; N_4–N_3O **80**; N_4–N_2S_2 **81**; N_3S–N_3O **82**; N_3S–N_2S_2 **83**; N_2S_2–N_2SO **84** were synthesized in decent yields under these coupling conditions [38,39,62]. NMR and absorption spectra of dimers **78**–**84** indicated a weak interaction between the porphyrin units. Since the porphyrins in unsymmetrical dimers

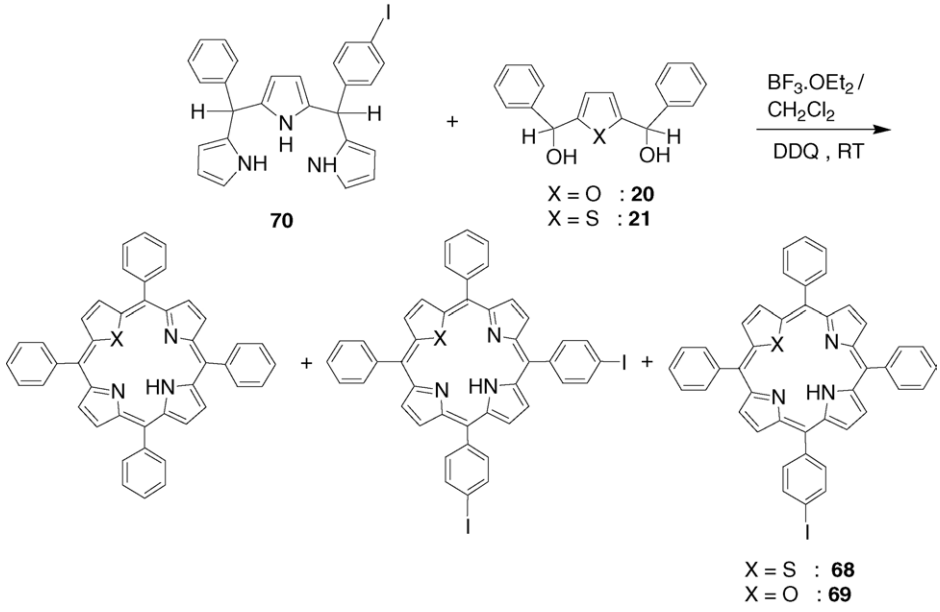

Scheme 10. Lee's approach for the synthesis of mono-functionalized 21-thia or 21-oxaporphyrins.

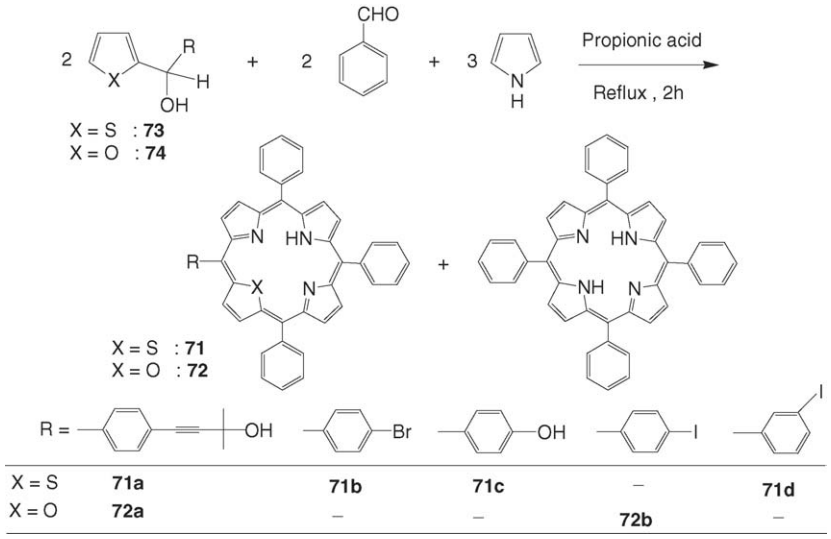

Scheme 11. Synthesis of mono-functionalized 21-thia and 21-oxaporphyrins by mono-ol method.

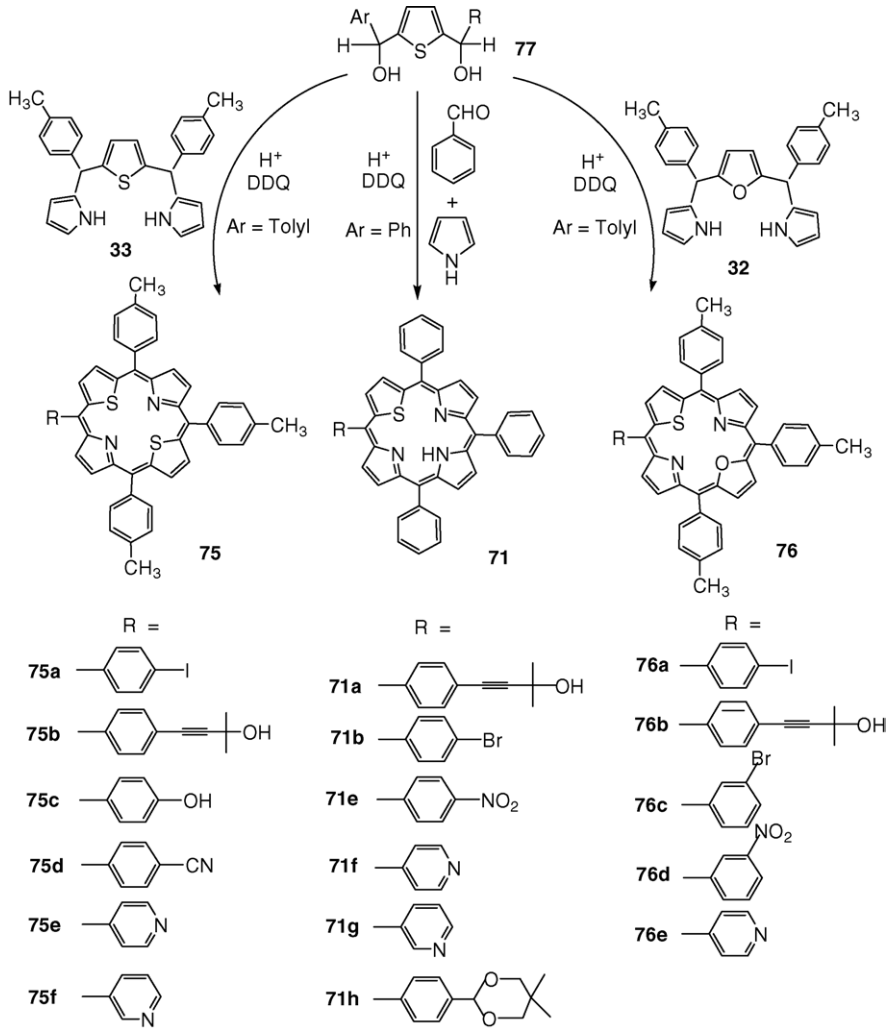

Scheme 12. Synthesis of mono-functionalized 21-thia, 21,23-dithia and 21-thia-23-oxaporphyrins using unsymmetrical thiophene diols.

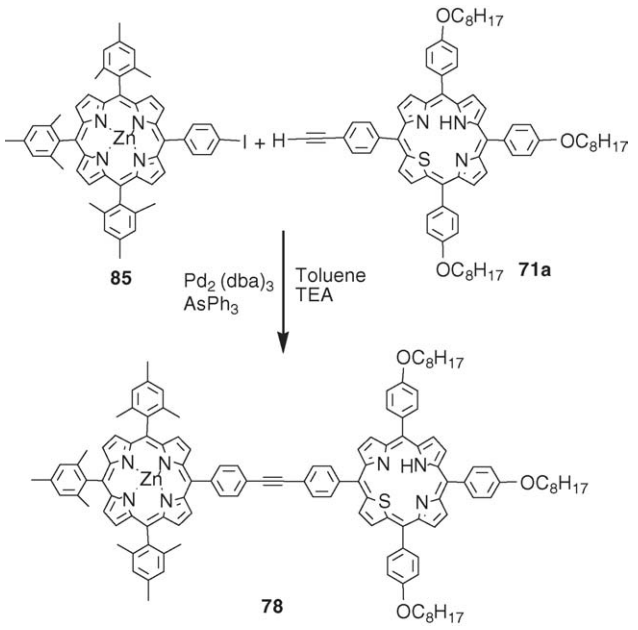

Scheme 13. Synthesis of unsymmetrical diarylethyne bridged covalent dimer.

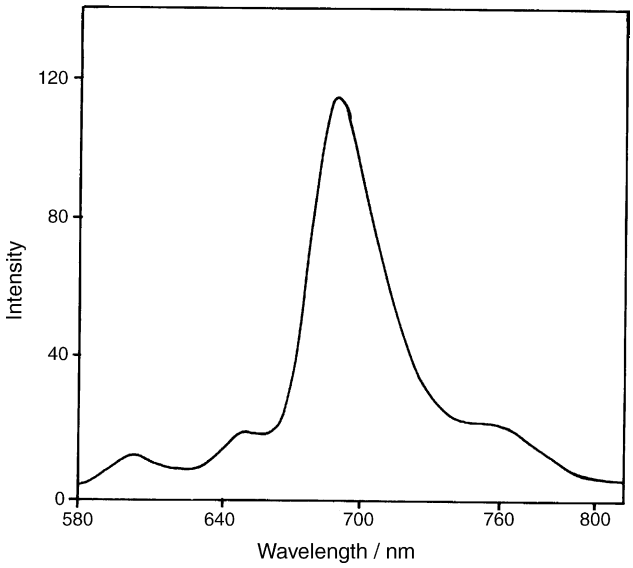

Fig. 6. Emission spectra of **78** recorded in toluene at λ_{ex} = 550 nm.

78–**84** absorb in two different regions, the photophysical properties of the dimers are expected to be interesting. A preliminary photophysical study was carried out on some of the unsymmetrical porphyrin dimers which exhibited interesting energy transfer properties from one porphyrin unit to the other on selective excitation of one porphyrin unit [39,62]. For example, a steady state fluorescence study of dimer **78** containing Zn(II) derivative of normal porphyrin and 21-thiaporphyrin sub-units was carried out with selective excitation at 550 nm where the Zn(II) derivative of normal porphyrin unit absorbs strongly. The major emission was observed from the 21-thiaporphyrin unit suggesting an efficient energy transfer from the Zn(II) derivative of the normal porphyrin unit to the 21-thiaporphyrin unit (Fig. 6). Similarly, the dimers **79**–**81** also showed an efficient energy transfer from donor porphyrin unit (normal porphyrin or its zinc(II) derivative) to acceptor porphyrin unit (21-thia, 21-oxa and 21,23-dithiaporphyrins) as confirmed by steady state fluorescence studies [39,62].

The mono-functionalized heteroporphyrins having pyridyl functional groups at *meso*-positions were used to synthesize unsymmetrical non-covalent porphyrin dimers **86**–**89** (Chart 9). The 21-thia **71f**,**g** and 21,23-dithiaporphyrin **75e**,**f** building blocks were reacted with RuTPP(CO)(EtOH) in toluene overnight and afforded dimers **86**–**89** (Chart 9) in decent yields [61,68].

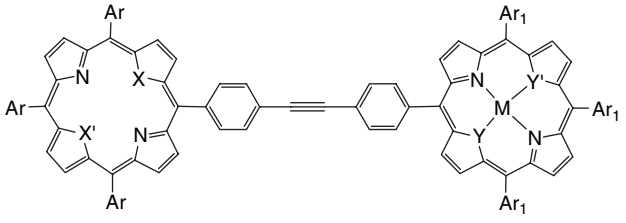

Chart 8. Unsymmetrical diarylethyne bridged covalent dimers.

6. β-Substituted heteroporphyrins

Porphyrins have two reactive positions—the β- and *meso*-positions at which suitable substituent(s) can be introduced to tune the electronic properties of the porphyrin for specific applications. The β-functionalization of porphyrins is of considerable chemical interest since the β-substituents are in direct conjugation with the porphyrin ring and small changes in the substituents alter the properties of the porphyrin macrocycle. There are several reports on both electron releasing and electron withdrawing substituents at β-pyrrole carbons of regular porphyrin systems [69,70]. Porphyrins with electron withdrawing substituents, such as –Br, NO_2 at β-pyrrole carbons of regular porphyrins are found to be robust catalysts for alkene epoxidation and alkane hydroxylation reactions [71,72,73]. However, until recently, there are no reports on β-substituted heteroporphyrins to understand the β-substituent effects on electronic properties of heteroporphyrins. Recently, a series of 21-thia and 21,23-dithiaporphyrins having bulky substituents at β-positions have been synthesized [74–79]. Both β-pyrrole [74,78] and β-thiophene substituted thiaporphyrins [75–77,79] have been synthesized and the spectroscopic properties were studied.

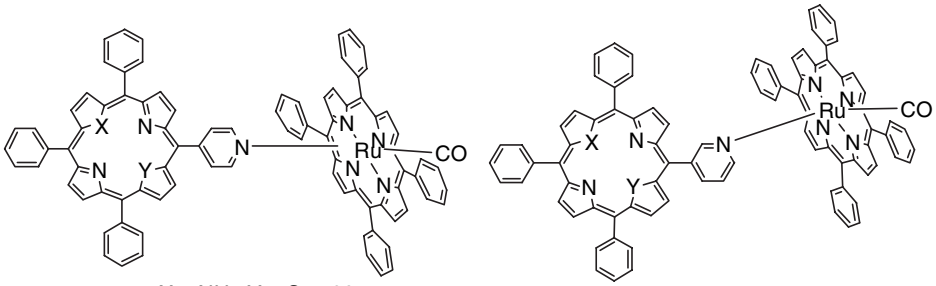

Chart 9. Unsymmetrical non-covalent porphyrin dimers.

6.1. β-Pyrrole substituted thiaporphyrins

We synthesized three β-pyrrole substituted 21,23-dithiaporphyrins by following the known synthetic methodologies (Chart 10). The tetrabrominated 21,23-dithiaporphyrin **90a** was synthesized in 70% yield by treating **7** with 4.2 equivalents of *N*-bromosuccinimide in chloroform at refluxing temperature. The bromines at the β-pyrrole carbon atoms of the thiaporphyrin **90a** resulted in upfield shifts of 0.26 ppm of the β-thiophene protons in ^{1}H NMR and red shifts of absorption and emission bands compared to **7** [74]. Unsuccessful attempts were made to use **90a** as a precursor to synthesize the β-aryl substituted thiaporphyrins by treating **90a** with different aryl boronic acids under Suzuki coupling conditions. However, the aryl substituted 21,23-dithiaporphyrins **90b** and **90c** (Chart 10) were obtained by condensing the corresponding 3,4-disubstituted pyrroles **91a**,**b** with thiophene diol **21** under mild acid conditions (Scheme 14) [74]. The large upfield shifts of the β-thiophene protons (0.44 ppm) in ^{1}H NMR and more red shifts in absorption and emission bands of **90b** compared to **7** (Table 3) indicated that the presence of bulky phenyl groups at the β-pyrrole carbon atoms alter the electronic properties of the porphyrin more drastically.

6.2. β-Thiophene substituted thiaporphyrins

We synthesized a series of β-thiophene substituted 21,23-dithia and 21-thiaporphyrins [75–77,79]. The 21,23-dithia **92a–d** and 21-thiaporphyrins **93a–d** having methyl and phenyl groups at β-thiophenes were synthesized by condensing the appropriate 3,4-disubstituted thiophene diols **94a–d** with pyrrole and with aryl aldehyde and pyrrole, respectively, under standard acid catalyzed conditions (Scheme 15). Spectroscopic studies on β-thiophene substituted thiaporphyrins showed the upfield shifts in ^{1}H NMR, red shifts in absorption and emission bands compared to the β-unsubstituted thiaporphyrins (Table 3). Furthermore, the magnitude of spectroscopic shifts were directly related to the number of β-substituents (Table 3). The comparison of absorption spectra of β-pyrrole and β-thiophene substituted thiaporphyrins **90b** and **92d**, respectively, along with unsubstituted thiaporphyrin **7** shown in Fig. 7 indicated that the maximum shifts were noted for **92d**. This suggested that the substituents at the β-thiophene carbon atoms alter the π-delocalization of porphyrin more effectively compared to the same substituents present at β-pyrrole carbons.

A series of cyclic substituents, such as propane-1,3-diyldioxy and its ethyl and benzyl derivatives substituted at the β-thiophene carbon atoms of 21,23-dithiaporphyrins **95a–c** and 21-monothiaporphyrins **96a–c** were synthesized (Scheme 16) [77]. 21,23-Dithiaporphyrins **95a–c** were prepared in 8–12% yields by condensing the substituted appropriate thiophene diols **97a–c** with pyrrole and 21-monothiaporphyrins **96a–c** were prepared in 7–9% yields by condensing the substituted thiophene diols with benzaldehyde and pyrrole under standard conditions (Scheme 16). The cyclic substituents introduced at the β-thiophene carbon atoms alter the electronic properties of the porphyrins moderately (Table 3). The moderate changes in the

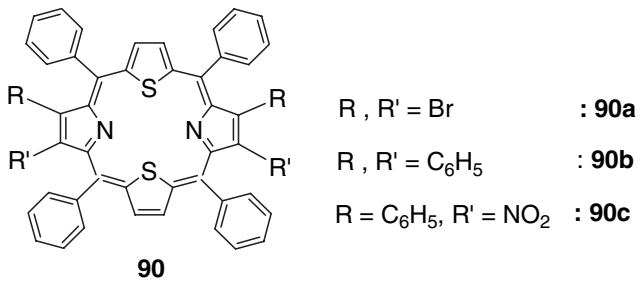

Chart 10. β-Pyrrole substituted 21,23-dithiaporphyrins.

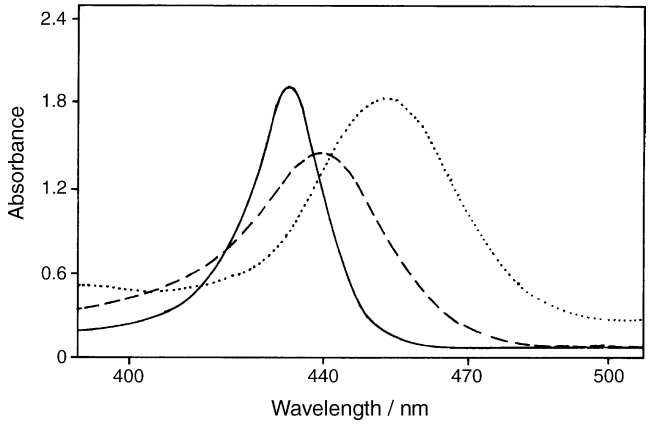

Fig. 7. Comparison of Soret band absorption spectra of **7** (—), **90b** (- - -) and **92d** (. . .) recorded in toluene.

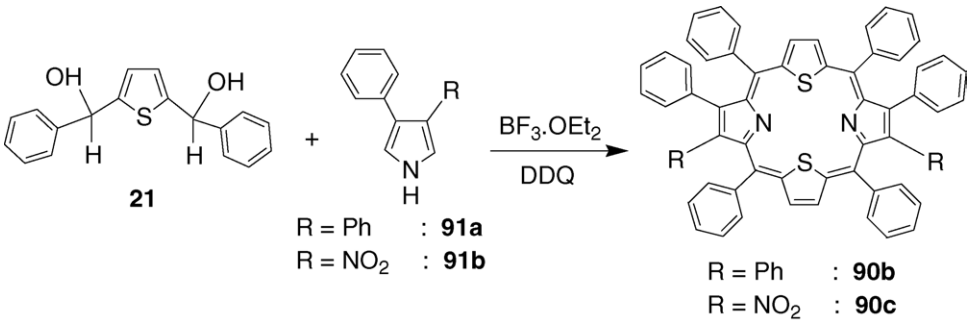

Scheme 14. Synthesis of β-pyrrole substituted 21,23-dithiaporphyrins.

Table 3
Selected spectroscopic data of β-thiophene and β-pyrrole substituted thiaporphyrins

Compound	β-Thiophene/β-furan (ppm)	β-Pyrrole (ppm)	Absorption		Emission	
			Soret (nm)	*Q*-band (nm)	λ_{em} (nm)	ϕ
7	9.68 (s)	8.67 (s)	435	696	706	0.0076
90b	9.23 (s)	–	440	700	735	0.0009
92d	–	8.10 (s)	454	715	736	0.0003
95c	–	8.39 (s)	443	708	713	0.0178
98a	–	8.26 (s)	446	714	744	0.0005
98d	–	8.30 (s)	441	705	713	0.0080
3	9.81 (s)	8.61 (d), 8.72 (d), 8.88 (s)	429	675	678	0.0168
93d	–	8.32 (s), 8.45 (q), 8.88 (s)	448	705	708	0.0139
96c	–	8.49 (s), 8.83 (q)	432	680	685	0.0399
99a	–	8.45 (d), 8.52 (d), 8.87 (m)	430	678	693	0.0023
99d	–	8.42 (s), 8.50 (d), 8.84 (d)	431	678	685	0.0035

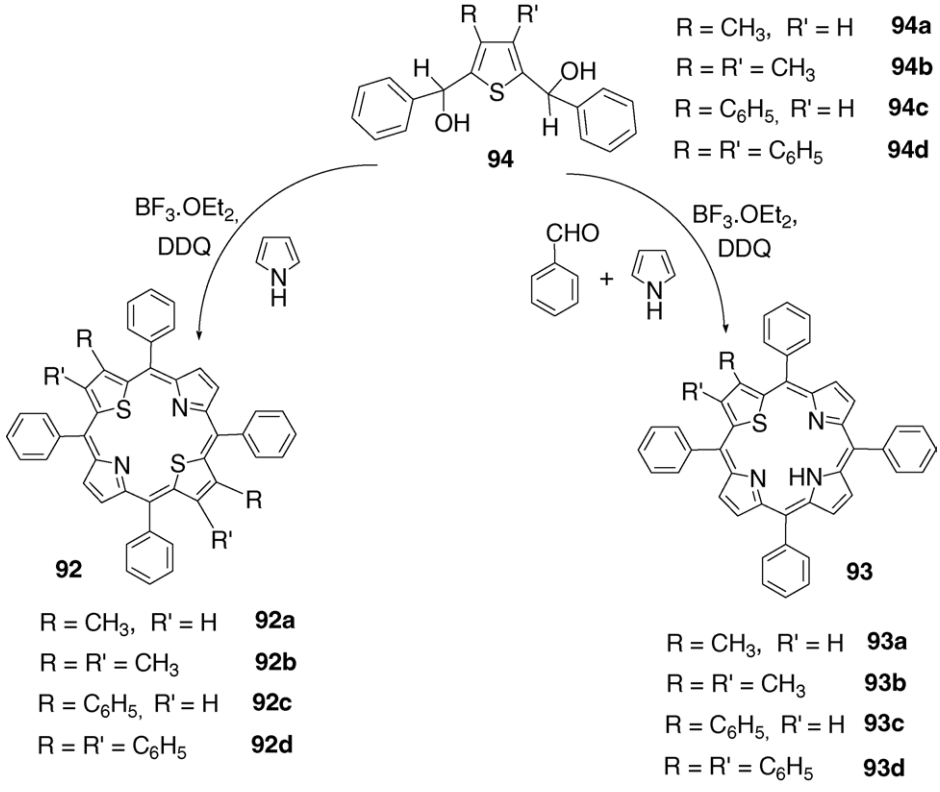

Scheme 15. Synthesis of β-thiophene substituted 21,23-dithia and 21-monothiaporphyrins.

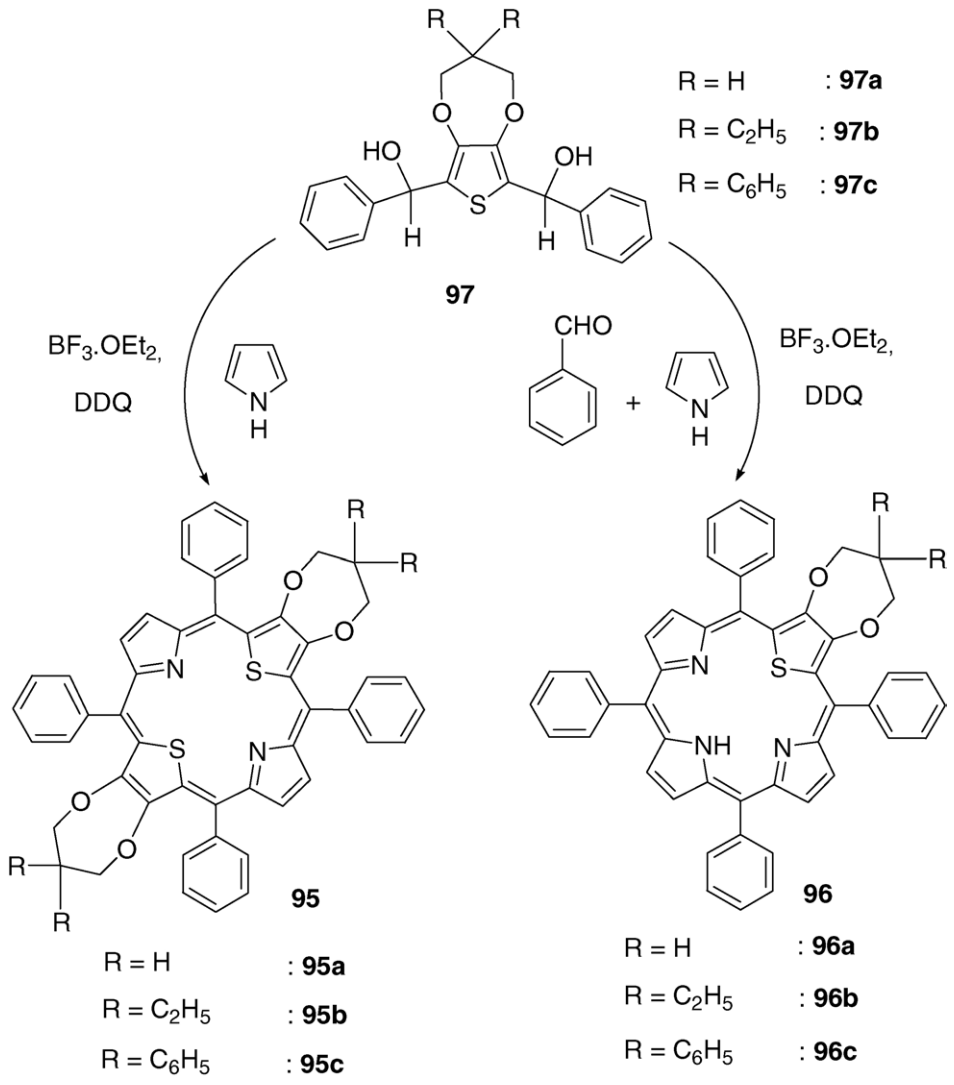

Scheme 16. Synthesis of β-thiophene substituted thiaporphyrins with cyclic substituents.

spectroscopic properties of the porphyrins were due to the flexible nature of the cyclic substituents at the β-thiophene carbon atoms.

The crystal structure solved for **96c** showed it is more planar [77] (Fig. 8) than the slightly saddle shaped β-unsubstituted **21-N_3SP 3b** [80] which was reflected in their dihedral angles. The dihedral angles between the plane of the *meso*-carbon atoms and the four five-membered rings of **96c** and **3b**, respectively, are: thiophene, 2.6° and 14.1°; pyrrole N(1), −4.9° and −11.5°; N(2), 5.6° and 10.0°; N(3), 0° and −7.4°. The non-bonded N(1)···N(3) distance in **96c** was almost the same as that of **3b** but the non-bonded S···N(2) distance in **96c** was slightly lower compared to **3b**. The C_α–S, C_α–C_β and C_β–C_β bond lengths of both the pyrrole and thiophene rings of **96c** were slightly altered compared with **3b** indicating that the π-delocalization was altered in the porphyrin macrocycle due to the presence of the substituent at the β-thiophene carbon atoms.

A series of tetraalkoxy and dialkoxy substituted 21,23-dithaporphyrins **98a–d** and 21-monothiaporphyrins **99a–d**,

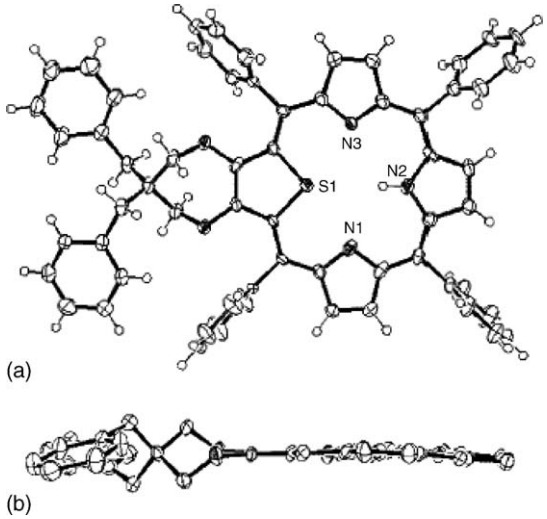

Fig. 8. X-ray structure of **96c** (a) top view and (b) side view (reproduced with permission from Ref. [77]).

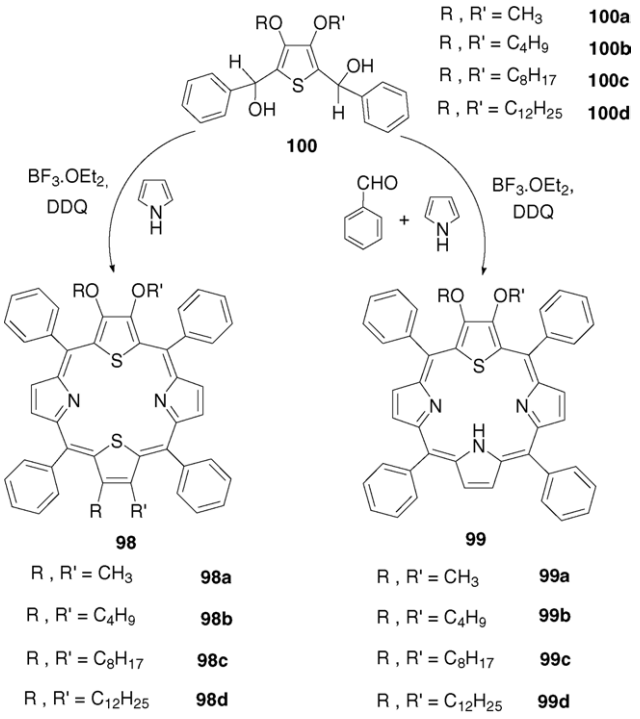

Scheme 17. Synthesis of β-thiophene substituted thiaporphyrins with alkoxy substituents.

respectively, having methoxy, butoxy, octyloxy and dodecyloxy substituents at β-thiophene carbon atoms [75,79]. These porphyrins, were synthesized by using appropriate alkoxy substituted thiophene diols **100a**–**d** as shown in Scheme 17.

The presence of alkoxy substituents at β-thiophenes resulted in shifts in ^{1}H NMR and red shifts of absorption and fluorescence bands compared to their unsubstituted **7** and **3** porphyrins (Table 3). The structures of **98b** (Fig. 9) and **99a** (Fig. 10) were elucidated by single crystal X-ray diffraction analysis [75,79]. Interestingly, **98b** was more planar compared to **7** [80] suggesting that the presence of butoxy substituents at the β-thiophene

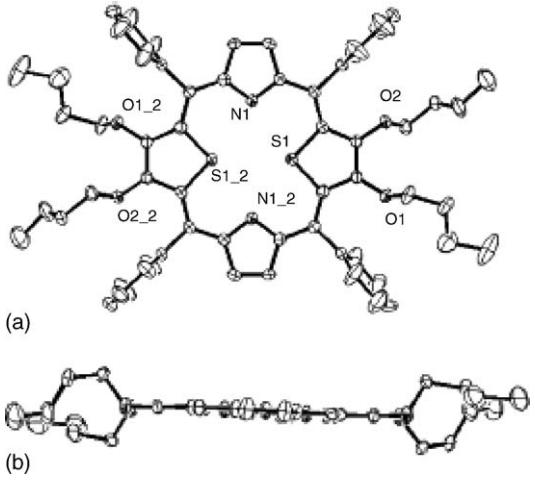

Fig. 9. X-ray structure of **98b** (a) top view and (b) side view (reproduced with permission from Ref. [75]).

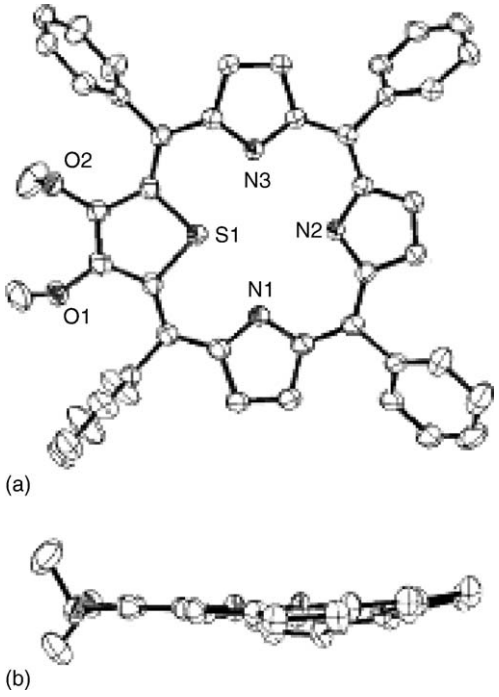

Fig. 10. X-ray structure of **99a** (a) top view and (b) side view (reproduced with permission from Ref. [79]).

carbon atoms induced more planarity. The four five-membered rings in **98b** were in the same plane with four *meso*-carbons with negligible deviation unlike **7** in which the four five-membered rings slightly deviated from the plane of the four *meso*-carbons [80]. The non-bonded S···S′ and the N···N′ distances were slightly increased and decreased, respectively, in **98b** compared to **7**. The presence of substitutents at β-thiophene **98b** also resulted in the decrease of the C_α–C_β and C_β–C_β distances of the thiophene rings in **98b** compared to **7**. The structure of **99a** (Fig. 10) was slightly saddle-shaped with a mean deviation of 0.16 Å for the atoms in the porphyrin core. This was similar to that of β-unsubstituted porphyrin **3b** [80] suggesting that the two methoxy groups at β-thiophene carbon atoms in **99a** did not influence the structure of the porphyrin. In **99a**, one of the methoxy groups on the β-thiophene carbon tilted upward and the other methoxy group was tilted downward [79]. The C_α–S, C_β–C_β distances in **99a** were almost similar to that of **3b**.

7. *meso*-Substituted heteroporphyrins

Porphyrin macrocycles are synthetically very flexible and by introducing substituents at β- or *meso*-positions, the properties can be tuned at will for any application. Most of the porphyrins and heteroporphyrins reported to date commonly have six-membered aryl groups at *meso*-positions. Recently, regular porphyrins having *meso*-substituents as five-membered heterocycles, such as thiophene [81–85] exhibited very interesting spectroscopic and electrochemical properties, which were attributed to the strong interaction between the porphyrin macrocycle and the five-membered *meso*-substituents. The interesting electronic properties of the porphyrins with five-membered heterocycles as *meso*-substituents suggests that these porphyrins

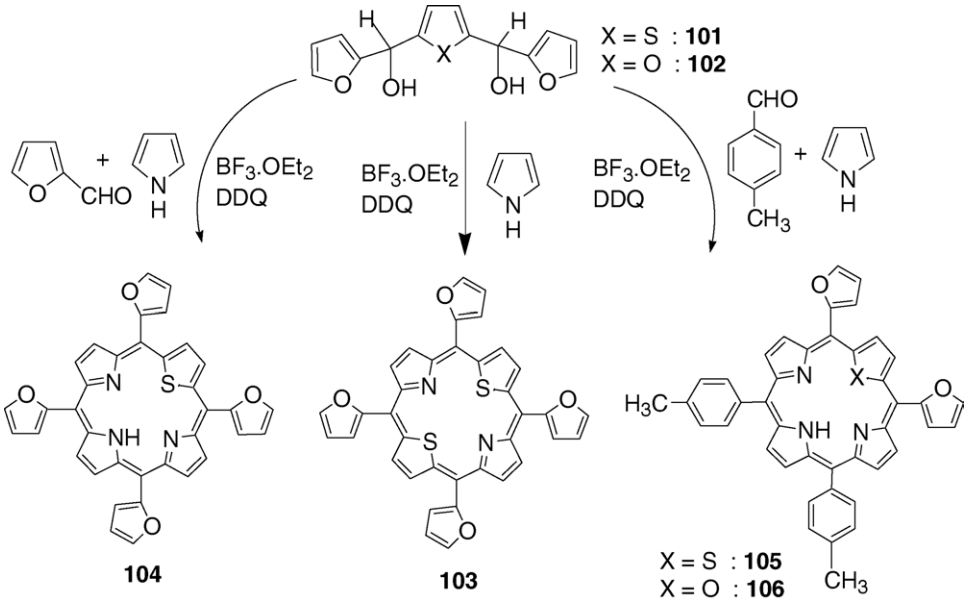

Scheme 18. Synthesis of *meso*-furyl substituted heteroporphyrins.

can be used as a substitute for *meso*-tetraarylporphyrins for various applications. We synthesized a series of heteroporphyrins having 2-furyl, 2-thienyl and 3-thienyl groups at the *meso*-positions and studied their ground and excited state properties [86–90]. The heteroporphyrins having two and four furyl groups at *meso*-positions were synthesized using 2,5-bis(2-furylhydroxymethyl)thiophene **101** or furan **102**. The tetrafuryl substituted 21,23-dithiaporphyrin **103** was prepared by condensing the diol **101** with pyrrole and the tetrasubstituted 21-thiaporphyrin **104** was prepared (Scheme 18) by condensing the same diol **101** with furan-2-carboxaldehyde and pyrrole under standard conditions [86]. The difuryl substituted 21-thiaporphyrin **105** and 21-oxaporphyrin **106** were prepared (Scheme 18) by condensing **101** and **102** respectively with *p*-tolylaldehyde and pyrrole under mild acid catalyzed conditions [86,87]. The introduction of five-membered furyl groups at *meso*-positions of heteroporphyrins altered the electronic properties drastically compared to the heteroporphyrins with six-membered aryl groups. This was reflected in the downfield shifts of the pyrrole and thiophene protons in ^{1}H NMR and red shifts of absorption and emission bands with reduction in intensity and lifetimes of singlet excited states of *meso*-furyl porphyrins [87] compared to *meso*-aryl analogues (Table 4). The changes in the spectroscopic properties were attributed to the greater resonance interaction between the porphyrin and five-membered heterocycles [87,89].

We also synthesized *meso*-thienyl substituted porphyrins with different cores, such as N_3S, N_3O and N_2S_2 [88]. The *meso*-2-thienyl substituted 21,23-dithiaporphyrin **111** and 21-thiaporphyrins **112a**,**b** were prepared using diol **107** and *meso*-2-thienyl substituted 21-oxaporphyrins **113a**,**b** were prepared using diol **108** under standard conditions (Chart 11). The heteroporphyrins **114**–**116** with two and four 3-thienyl groups at *meso*-positions were synthesized using diols **109** and **110** (Chart 11). Similar to *meso*-furyl heteroporphyrins, the *meso*-thienyl heteroporphyrins also exhibited changes in ^{1}H NMR, absorption and emission properties [88,90] (Table 4). However, the effects observed for *meso*-thienyl heteroporphyrins were comparatively less in magnitude than *meso*-furyl heteroporphyrins (Table 4).

The X-ray structures were solved for *meso*-thienyl heteroporphyrins **111** and **115** [88]. The structure of **111** was almost

Table 4
Comparison of selected spectroscopic data of *meso*-furyl and *meso*-thienyl heteroporphyrins and their *meso*-aryl analogues

Compound	β-Thiophene/β-furan (ppm)	β-Pyrrole (ppm)	Absorption		Emission		Lifetime
			Soret (nm)	*Q*-band (nm)	λ_{em} (nm)	ϕ_f	τ_f (ns)
7	9.68 (s)	8.67 (s)	435	696	706	0.0076	1.34
104	10.05 (s)	8.97 (s)	458	740	773	0.0025	1.20
111	9.91 (s)	8.86 (s)	447	713	738	0.0004	1.12
114	9.82 (s)	8.8.1 (s)	440	704	717	0.0001	1.20
3	9.81 (s)	8.61 (d), 8.72 (d), 8.88 (s)	429	675	678	0.0168	1.77
103	10.21 (s)	8.85 (d), 9.01 (d), 9.22 (d)	448	705	708	0.0139	1.06
112a	9.99 (s)	8.77 (d), 8.88 (d), 9.15 (d)	440	692	709	0.0002	0.97
2	9.16 (s)	8.52 (d), 8.62 (d), 8.89 (s)	419	671	676	0.0758	8.18
113a	9.59 (s)	9.21 (d), 9.47 (s)	430	682	690	0.0047	5.84

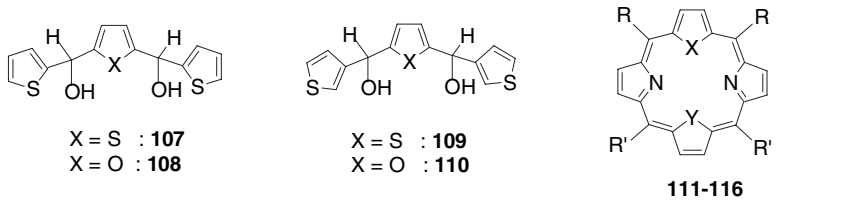

	R = R' =	R = R' =	R = / R' =	R = / R' =
X , Y = S	**111**	**114**	-	-
X = S ; Y = NH	**112a**	-	**112b**	**115**
X = O ; Y = NH	**113a**	-	**113b**	**116**

Chart 11. *meso*-Thienyl substituted heteroporphyrins and *meso*-thienyl heterocycle diols.

planar (Fig. 11). The four five-membered rings were in the same plane as the four *meso*-carbon atoms with negligible deviation from planarity and the *meso*-thienyl substituents were out of the plane of porphyrin. Two of the *meso*-thienyl sulfur atoms were above the plane and other two were below the plane. The non-bonding N···N′ (4.61 Å) and S···S′ distances (3.058 Å) were shorter in **111** than in **7** (N···N′: 4.65 Å, S···S′: 3.069 Å) [80], indicating that **111** is more planar than **7**. The C_β–C_β distances of thiophene and pyrrole rings in **111** [1.353(5) and 1.3331(6) Å, respectively] were significantly shorter than in **7** [80], due to the altered π-delocalization in **111** because of the thienyl substituents at the *meso*-positions. The most novel feature of **111** was the observation of intermolecular hydrogen bonding holding the porphyrin rings in a supramolecular array formed due to the presence of a C–H···N hydrogen bond between the *meso*-thienyl CH group of one porphyrin ring and the pyrrole N atom of another porphyrin [88]. This H-bonding was limited to the single strand to form a ladder-type supramolecular assembly and was not extended between the strands. The structure of 21-thiaporphyrin **115** (Fig. 12) with two *meso*-thienyl groups and two *meso*-aryl groups [88] was planar (Fig. 12) compared to the saddle-shaped structure of **3b** [80]. In **115**, the non-bonding N(1)···N(3) distance (4.392 Å) was almost the same as that of **3b** but the non-bonding S···N(2) distance (3.570 Å) was longer than **3b** (3.547 Å) supporting the planarity observed for **115**.

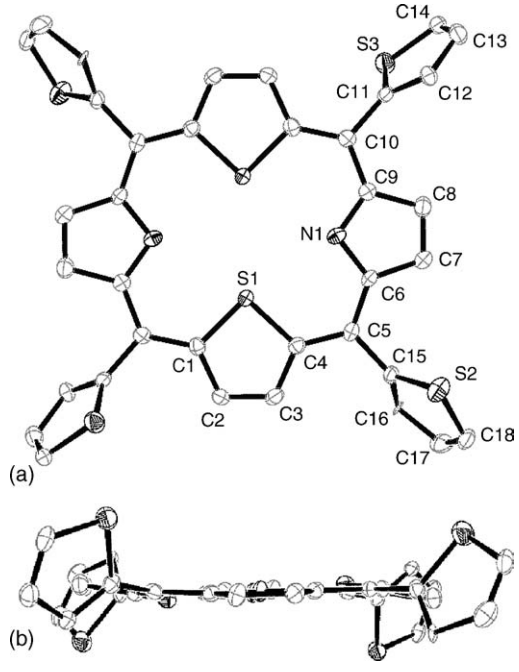

Fig. 11. X-ray structure of **111** (a) top view and (b) side view (reproduced with permission from Ref. [88]).

Porphyrins having bulky dendritic wedges at the *meso*-positions have received a lot of attention in recent years because of their importance as biomimic models [91,92], for catalytic applications [93] and also as attractive building blocks for the formation of supramolecular architectures having well defined shapes and dimensions [94,95]. However, to date there is only one report on heteroporphyrins having phenyl ether based second generation dendrons at *meso*-position [96]. The 21-oxaporphyrin **117** (Scheme 19) having a bulky phenyl ether based second generation dendron at two *meso*-positions in *cis* fashion was synthesized in 4.6% yield by condensing furan diol **20** with a second generation dendritic aldehyde **118** and pyrrole in propionic acid at refluxing temperature [96].

The emission study showed an energy transfer from dendritic wedges to porphyrin unit. The material properties of **117** and its Cu(II) derivative **Cu117** were studied by optical microscopy and AFM analysis in contact mode. The optical microscopy of 100 μM solutions of the Cu(II) derivative of **2** (CuOTPPCl) showed random aggregates but **Cu117** showed the formation of large and small spherical aggregates up to 7.5 μm size [96]. The AFM analysis supported the formation of large spherical structures of **Cu117** and showed that the **Cu117** formed nearly spherical, robust and isolated assemblies whereas CuOTPPCl formed random aggregates on a glass surface (Fig. 13). This study suggested that the dedritic wedges assist in the formation of large spherical supra structures with well-defined dimensions.

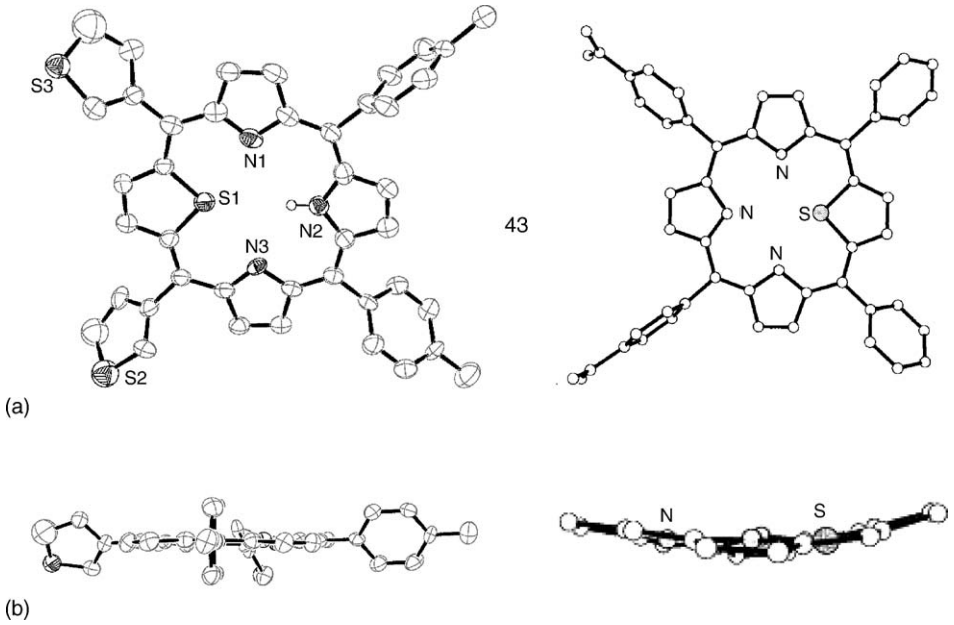

Fig. 12. A comparison of X-ray structures of **115** and **3b** (a) top view and (b) side view (reproduced with permission from Ref. [88] and Ref. [80] respectively).

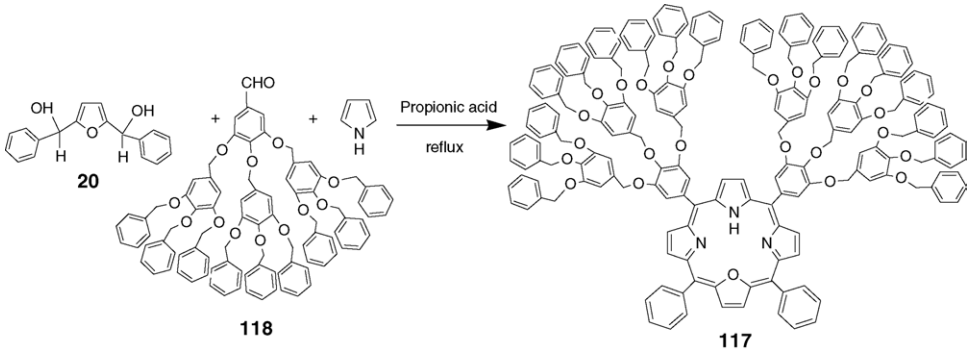

Scheme 19. Synthesis of 21-oxaporphyrin with second generation dendritic wedges.

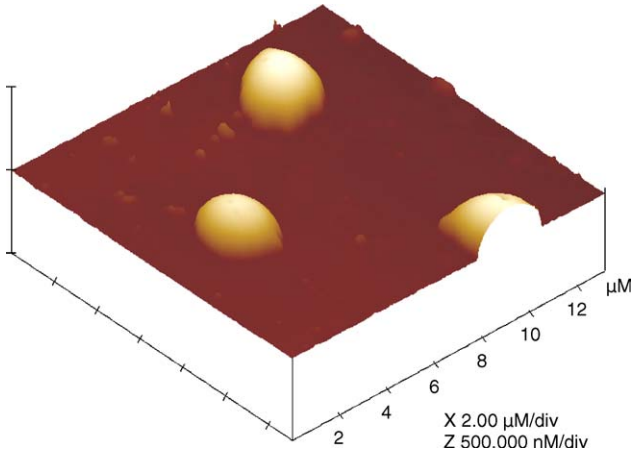

Fig. 13. AFM image of **Cu117** on glass substrate (reproduced with permission from Ref. [96]).

8. *meso*-Unsubstituted heteroporphyrins

Porphyrins with *meso*-unsubstituted carbon(s) played a vital role in synthetic porphyrin chemistry. The high reactivity of the *meso*-carbon bridge of the *meso*-unsubstituted porphyrins made these porphyrins ideal precursors for the synthesis of more complex systems with special physical and chemical properties. The β-unsubstituted *meso*-unsubstituted porphyrin or porphin, has not been well studied because of its very poor solubility characteristics. Broadhurst and Grigg [15] in the early 1970s synthesized 21-monoheteroporphyrins **15** and **16** as well as 21,23-diheteroporphyrins **28**–**30** with four *meso*-unsubstituted carbons (Schemes 1a and 2a). Chmielewski et al. reported the synthesis of 21-oxaporphyrin with one *meso*-unsubstituted carbon but its chemistry was not extended further [2,9]. We recently reported the synthesis of a series of thiaporphyrins with four, and two *meso*-unsubstituted carbons (Chart 12) using simple thiophene diols [97,98]. The synthesis of 21,23-dithiaporphyrin **120** with four *meso*-unsubstituted carbon atoms as well as β-unsubstituted carbon atoms was attempted using thiophene diol **119**. However, the compound was not isolated due to the

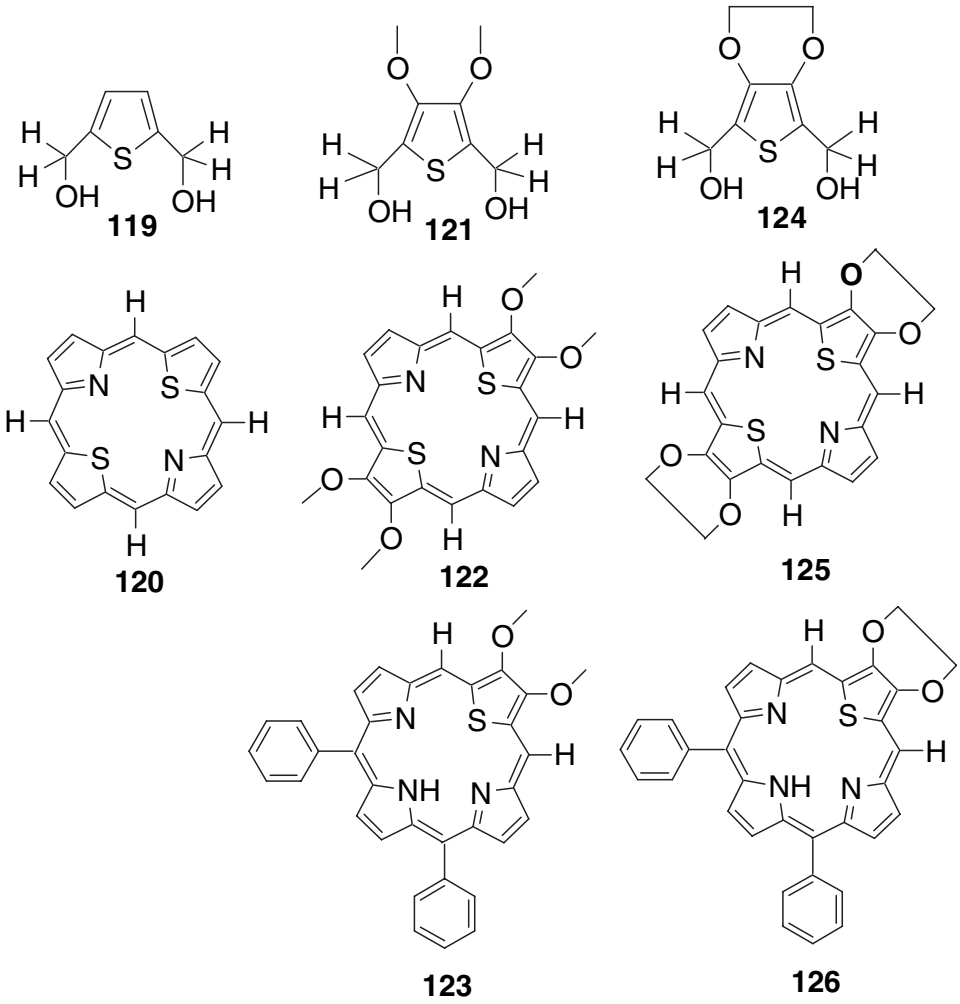

Chart 12. Four and two *meso*-unsubstituted thiaporphyrins and their precursor diols.

unstable nature of the porphyrin. The four *meso*-unsubstituted but β-substituted 21,23-dithiaporphyrin **122** and two *meso*-unsubstituted 21-thiaporphyrin **123** were synthesized using thiophene diol **121**. Similarly, the thiophene diol **124** was used to synthesize the four *meso*-unsubstituted 21,23-dithiaporphyrin **125** and two *meso*-unsubstituted 21-thiaporphyrin **126**. The crystal structure solved for **126** exhibited the formation of a supramolecular assembly [98] due to intermolecular C–H···O and C–H···N hydrogen bonded interactions (Fig. 14).

A series of mono *meso*-unsubstituted heteroporphyrins with different cores, such as N_3S, N_3O, N_2S_2, N_2O_2, N_2SO and N_2OS **127**–**132** were synthesized [99] by following three different strategies (Scheme 20). The mono *meso*-unsubstituted 21-thiaporphyrin **127** and 21-oxaporphyrin **128** were synthesized by condensing the unsymmetrical thiophene diol **133** and furan diol **134**, respectively, with aldehyde and pyrrole (Scheme 20a). The mono *meso*-unsubstituted 21,23-dithiaporphyrin **129**, 21,23-dioxaporphyrin **130**, 21-thia-23-oxaporphyrin **131** and 21-oxa-23-thiaporphyrin **132** were prepared by condensing appropriate unsymmetrical diols (**133** and **134**) and symmetric tripyrranes (**33b** and **32b**) as shown in Scheme 20b. The mono-*meso*-unsubstituted 21-thia-23-oxaporphyrin **131** and 21-oxa-23-thiaporphyrin **132** were also prepared alternately as presented in Scheme 20c by condensing the corresponding unsymmetrical tripyrrane (**135** and **136**) with an appropriate symmetrical diol (**20b** and **21b**).

The reactivity of *meso*-unsubstituted porphyrins was tested towards electrophilic and nucleophilic substitution reactions. The dibromo derivative **137** was synthesized in 55% yield by treating porphyrin **126** with *N*-bromosuccinimide in $CHCl_3$ at room temperature [98]. The diethynyl porphyrin **138** was synthesized in 58% yield by treating **137** with trimethylsilylacetylene in the presence of catalytic amounts of $PdCl_2(PPh_3)_2$/CuI in THF/triethylamine followed by deprotection of the trimethylsilyl group with K_2CO_3 in THF/CH_3OH (Scheme 21). *meso*-Bis(palladio)porphyrin **139** was synthesized [98] in 28% yield under Arnold et al. [100] conditions by treating **137** with $Pd_2(dba)_3/PPh_3$ in toluene at room temperature (Scheme 21). The *meso*-butyl porphyrin **140** was synthesized using Kalisch and Senge method [101] by treating porphyrin **127** with *n*-BuLi at 0 °C in THF followed by oxidation with DDQ (Scheme 22). The mono bromo derivative **141** was synthesized similarly by treating **127** with *N*-bromosuccinimide in $CHCl_3$ at room temperature which was then coupled with **71a** under palladium

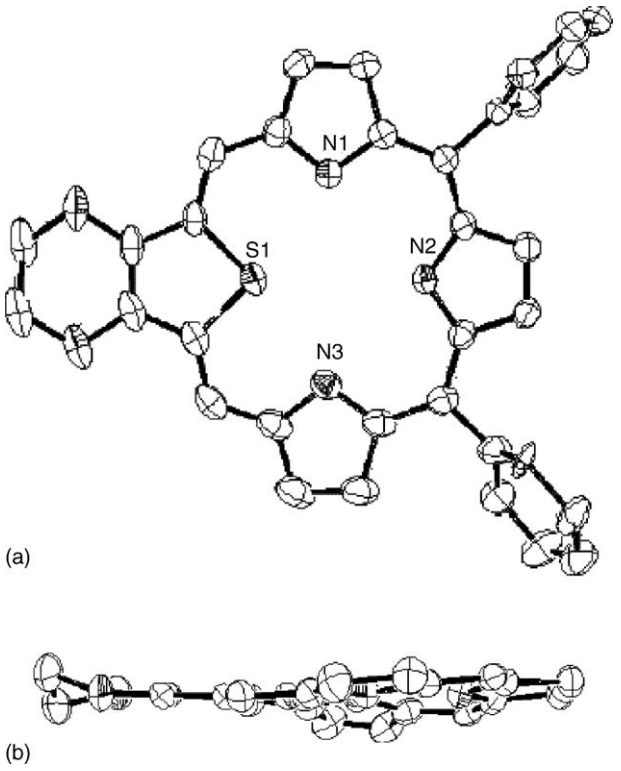

Fig. 14. X-ray structure of **126** (a) top view and (b) side view (reproduced with permission from Ref. [98]).

coupling conditions to yield the symmetrical covalently linked phenylethyne bridged dimer **142** containing two N_3S porphyrin cores (Scheme 23).

9. Heteroatom substituted corroles, carbaporphyrins, chlorins, bacteriochlorins and tetrabenzoporphyrins

9.1. Heterocorroles

A corrole molecule is an 18 π-electron aromatic tetrapyrrole macrocycle with a direct α–α pyrrole–pyrrole link. Since corroles have three ionisable hydrogen atoms, these molecules can stabilize metals in +3 oxidation state whereas porphyrins, which have two ionisable hydrogen atoms tend to stabilize only +2 metal ions. Hence, much attention has been directed recently on corrole chemistry [102,103]. Johnson and Kay [104,105] were the first to report the synthesis of β-alkylated 21,23-dioxacorrole, 21-oxacorrole and 22-oxacorrole by ring closure reaction of the corresponding heteroatom containing metallo linear tetrapyrroles. Later, Broadhurst et al. [106,107] synthesized a variety of heteroatom containing metallocorroles by 2 + 2 Macdonald type of condensation of dipyrromethanes and 2,2′-bifuran or 2,2′-bithiophene at elevated temperatures. The first synthesis of core-modified *meso*-aryl corrole was reported by Chandrashekar and co-workers [108]. They isolated 5,10,15-triaryl-21-oxacorrole **143** as a byproduct in 8%

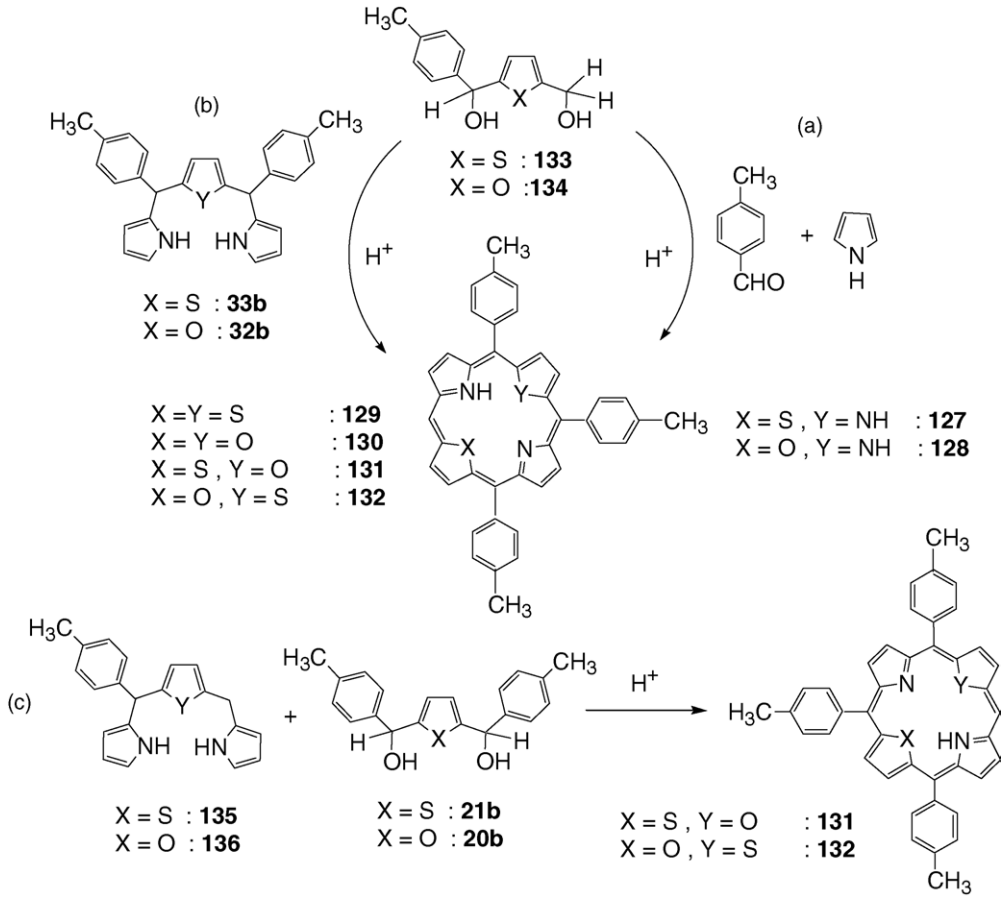

Scheme 20. Three different synthetic routes for *meso*-unsubstituted heteroporphyrins.

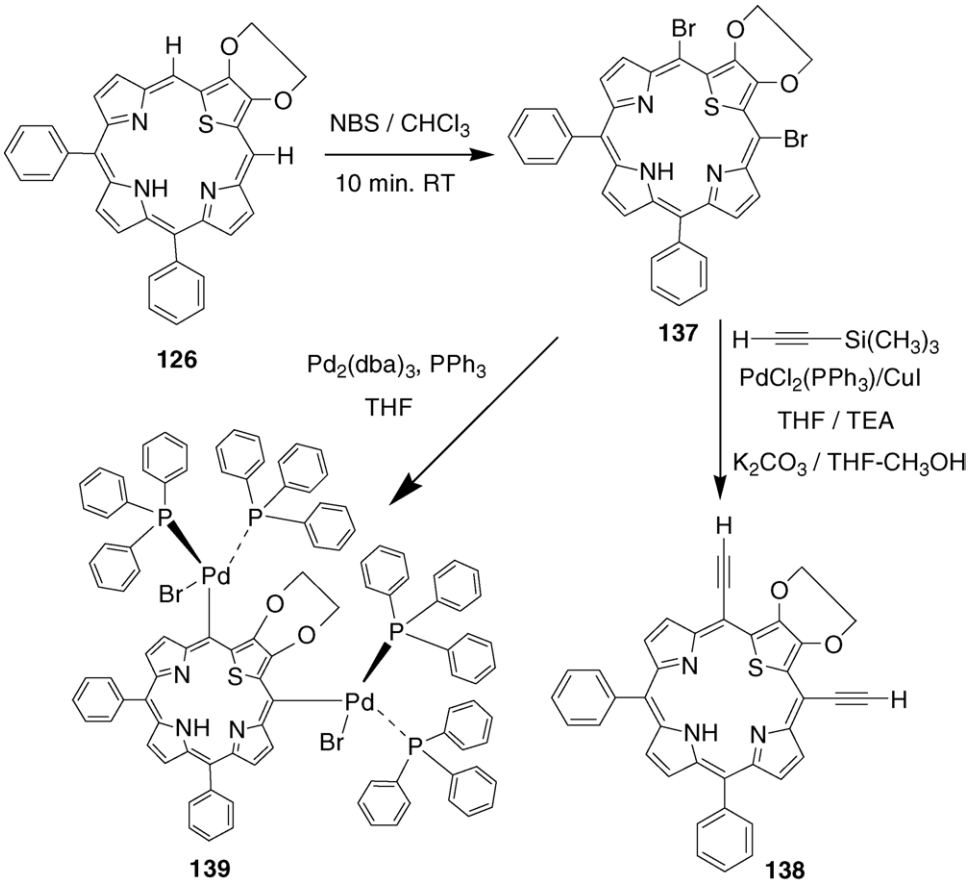

Scheme 21. Synthesis of *meso*-functionalized 21-thiaporphyrins.

yield in their attempts to synthesize oxa-smaragdyrin **144** by an acid catalyzed oxidative coupling reaction of **32a** and *meso*-phenyldipyrromethane **25** (Scheme 24). Since **143** was formed in acid, the formation of **143** was attributed to the acidolysis of dipyrromethanes followed by the recombination of fragmented products [108].

NMR studies revealed that **143** exhibits asymmetric tautomerism where the NH proton adjacent to the furan ring was localized and the other NH proton on the bipyrrolic unit was changing sites between the two nitrogen atoms of the bipyrrolic unit. The 21-oxacorrole **143** showed usual intense Soret and four *Q*-bands in the visible region. On protonation, the Soret band split due to the lowering of symmetry. The emission spectrum of **143** was blue shifted compared to **2** with a high quantum yield (0.88) relative to **2** (0.075). Interestingly, even the protonated species of **143** was highly emitting with a quantum yield of 0.23. The X-ray structure of **143** (Fig. 15) exhibited an almost planar structure with only a small deviation of the inner-core heteroatoms from planarity varying from 5.48° to 7.74° [109]. The planarity of **143** was attributed to less steric hindrance in the macrocyle because of the presence of only two hydrogen atoms unlike regular corroles which showed small deviations from planarity due to three inner hydrogen atoms causing strain in the macrocycle. Furthermore, **143**

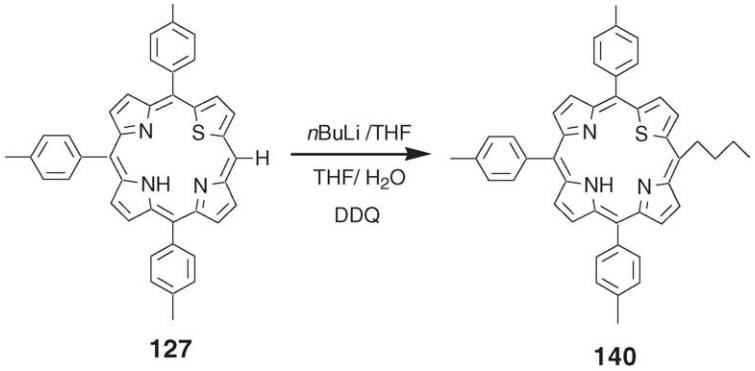

Scheme 22. Synthesis of *meso*-butyl derivative of 21-thiaporphyrin.

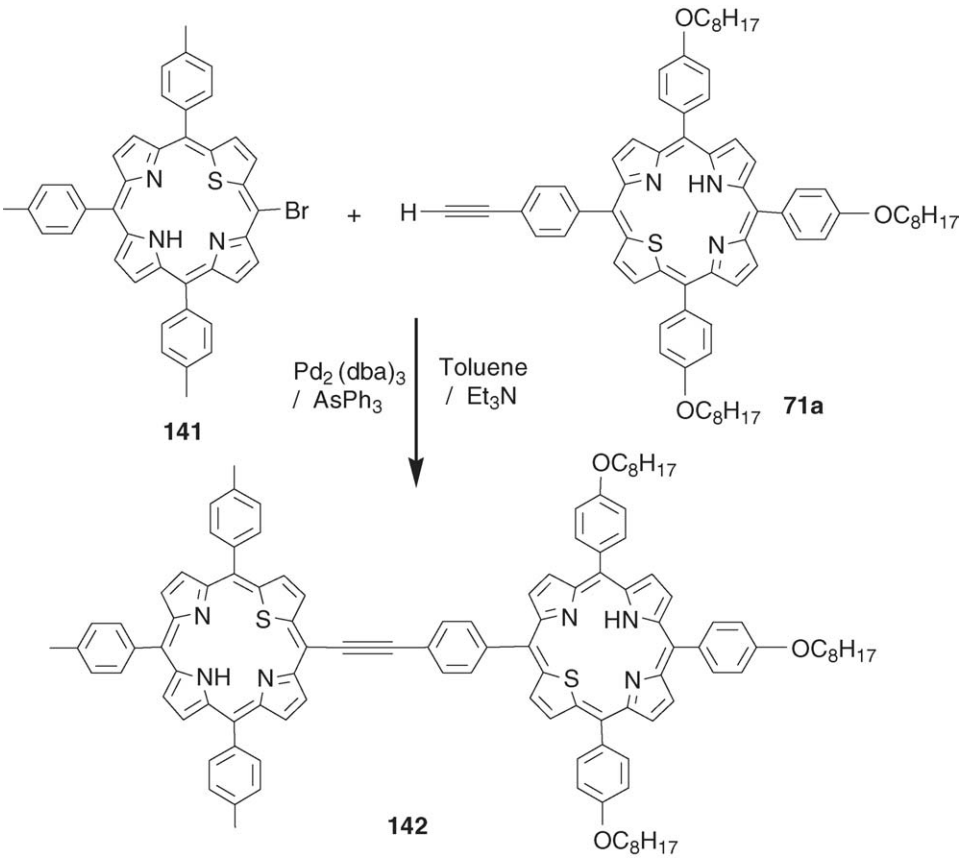

Scheme 23. Synthesis of phenylethyne bridged covalent dimer.

showed columnar structures due to π–π interactions between the macrocycles.

A variety of metal complexes of **143** have been investigated [109]. Since **143** is a dianionic ligand, it stabilizes metals in the +2 oxidation state provided that all the heteroatoms in the core participate in the coordination. Four metal derivatives (Rh, Cu, Ni and Co) of **143** were prepared by reacting **143** with appropriate metal precursors [109]. **143** stabilizes Ni, Cu, Co in +2 oxidation states with the participation of all heteroatoms in the coordination. However, **143** stabilizes Rh in the +1 oxidation state since it binds to only two heteroatoms of the macrocycle. These observations were in contrast with corroles that act as trianionic ligands favoring higher oxidation states. The metal insertion into **143** was found to be difficult compared to normal corroles. The crystal structures of Rh(I) and Ni(II) complexes of **143** were analyzed [109]. The Rh(I) complex of **143** was non-planar and the Rh(I) ion was located above the corrole plane (Fig. 16). Rh(I) binds to only one imino and one amino nitrogen of the macrocycle and other two coordination sites were occupied by carbonyl ligands providing square planar geometry around the Rh(I) ion. This type of coordination was preferred by Rh(I) possibly to avoid strain in the macrocycle. The Ni(II) complex of **143** is almost planar with a distorted square planar geometry around the Ni(II) ion (Fig. 17). The Ni(II) ion lies above the mean plane of the macrocycle by only 0.008 Å and acquired distorted square planar geometry around the metal ion. The comparison of Ni–N and Ni–O distances of **143** with that of corresponding Ni(II) derivative of **2** [9] showed that in **143** the bond distances were much shorter reflecting the reduced core size in **Ni(II)143**.

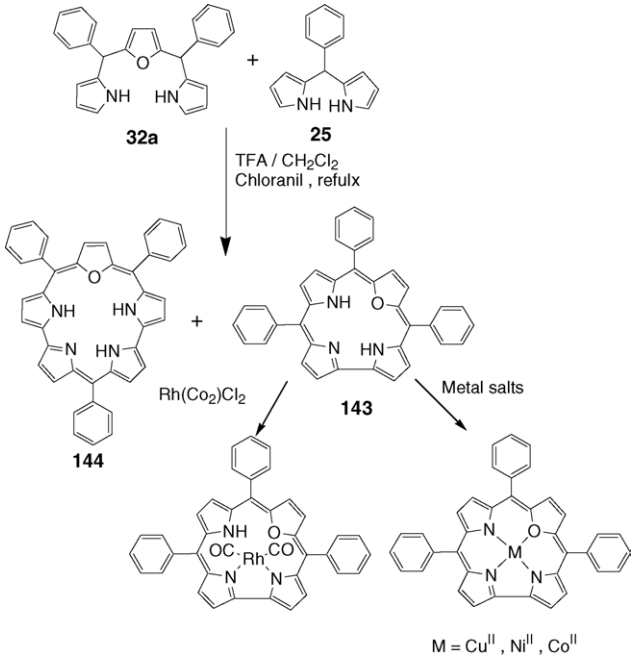

Scheme 24. Synthesis of 21-oxacorrole and its metal derivatives.

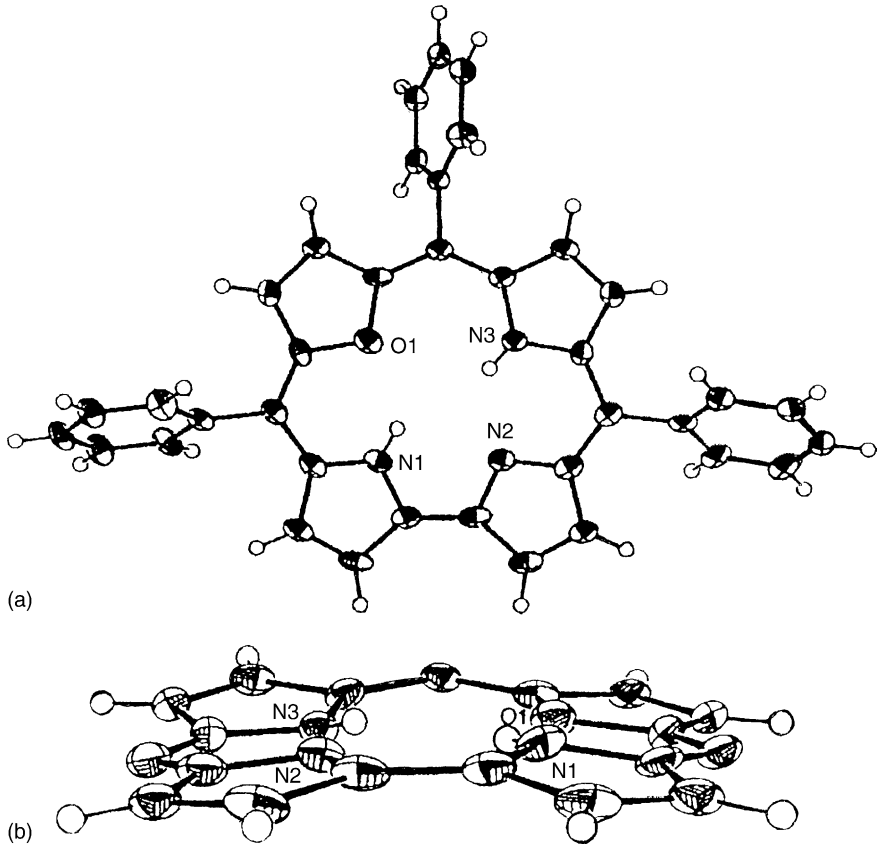

Fig. 15. X-ray structure of **143** (a) top view and (b) side view (reproduced with permission from Ref. [109]).

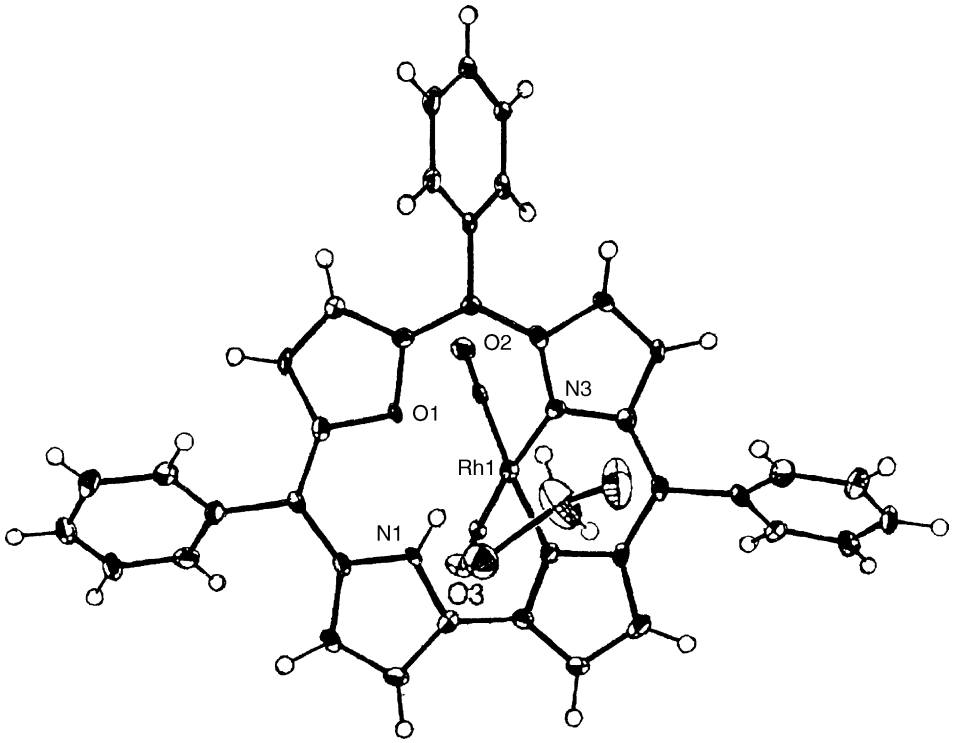

Fig. 16. X-ray structure of Rh(I)**143** (reproduced with permission from Ref. [109]).

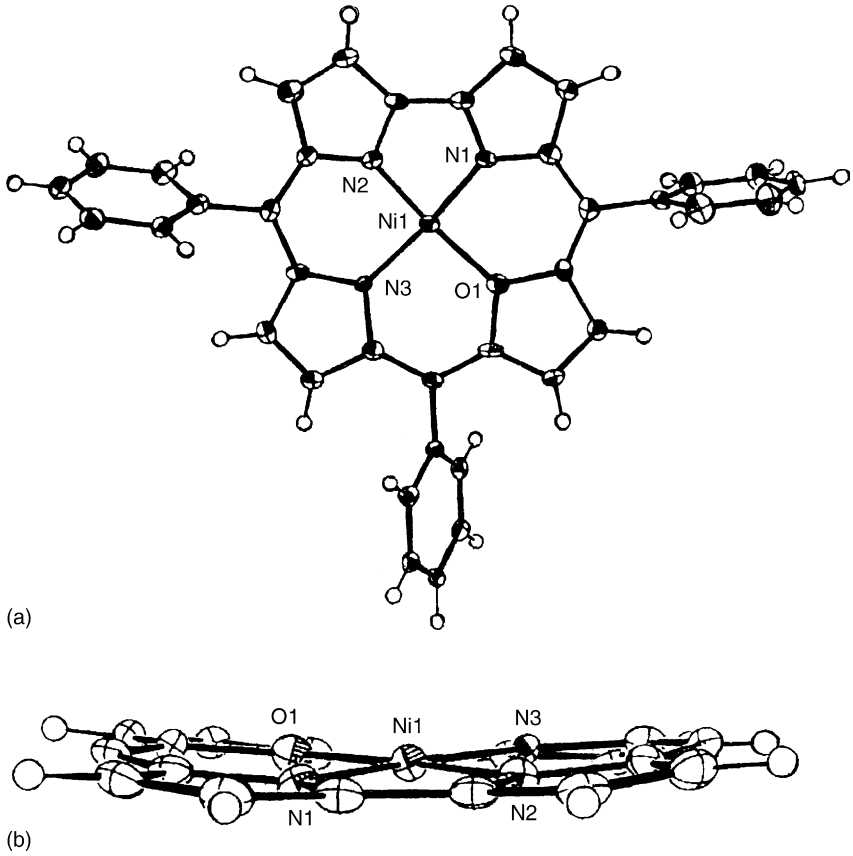

Fig. 17. X-ray structure of Ni(II)**143** (a) top view and (b) side view (reproduced with permission from Ref. [109]).

The absorption spectra of metal derivatives showed the characteristic Soret type and *Q*-type bands in the 400–700 nm region. The presence of inner NH ($\delta = -1.15$) in NMR of **Rh(I)143** supported the coordination of Rh(I) ion to only two nitrogen atoms. The NMR studies also showed the diamagnetic nature of **Ni(II)143** which was in contrast with paramagnetic Ni(II) derivative of **2** [9]. Electrochemical studies on **143** and its metal complexes indicated that **143** and its metal complexes were easier to oxidize and harder to reduce compared with the corresponding porphyrin derivatives. Surprisingly, the metal derivatives of **143** did not show their characteristic metal reductions unlike corresponding metalloporphyrins [2].

Chandrashekar and co-workers further extended their work on 21-oxacorroles and synthesized 21-oxacorroles with one *meso*-free carbon **144** by three different routes [110,111]. The "3 + 1" condensation of **32** with 2-pyrrole carboxaldehyde in the presence of trifluoroacetic acid in CH_2Cl_2 followed by oxidation with *p*-chloranil (Scheme 25) gave the 21-oxacorroles with one *meso*-free carbon in 9–15% yield depending on the concentration of acid catalyst used (Scheme 25a). Alternately, **144** was also prepared in 13–15% yield by condensing **32** with pyrrole and *para*-formaldehyde or formalin in the presence of 0.5 equivalent of TFA followed by oxidation with *p*-chloranil (Scheme 25b). The 21-oxacorrole **144** was also prepared by condensing **32** with 2-(hydroxyphenylmethyl)pyrrole under the same acid catalyzed conditions (Scheme 25c). In all three methods, both condensation and oxidative coupling reactions

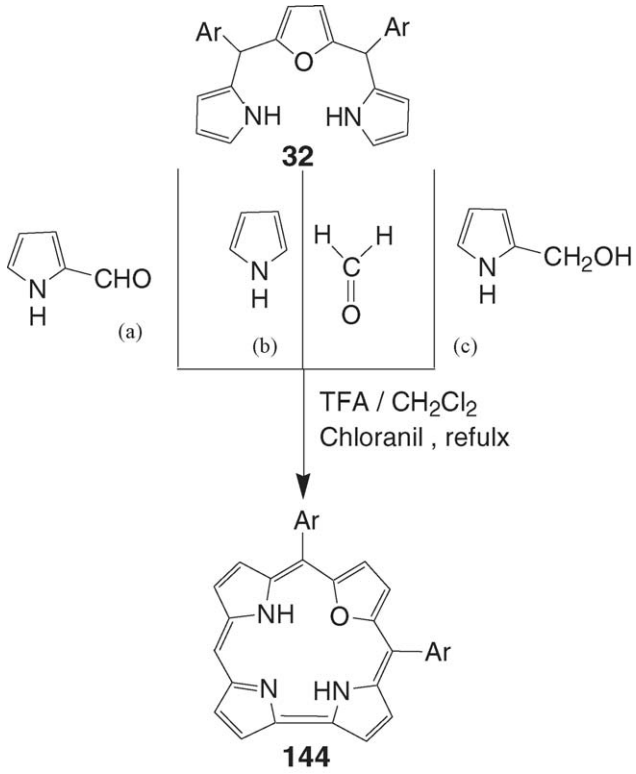

Scheme 25. Synthesis of mono *meso*-unsubstituted 21-oxacorrole.

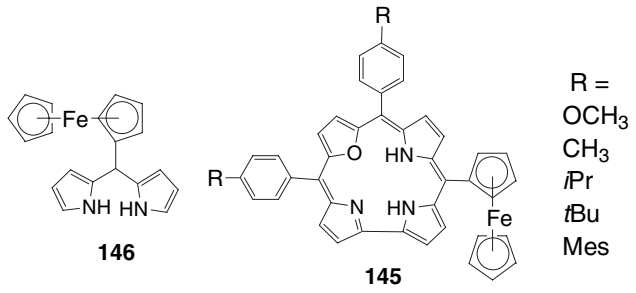

Chart 13. *meso*-Ferrocenyl dipyrromethane and ferrocenyl -21-oxacorrole conjugates.

takes place simultaneously. Chandrashekar and co-workers used the same strategy and synthesized the ferrocenyl-oxacorrole conjugates **145** (Chart 13) by condensation of the *meso*-ferrocenyl dipyrromethane **146** with various *para*-substituted 5,10-diphenyl-16-oxatripyrranes **32** under acid catalyzed conditions [112].

The electronic spectra of **145** showed that the ferrocene substitution at the *meso*-position resulted in the shift of both the Soret and *Q*-bands relative to oxacorrole **143** indicating the presence of a strong electronic interaction between the ferrocene moiety and the oxacorrole π-system [112]. Electrochemical studies of **145** showed three quasi-reversible oxidations (ΔE_p = 70–130 mV) of which one was based on the ferrocene and the other two were on the corrole ring. The corrole ring oxidations in **145** were shifted to more positive potentials compared with **143**, which was attributed to the combined effect of electronic coupling between the corrole π-system and the ferrocene moiety as well as the non-planarity of the corrole ring. The corrole ring reductions in **145** were shifted towards less negative potentials compared with **143** due to the electron deficient nature of corrole ring in **145** [112].

Cho and Lee [113,114] adopted a "2 + 2" methodology of acid catalyzed condensation of two different regio-isomers of furylpyrromethane alcohols **147** and **148** with dipyrromethane **25b** and synthesized 21-oxacorrole **143** and 22-oxacorrole **149**, respectively, bearing an oxygen atom at the designated site (Scheme 26). The absorption spectra of **143** and **149** have dis-

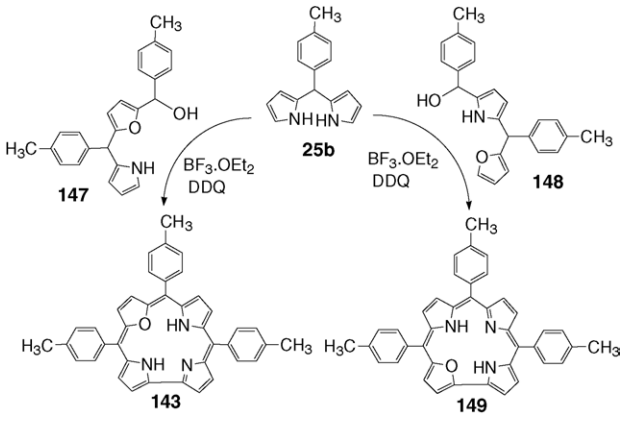

Scheme 26. Synthesis of 21-oxacorrole and 22-oxacorrole by 2 + 2 condensation.

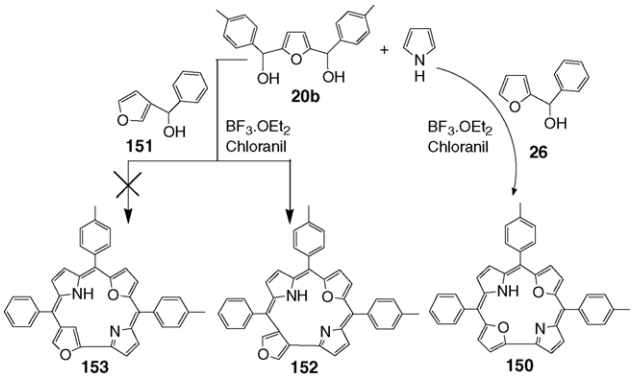

Scheme 27. Synthesis of 21,23-dioxacorrole and its inverted isomers.

tinct features [114]. The Soret and *Q*-bands of **143** were more red shifted compared with **149**. The blue shifted absorption bands of **149** indicated that it was less flexible and more resonance stabilized than **143**. The ^{1}H NMR spectroscopic analysis was also in agreement with this assumption. The β-pyrrolic protons and inner NH protons in ^{1}H NMR of **149** were shifted more downfield and upfield, respectively, compared with the corresponding protons of **143** supporting the view that **149** was more resonance stabilized.

Latos-Grażyński and co-workers [115] reported the synthesis 21,23-dioxacorrole **150** in 8% yield by condensing **20**, **26** and pyrrole under acid catalyzed conditions (Scheme 27). The use of **26** was essential for the creation of direct pyrrole-furan α–α bond to form **150**. The UV–visible spectrum of **150** showed a corrole-like spectrum with split Soret band (397 and 422 nm) and a series of *Q*-bands in the 480–640 nm region [115]. The ^{1}H NMR spectrum of **150** confirmed the aromaticity of the corrole with a characteristic downfield positions of furan and pyrrole resonances and upfield position of inner NH resonance. The temperature dependent NMR studies indicated the existence of two tautomers protonated alternatively on two nitrogen atoms. The crystal structure analysis [115] of the cation of **150** which was complexed to $ZnCl_4^{2-}$ anion showed that $ZnCl_4^{2-}$ anion was located in the clam-shell like cavity formed by two cations of **150** (Fig. 18). In the structure of cation **150** the dihedral angle between the two corrole cation planes equals 61.5. The C_α–C_β and the C_β–C_β distances were longer and shorter, respectively, in the corrole macrocycle than in free furan indicated the π-delocalization the furan ring was altered in **150**. The nickel(II) complex of **150** is high spin (paramagnetic) and five coordinate [115] unlike the Ni(II) complex of **143** which was diamagnetic [109].They have also synthesized the non-aromatic isomer of **150** with a protruding furan ring **152** by condensing 3-phenylhydroxymethylfuran **151** in place of **26** with **20** and pyrrole under similar reaction conditions (Scheme 27) [115]. In this reaction, instead of the expected isomer **153**, the isomer with protruding furan ring **152** was formed because the condensation took place only at the sterically hindered β-position and not at the expected α-position The UV–visible and ^{1}H NMR spectra confirmed the non-aromatic nature of the macrocycle. The crystal structure of protonated species (**152**-H)Cl (Fig. 19) showed that the macrocycle was

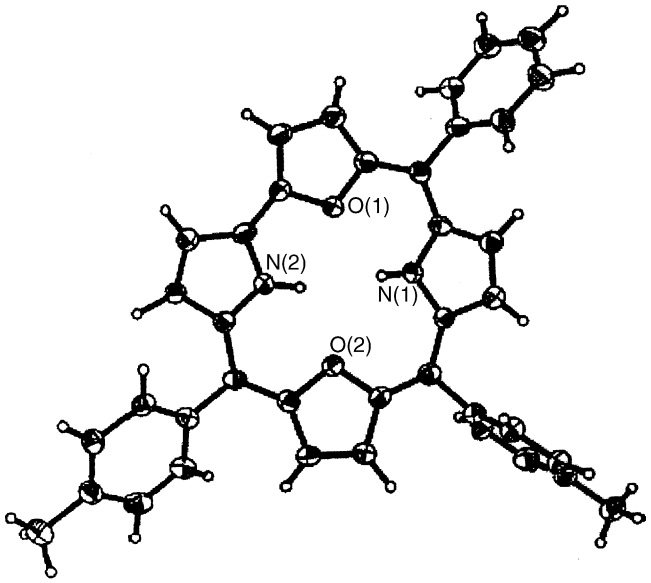

Fig. 18. X-ray structure of **150**, top view (reproduced with permission from Ref. [115]).

strongly puckered [115]. The chloride anion was located over the centre of the macrocycle and was involved in two intramolecular NH···Cl and two intermolecular (C)H···Cl interactions. The protruded furan ring preserved all features of the isolated furan and bond lengths were identical to that of free furan. However, the bond lengths of the second furan moiety were altered indicating appreciable π-delocalization in the second furan ring [115].

9.2. Heterocarbaporphyrins

Carbaporphinoids, which are porphyrin analogues where one or more of the pyrrole units have been replaced by carbocyclic rings received much attention in the mid 1990s. Lash carried out extensive work on carbaporphyrins and explored their unusual physico-chemical properties [116–120]. The carbaporphyrins were mainly synthesized through a [3 + 1] acid catalyzed MacDonald type condensation reaction of appropriate precursors. Lash and co-workers have shown that these carbaporphyrins form very interesting stable organometallic derivatives with a range of metals, such as Pd(II), Pt(II) and Ag(III) to name a few [121–129]. The chemistry of carbaporphyrins has been reviewed recently by Lash in "The Porphyrin Handbook" [130]. The first examples of carbaporphyrins containing heteroatoms, such as S and O in addition to pyrrole nitrogen atoms were synthesized [131] by following their well established 3 + 1 synthetic strategy used for the synthesis of the aza carbaporphyrins [130]. They attempted to synthesize the thia azuliporphyrin **154**, selena azuliporphyrin **155** and oxa azuliporphyrin **156** using a novel tripyrrane **157** (Scheme 28) [131,132].

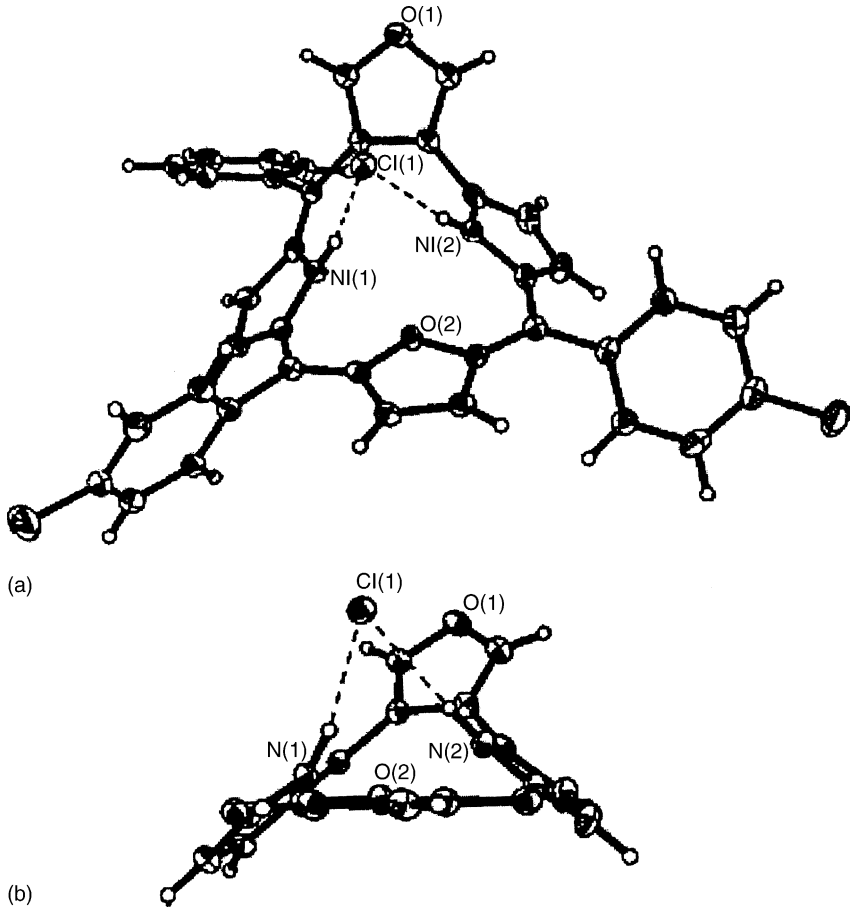

Fig. 19. X-ray structure of (**152**-H)Cl. (a) Top view and (b) side view (reproduced with permission from Ref. [115]).

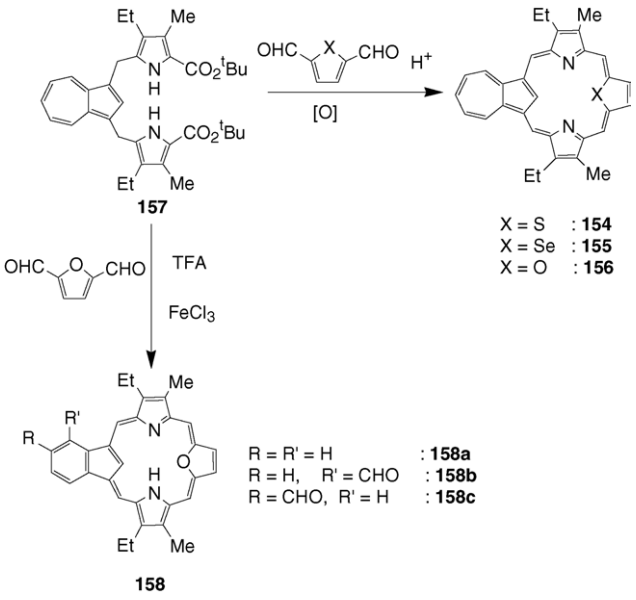

Scheme 28. Synthesis of hetero azuliporphyrins.

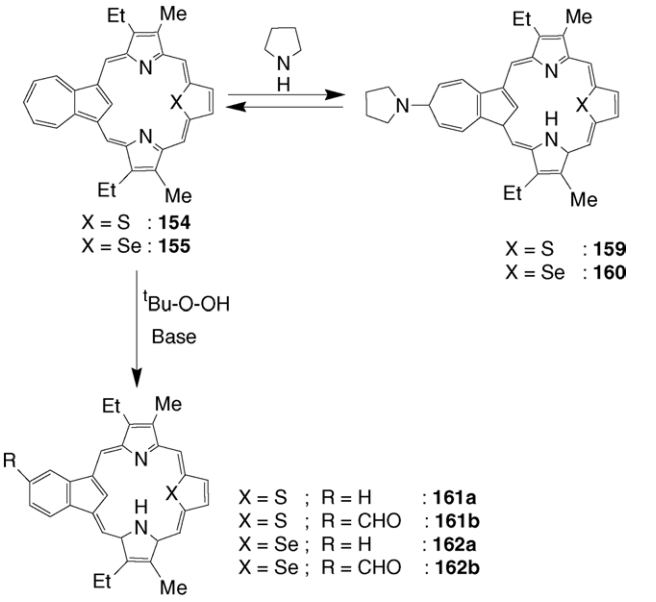

Scheme 29. Reactivity of hetero azuliporphyrins in the presence of pyrrolidine and alkaline ^{t}BuOOH.

The tripyrrane **157** was condensed with 2,5-diformylthiophene in the presence of TFA followed by oxidation with 0.1 aqueous $FeCl_3$ solution of yielded the thia azuliporphyrin **154** in 45% yield (Scheme 28). Similarly, the condensation of **157** with 2,5-diformylselenophene under the same reaction conditions gave selena azuliporphyrin **155** in 27% yield. Interestingly, the condensation of tripyrrane **157** with 2,5-diformylfuran did not give the expected oxaazuliporphyrin **156** but gave a mixture of three fully aromatic oxacarbaporphyrins **158a**–**c** in a combined yield of 15% (Scheme 28). The compounds **158a**–**c** were formed due to ring contraction of the seven-membered ring as observed previously for related aza analogues [133].

The free base forms of thia- **154** and selenaazuliporphyrins **155** exhibited borderline aromatic properties that was enhanced on protonation as confirmed by detailed UV–visible and NMR studies. The azuliporphyrins were susceptible to nucleophilic attack to give carbaporphyrin adducts because of the electron deficient cycloheptatriene ring [133]. The thia- and selena azuliporphyrins **154** and **155** also showed similar reactivity [132]. On addition of pyrrolidine to **154** and **155** gave their corresponding pyrrolidine adducts **159** and **160**, respectively (Scheme 29). However, the hetero azuliporphyrins **154** and **155** requires more pyrrolidine as compared to the aza analogue to form pyrrolidine adducts. This was attributed to the larger size of sulfur and selenium atoms, which reduces the favorability of pyrrolidine adducts by decreasing the planarity of the macrocyclic core. The reactivity of **154** and **155** was further explored with alkaline solutions of *tert*-butyl hydroperoxide [132]. **154**, upon treatment with *t*-BuOOH in the presence of KOH gave thiacarbaporphyrin **161a** in 10% yield. However, when **154** was treated with *t*-BuOOH in the presence of *t*-BuOK, an inseparable mixture of **161a** and **161b** was formed in 50% yield (Scheme 29). Similarly, **155** on treatment with *t*-BuOK gave **162a** in 10% yield and when treated with KOH gave two major products **162a** and **162b**, which were separated by flash column chromatography.

The UV–visible and NMR studies of the carbaporphyrins **161** and **162** clearly showed that these hetero carbaporphyrins like aza carbaporphyrins are completely aromatic.

Chandrashekar and co-workers [134] also synthesized the thia- **163** and selenaazuliporphyrins and **164** by following the "3 + 1" strategy used by Lash [130] to synthesize several aza carbaporphyrins. The thia- and selenaazuliporphyrins **163** and **164** were prepared by acid catalyzed condensation of **33** and **34**, respectively, with azulene-1,3-dicarboxaldehyde in dichloromethane followed by DDQ oxidation [134] (Scheme 30). They also observed borderline aromaticity for these hetero azuliporphyrins in free base form and enhanced aromatic behaviour in their protonated form using absorption and NMR studies.

The X-ray structure solved for **163** indicated that the molecule was completely planar and azuline moiety was in the plane defined by four *meso*-carbon atoms [134] (Fig. 20). The aromatic nature was evident from the smaller C_β–C_β distances than C_α–C_β distances of pyrroles and thiophene in macrocycle **163**. There was a strong intramolecular C–H···S hydrogen bonding {bond distance 2.53(1) Å, bond angle 177.00(18)°} interaction present inside the azuliporphyrin cavity. The interesting aspect of the structure was the observation of non-classical hydrogen bonding interactions, such as C–H···π interactions between one of the β-hydrogen atoms of the pyrrole ring and the π-cloud of the *meso*-mesityl ring [C–H distance 0.950(2) Å, H···π distance 2.79(1) Å, C–H···π angle 137.10(12)°]. These C–H···π interactions helped in the formation of a one dimensional zigzag polymeric supramolecular array where the two adjacent porphyrin rings were aligned perpendicular to each other [134].

Although Lash and co-workers reported rich coordination chemistry for aza azuliporphyrins [123,126] and showed that the azuliporphyrins form very interesting organometallic derivatives with various metals, such as Ni(II), Pd(II), Pt(II) and Ag(III),

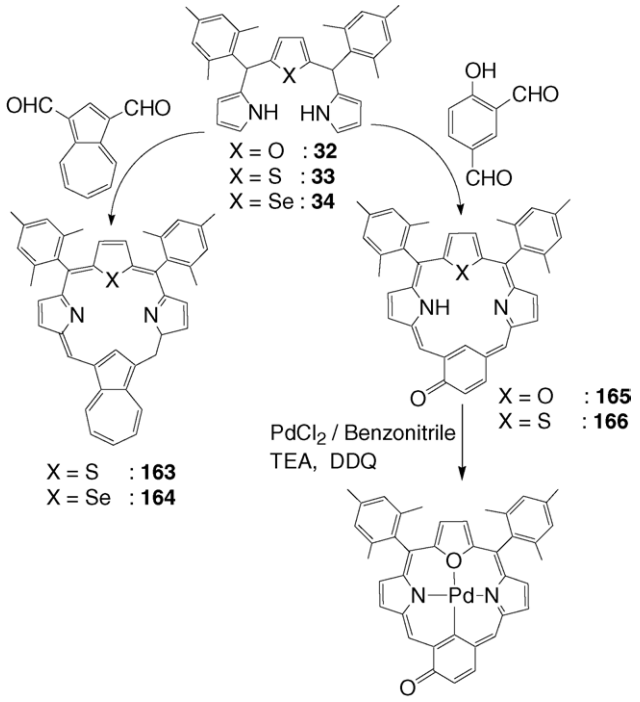

Scheme 30. Synthesis of hetero analogues of oxybenzi and azuliporhyrins.

there have been no reports on metallation studies of hetero analogues of azuliporphyrins.

Chandrashekar and co-workers also synthesized the hetero analogues of benziporphyrins [135] by following Lash's synthetic strategy of carbaporphyrins [130]. The oxa and thia derivatives of oxybenziporphyrins **165** and **166** were synthesized by "3 + 1" acid catalyzed condensation of 5-formyl salicylaldehyde with corresponding modified tripyrranes **32** and **33**, respectively (Scheme 30). In ^{1}H NMR, the upfield shifts of the inner CH and NH protons of **165** (−3.5 and −4.7 ppm) and **166** (−4.32 and −2.90 ppm) supported the aromatic nature of the macrocycles. The absorption spectra of **165** and **166** showed strong Soret type bands in 430–480 region and multiple *Q*-bands in the 500–750 region because of the porphyrinoid nature of the compounds. These observations were in line with the earlier observations made on aza carbaporphyrins The aza oxybenziporphyrin forms an organometallic complex with Pd(II) [6]. Chandrashekar and co-workers also successfully synthesized an organometallic palladium derivative of **165** and the spectroscopic data indicated the retention of aromatic character of porphyrin on metal insertion [135].

Lash and co-workers by following their well established strategy synthesized a series of β-substituted and *meso*-unsubstituted S and O containing oxybenziporphyrins **167**, **168**, oxypyriporphyrins **169**, **170** and benzocarbaporphyrins **171**, **172** [136,137] by condensing the appropriate modified β-substituted tripyrranes **173** and **174** with 5-formylsalicylaldehyde, 3-hydroxy-2,6-pyridinedicarboxaldehyde and indene-1,3-dicarboxaldehyde in dichloromethane in the presence of trifluoroacetic acid followed by oxidation with DDQ (Scheme 31). UV–visible spectra of all hetero carbaporphyrinoids showed strong Soret bands and their ^{1}H NMR exhibited large diatropic ring currents similar to their corresponding aza analogues, supported their aromatic nature. This kind of carbaporphyrin was known to form novel organometallic complexes. The organometallic Ni(II), Pd(II) and Pt(II) complexes of **171** were prepared and the studies indicated that all three complexes retained their aromatic character [136,137]. The X-ray structure solved for Pd(II) complex of **171** [137] exhibited a planar macrocycle with dihedral angles of the component pyrrole, furan and indene rings all $\leq 2.1^\circ$ relative to mean [18]annulene plane were (Fig. 21).

Recently, Miyake and Lash reported the synthesis of a new class of heteroatom substituted benziporphyrins [138] using a

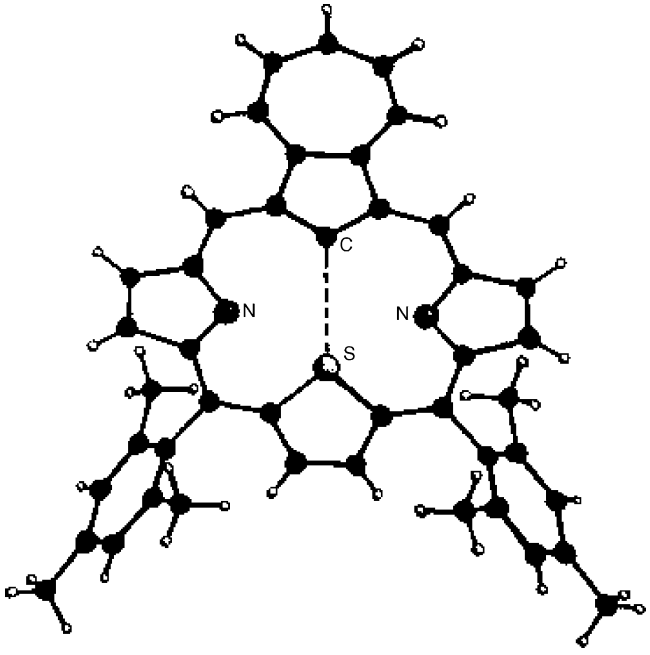

Fig. 20. X-ray structure of **163** (reproduced with permission from Ref. [134]).

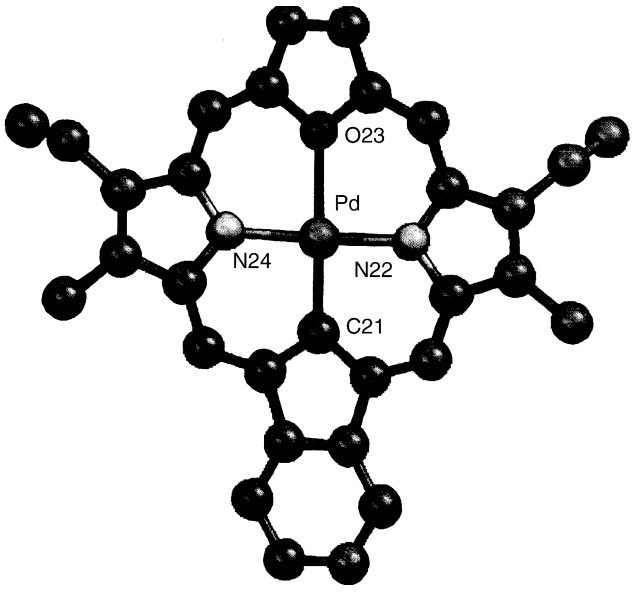

Fig. 21. X-ray structure of **Pd(II)171**, top view (reproduced with permission from Ref. [137]).

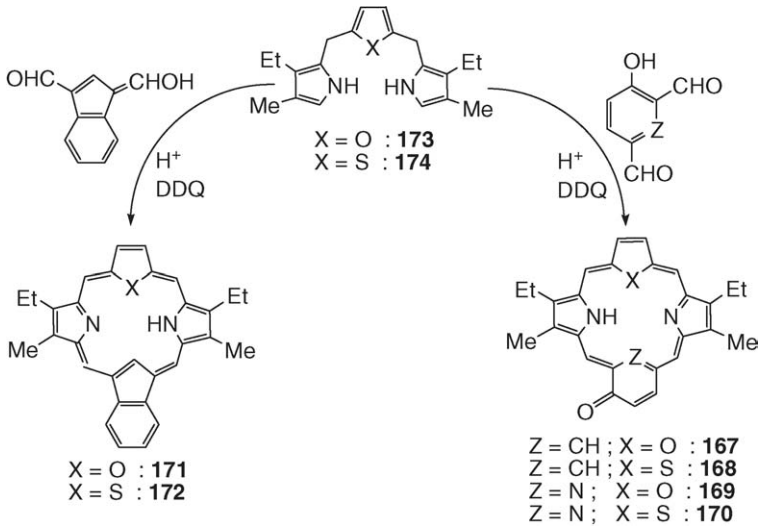

Scheme 31. Synthesis of hetero analogues of oxybenzi, oxypyri and benzocarbaporphyrins.

novel tripyrranes **175a**,**b** which was synthesized by acid catalyzed condensation of resorcinol or 2-methyl resorcinol with two equivalents of an acetoxymethyl pyrrole. Condensation of **175a** with 2,5-diformylthiophene or 2,5-diformylfuran in the presence of TFA followed by oxidation with dilute aqueous $FeCl_3$ solution gave the corresponding porphyrinoids **176** and **177**, respectively (Scheme 32). These porphyrinoids were not characterized due to insolubility. However, when they condensed **175b** with 2,5-diformylthiophene under similar reaction conditions there resulted a mixture of **178** and **180**. The crude mixture of **178** and **180** was further oxidized with $PhI(OCOCF_3)_2$ and afforded **180** in 20% yield (Scheme 32). Similarly, the condensation of **175b** with 2,5-diformylfuran gave a mixture of **179** and **181**, which upon oxidation under similar conditions gave **181** in 6% yield (Scheme 32). The NMR studies indicated that the porphyrinoids **180** and **181** were fully aromatic [138]. Metal derivatives of these novel porphyrinoids are not yet known.

9.3. Heterotetrabenzoporphyrins

The first examples of tetrabenzoporphyrins with N_3S, N_2S_2 and N_2SO cores **182**–**184** were reported recently by Ono and co-workers [139]. In the first step, the bicyclo[2.2.2]octadecane (BCOD) fused porphyrins **185**–**187** were synthesized by the TFA catalyzed condensation of BCOD-fused 16-thiatripyrrane **188** with corresponding BCOD-fused pyrrole, thiophene and furan dialdehydes **189**, **190** and **191**, in CH_2Cl_2 followed by oxidation with DDQ (Scheme 33). The BCOD-fused porphyrins with N_3S **185**, N_2S_2 **186** and N_2SO **187** cores were obtained as a mixture of diastereomers in 42, 37 and 23% yields, respectively. The BCOD-fused porphyrins **185**, **186** and **187** were heated at 230 °C under vacuuo for 30 min and afforded the heterotetrabenzoporphyrins **182**, **183** and **184** respectively as dark green solids in nearly quantitative yields.

The absorption spectra of heterotetrabenzoporphyrins unlike their corresponding porphyrin analogues showed split Soret bands [139] (Table 5). Furthermore, the longest wavelength *Q*-band in **182**–**184** was more bathochromically shifted and very intense compared to their corresponding core-modified porphyrins (Table 5). The fluorescence spectra of **182**–**184** were also red-shifted with greater quantum yield compared to their corresponding core-modified porphyrins (Table 5).

9.4. Heterochlorins

The first examples of chlorin and bacteriochlorin with an N_2S_2 core were reported recently by Bruckner and co-workers

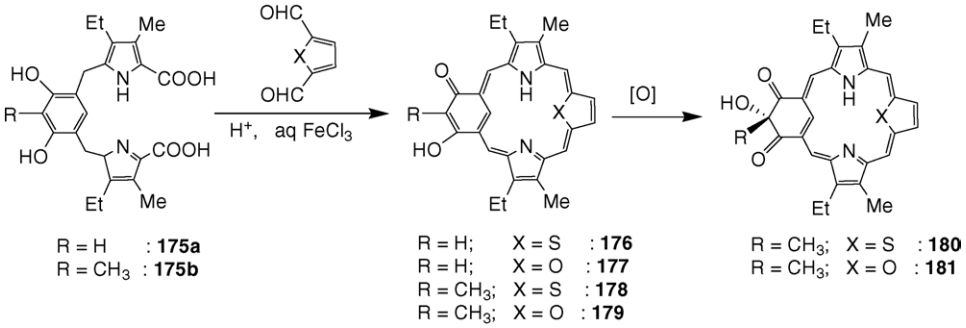

Scheme 32. Synthesis of hetero benziporphyrins.

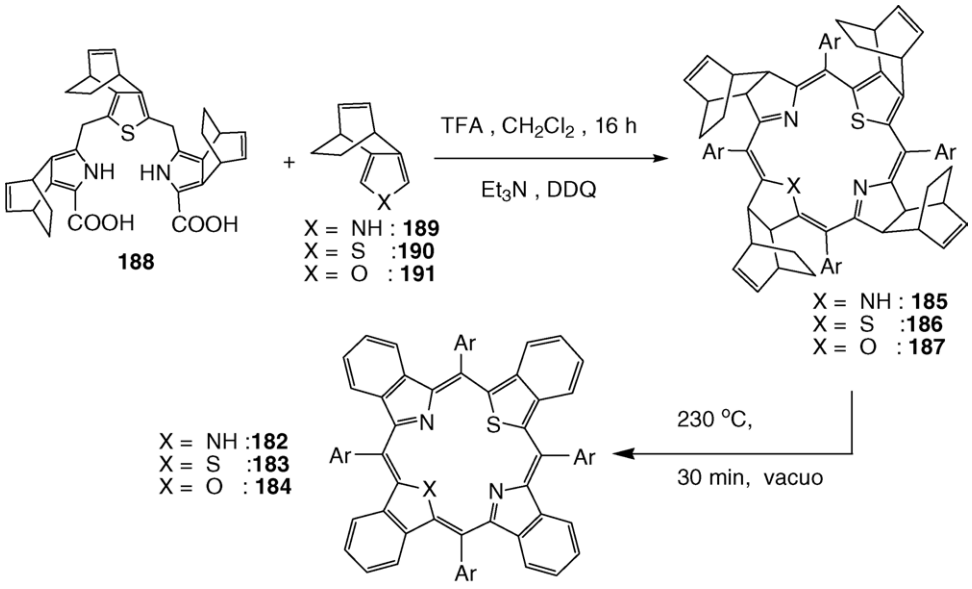

Scheme 33. Synthesis of heterotetrabenzoporphyrins.

[140]. The **7a** or **7b** were treated with 1.2 equivalents of OsO_4 in $CHCl_3$/pyridine for 24 h followed by quenching with H_2S and column chromatographic purification gave chlorin **192** as a major product (20%) and an isomeric mixture of two bacteriochlorins **193** as minor products (<5%) (Scheme 34). ^{1}H NMR spectroscopy confirmed that OsO_4 only reacts with double bonds of the pyrrole(s) to yield **192** and **193**. **192** when treated with an aqueous solution of $KMnO_4$ in the presence of 18-crown-6, underwent oxidative ring opening reaction and formed the dithiaporpholactone **194**.

The UV–visible spectra of **192** showed a broadened Soret band and the longest wavelength absorption band (λ_{max} = 687 nm) was only minimally more intense and surprisingly little blue shifted when compared to the porphyrin **7** (λ_{max} = 699 nm). The UV–visible spectra of both the isomers of **193** were identical and showed the typical three band pattern of the bacteriochlorin chromophore. The absorption bands of **193** were significantly red shifted (λ_{max} = 734 nm) when compared to the porphyrin **7** [140].

Table 5
Selected absorption and emission data of core-modified tetrabenzoporphyrins and their corresponding core-modified porphyrins

Compound	Soret bands, λ_{abs} (nm)	*Q*-band, λ_{abs} (nm)	Emission	
			λ_{em} (nm)	ϕ_f
2[a]	428	680	685	0.016
182[b]	394, 423, 442	692	693	0.053
7[a]	435	699	706	0.007
183[b]	399, 429, 449	718	718	0.013
9[a]	428	707	713	0.005
184[b]	394, 421, 444	714	714	0.018

[a] CH_2Cl_2.
[b] DMF.

9.5. Heteroatom substituted confused porphyrins

N-confused porphyrins, a group of porphyrin isomers that have an inverted pyrrole sub-unit were independently isolated and characterized by Furuta et al. in Japan [141] and Latos-Grażyński and co-workers in Poland [142] in 1994. Since N-confused porphyrins have the presence of inner CH, external and internal nitrogen atoms, these porphyrins exhibited very interesting metal coordination properties, such as being organometallic in nature, exhibiting multivalency and formation of inner and outer coordination complexes and supramolecular structures [143–153]. Thus, the N-confused porphyrins have been explored to synthesize metal complexes in various oxidation states, such as Ni(II), Pd(II), Ag(III), Sb(V), Cu(II), Fe(II), Rh(I) and Zn(II) [154]. Furthermore, Furuta et al. recently synthesized unique N-fused porphyrins [155,156] and *cis*-doubly N-confused porphyrins [157–159] and studied their metal bonding properties [160]. Recently, some confused heteroporphyrins have appeared. In heteroporphyrins, the confusion can occur with the pyrrole ring or with the other heterocycle, such as thiophene, furan, selenophene and tellurophene of porphyrin macrocycle. Thus, these porphyrins were sub-classified into N-confused heteroporphyrins and heteroatom confused heteroporphyrins.

9.5.1. N-confused heteroporphyrins

Lee and Kim [161–163] synthesized the first N-confused 21-thiaporphyrin **195** and 21-oxaporphyrin **196** by 3 + 1 condensation of 2,4-bis(α-hydroxy-α-phenylmethyl)pyrrole or its *N*-alkyl derivative **197** with modified tripyrrane **33** and **32** respectively under mild acidic conditions (Scheme 35). In **195** and **196**, the confused pyrrole was in the position *trans* to the thiophene and furan rings, respectively. Chandrashekar and co-workers [164] synthesized, by using different precursors, the N-confused 21-selenaporphyrin **198** in addition to the **195** and **196** having a

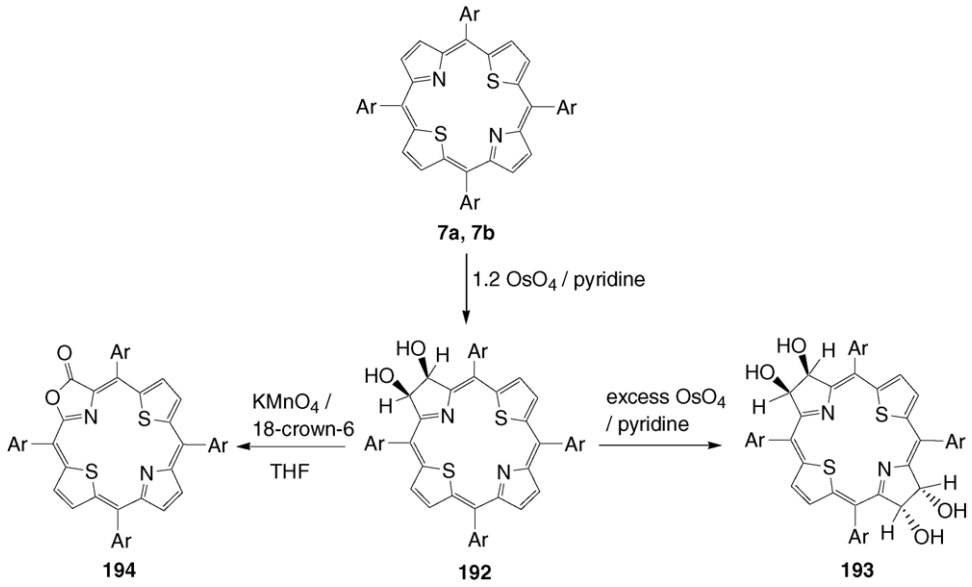

Scheme 34. Synthesis of dithia analogues of chlorin, bacteriochlorin and porpholactone.

confused pyrrole opposite to the heteroatoms. The tripyrrane containing the middle N-confused pyrrole ring **199** was condensed with the corresponding diol **21**, **20** and **22** under standard conditions and afforded **195**, **196** and **198**, respectively, in 19–32% yields (Scheme 36a). The advantage of Chandrashekar and co-workers strategy of using **199** as a synthon resulted in the exclusive formation of the desired N-confused heteroporphyrins in high yields with only a trace amount of normal porphyrin making their column separation very easy.

Latos-Grażyński and co-workers [165] synthesized N-confused 21-selenaporphyrin **200** in which the confused pyrrole ring was adjacent to the selenophene ring unlike **198** in which the confused pyrrole was opposite to the selenophene ring. The compound **200** was obtained as a side product in 1% yield along with the expected 21-selenaporphyrin **4** in 19% yield in a typical acid catalyzed condensation of **22** with **24** (Scheme 36b). Similarly they [166] also obtained the N-confused 21,23-dithiaporphyrin **201** as one of the products in 4.7% yield by acid catalyzed condensation of **21** with pyrrole (Scheme 36c).

A detailed NMR studies has been carried out on free base and protonated forms of N-confused heteroporphyrins at different temperatures to identify the tautomers. Lee et al. [162] proposed the existence of three different tautomeric forms of N-confused porphyrins **195a** and **196a** depending on the location of the inner NH proton. (Chart 14). In tautomers **I** and **II**, the hydrogen was located on either of the inner pyrrole nitrogen atoms whereas in tautomer **III**, the proton was located on the nitrogen of the N-confused ring. The tautomer **I** was the only stable form for 21-oxaporphyrin **196a**. However, studies on 21-thiaporphyrin **195a** suggested that tautomer **III** was the major and tautomer **I** was the minor isomer at room temperature. Furthermore, studies at 223 K suggested that **195a** existed in all three tautomeric forms **I**, **II** and **III** in the ratio 1:0.5:1. Interestingly, the *N*-alkyl substituted N-confused porphyrins existed only as tautomer **III** because of the bulkiness of the alkyl group [163]. Density functional theory also supported the existence of different tautomeric forms for N-confused 21-thiaporpyrins [167].

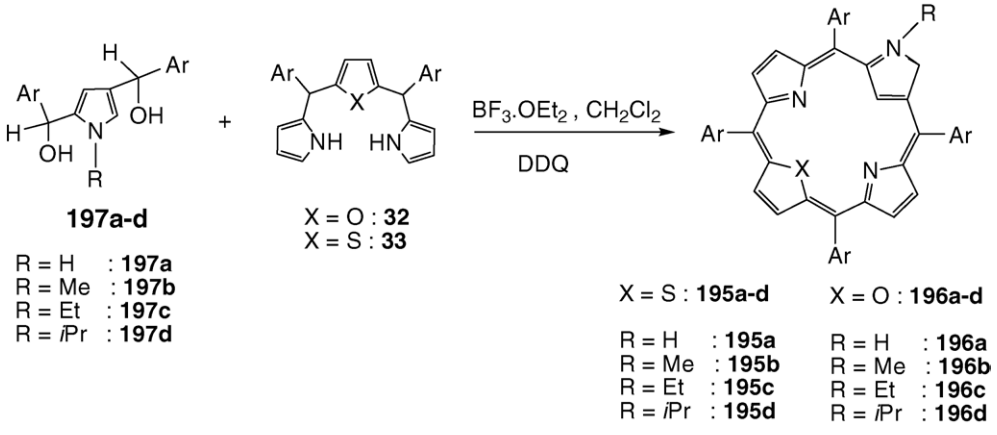

Scheme 35. Synthesis of N-confused 21-thiaporphyrins and 21-oxaporphyrins.

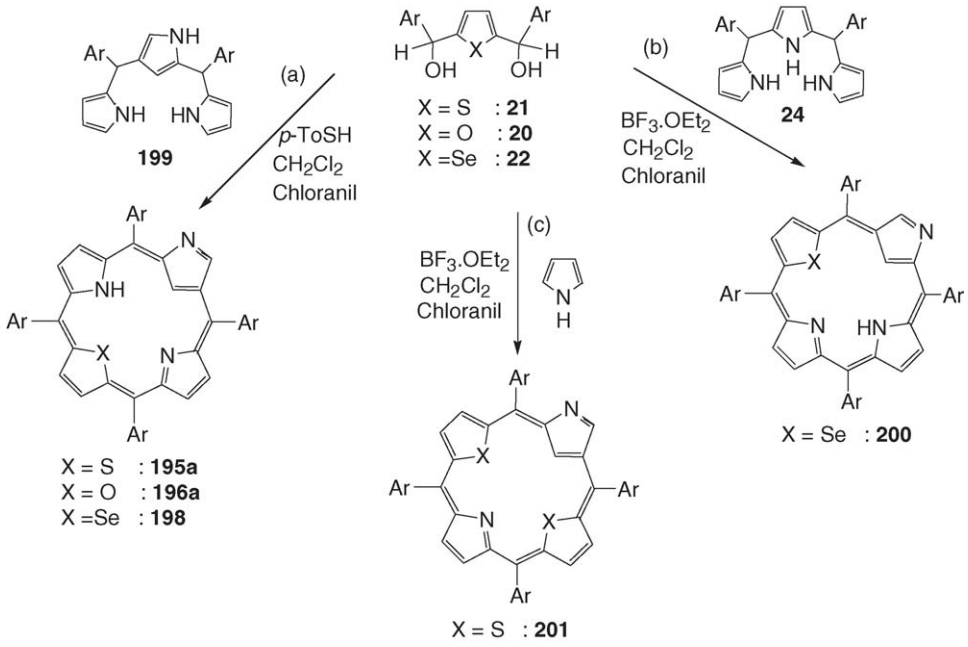

Scheme 36. Different synthetic approaches for N-confused heteroporphyrins.

Detailed NMR studies were carried out by Chandrashekar and co-workers for N-confused porphyrins **195a**, **196a** and **198** [164]. They also observed a single dominant tautomer as in **I** for **196a**. Furthermore, their studies also confirmed the existence of three different tautomeric forms in equilibrium for **195a** at low temperature. However, they claimed that for **195a**, the tautomer **I** was the major component rather than tautomer **III** at room temperature based on NMR and X-ray structural studies [164]. In ^{1}H NMR, the observation of the inner NH signal in the shielded region and the outer NH signal in the deshielded region on careful titration of **195a** with TFA supported the tautomer form **I** was the dominant at room temperature. The X-ray structure shows formation of a cyclophane dimer in the unit cell because of the presence of strong hydrogen bonding interaction between the inner NH of one molecule and the outer nitrogen of the other molecule; this may support the view that the predominant form of **195a** at room temperature is tautomer **I**.

Latos-Grażyński and co-workers [165] also proposed the existence of the three tautomers **IV**, **V** and **VI** for N-confused 21-selenaporphyrin **200** in which the N-confused pyrrole was adjacent to the selenophene ring (Chart 15). NMR studies on **200** indicated that in pyridine-d_5, only tautomer **VI** was exclusively formed but in chloroform-d, the tautomers **V** and **VI** were formed in equilibrium.

The N-confused heteroporphyrins exhibited split Soret bands in the region 425–450 nm and *Q*-bands in the region 500–750 nm [162–166]. The presence of split Soret bands indicated the less planar character of N-confused heteroporphyrins relative to regular heteroporphyrins. The crystal structures of N-confused heteroporphyrins **195a** [164] and **200** [165] have been solved. The structure of **195a** shown in the Fig. 22 clearly indicated the non-planarity of the macrocycle in a ruffled conformation where the *meso*-carbons were formed alternately above and below the mean plane defined by four *meso*-carbon atoms. The non-planarity in **195a** was also clearly reflected in the dihedral angles of individual heterocyclic rings w.r.t. the mean plane defined by four *meso*-carbon atoms. The dihedral angles were 2.82(6)° for the thiophene ring, 21.11(9)° for the N-confused pyrrole ring and 15.77(9)° and 31.23(9)° for the two pyrrole rings, respectively, indicating that the N-confused pyrrole ring and one of the adjacent pyrrole ring showed the maximum deviation [164]. The presence of the large sulfur atom increased the repulsion between the inner NH and the sulfur atom resulting in the deviation of the pyrrole away from the mean plane. The

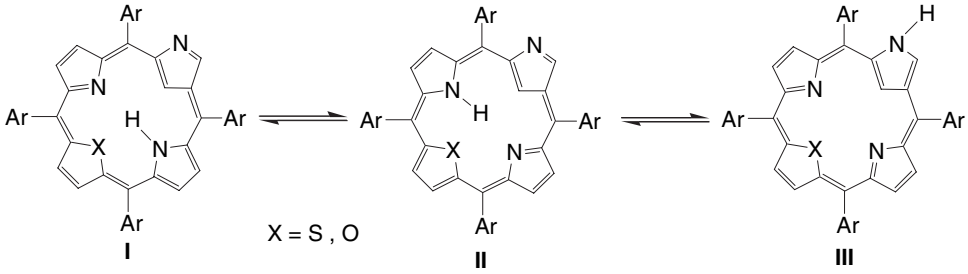

Chart 14. Proposed tautomeric forms of 21-heteroatom substituted N-confused porphyrins.

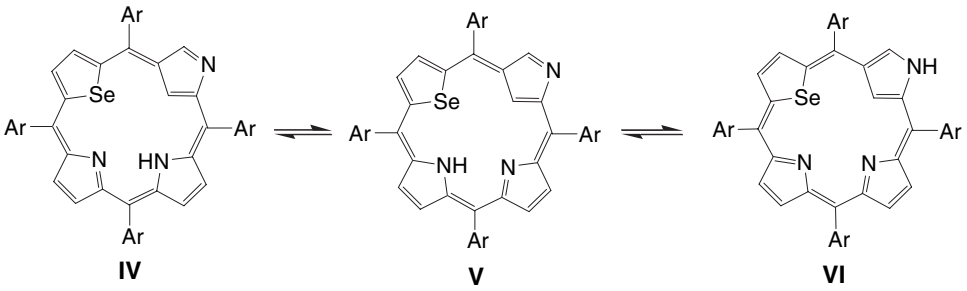

Chart 15. Different tautomeric forms of **200**.

alteration of π-delocalization in **195a** was evident in the significant changes in C_α–X, C_α–C_β and C_β–C_β distances relative to free thiophene and pyrrole units. The packing diagram of **195a** showed that the unit cell contained two molecules which were linked to each other through a non-covalent weak N–H···N and C–H···N intermolecular hydrogen bonds involving the pyrrole NH and N atom of the N-confused ring and C atom of pyrrole ring. These interactions lead to a cyclophane-like dimeric structure where the two N-confused rings were almost one above the other [164]. In addition, there were two intramolecular N–H···S hydrogen bonds and one C–H···S hydrogen bond in each molecule between N1–H, N3–H, pyrrole C13 and thiophene sulfur with an average distance of 2.74 and 3.45 Å for N–H···S and C–H···S hydrogen bonds, respectively. The X-ray structure of **200** (Fig. 23) exhibited saddle distortion [165]. The Se–C_α, C_α–C_β and C_β–C_β distances of **200** were similar

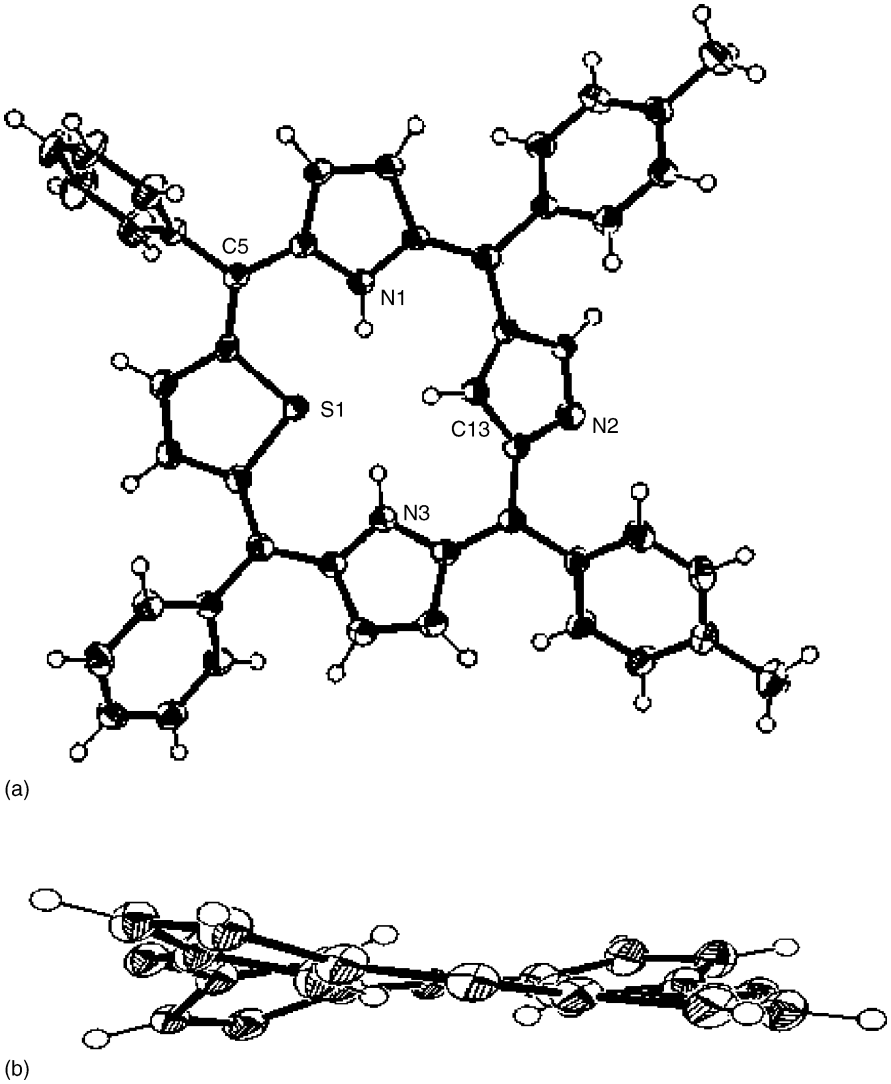

Fig. 22. X-ray structure of **195a**. (a) Top view and (b) side view (reproduced with permission from Ref. [164]).

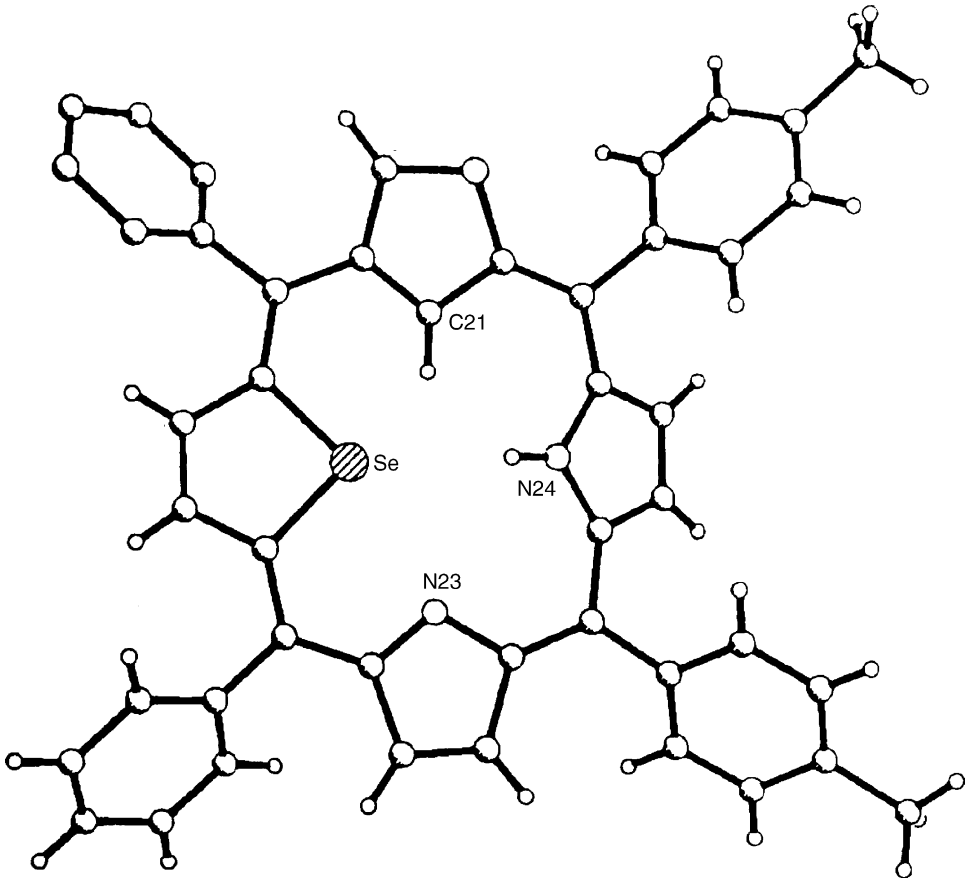

Fig. 23. X-ray structure of **200**, top view (reproduced with permission from Ref. [165]).

to those of **4** indicating the perseverance of aromatic character of the macrocycle, on inversion of one of the pyrrole ring in **200**.

9.5.2. Heteroatom confused heteroporphyrins

Latos-Grażyński and co-workers [168,169] prepared the first S-confused porphyrin **202** by condensing 2,4-bis(phenylhydroxymethyl) thiophene **203** with benzaldehyde and pyrrole via one pot two step reaction or by the [3 + 1] condensation of the **203** and 5,10-diphenyltripyrrane **24** (Scheme 37). The oxidation of **202** with DDQ or with an excess of *p*-chloranil gave a new compound **204**. The ^{1}H NMR study on **202** showed that the inner NH appeared as a singlet at 5.81 ppm and inner CH resonance of the inverted thiophene ring appeared at 4.76 ppm suggesting that this porphyrinoid exhibiting borderline aromaticity. However, an ^{1}H NMR study of **204** exhibited typical aromatic features with inner CH and two inner NH resonances appearing at −5.31, −3.37 and −2.93 ppm, respectively [168].

Pawlicki and Latos-Grażyński [170] attempted to synthesize the O-confused oxaporphyrin **205** by condensing 2,4-bis(phenylhydroxy methyl)furan **206** with *p*-tolylaldehyde and pyrrole in a 1:2:3 molar ratio under mild acid conditions (Scheme 38). However, this condensation did not yield the expected O-confused oxaporphyrin **205** but gave the pyrrole addition product **207** in 10% yield. The electronic absorption spectrum of **207** showed a strong Soret band and a set of four *Q*-bands like any other aromatic carbaporphyrinoids [170]. The aromatic nature and the ring current effects of the compound **207** were also evident in the upfield positions of the inner CH ($\delta = -5.11$ ppm) and inner NH protons ($\delta = -2.4$, -2.79 ppm). The macrocycle **207** can act as a dianionic or trianionic ligand and complexes metal ions to match the oxidation state of

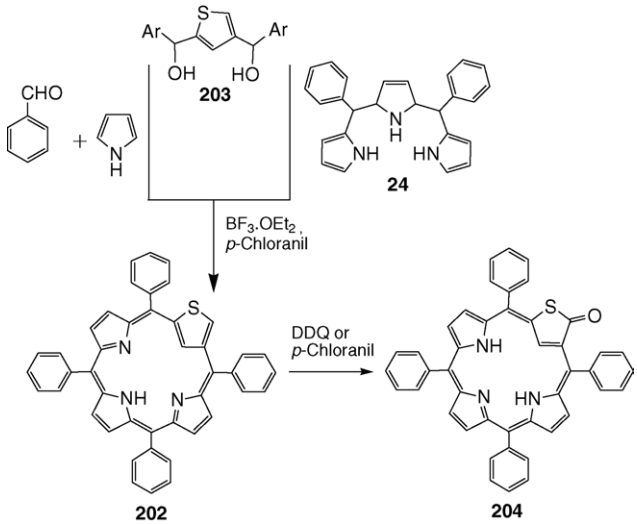

Scheme 37. Synthetic approaches for S-confused porphyrin.

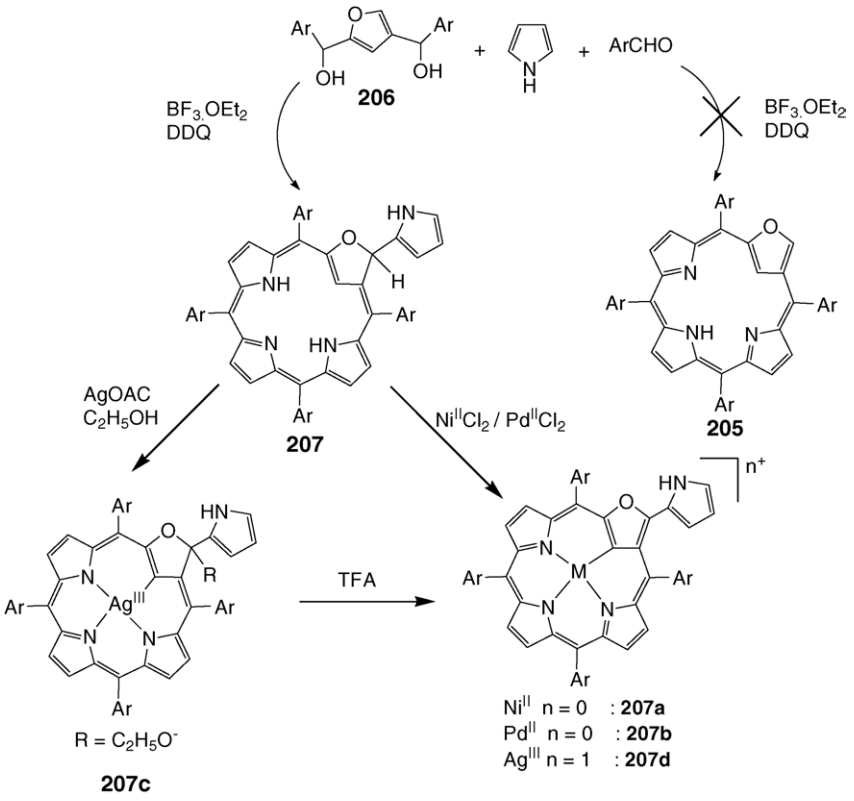

Scheme 38. Synthesis of pyrrole appended O-confused porphyrins.

metal ion. Thus, the Ni(II), Pd(II) and Ag(III) complexes of **207** were prepared under standard metallation conditions [170]. The insertion of Ni(II) and Pd(II) metal ions resulted in related dehydrogenated organometallic complexes **207a** and **207b**, respectively, in which the metal ions were coordinated to three pyrrolic nitrogen atoms and the trigonally hybridized C21 atom of the inverted furan [170]. The electronic spectra of **207a** and **207b** showed several Soret like bands and less intense *Q*-bands with low extinction coefficients compared with **207** indicating that the aromatic character of ligand **207** was lowered on metal complexation. Interestingly, the insertion of Ag(III) into **207** on treatment with silver acetate followed by addition of ethanol initially gave a stable Ag(III) complex **207c** which was substituted at the C3 position by the ethoxy and pyrrole moieties. However, when this macrocycle **207c** was treated with TFA it resulted in a new aromatic Ag(III) complex **207d** due to elimination of the ethoxy group. The compound **207d** was converted back to **207c** on treatment with sodium ethoxide in ethanol [170].

A set of canonical structures **VII**, **VIII** and **IX** was proposed for **207a**, **207b**, **207d** (Chart 16) to account for their non-aromatic and aromatic behavior [170]. The canonical structure **VII** was non-aromatic with less interaction between the macrocycle and appended pyrrole moiety. However, the structures **VIII** and **IX** were aromatic and the direct conjugation between the appended pyrrole fragment and the carbaporphyrinoid π-system was expected for **VIII** and **IX** structures. The electronic structures of **207a**, **207b**, **207d** (Chart 16) were a combination of aromatic and non-aromatic canonical structures and the most aromatic character observed for **207d** was due to the dominant contribution of canonical structures **VIII** and **IX** and relatively less aromatic nature noted for **207a** and **207b** was due to the major contribution from canonical structure **VII**. Support

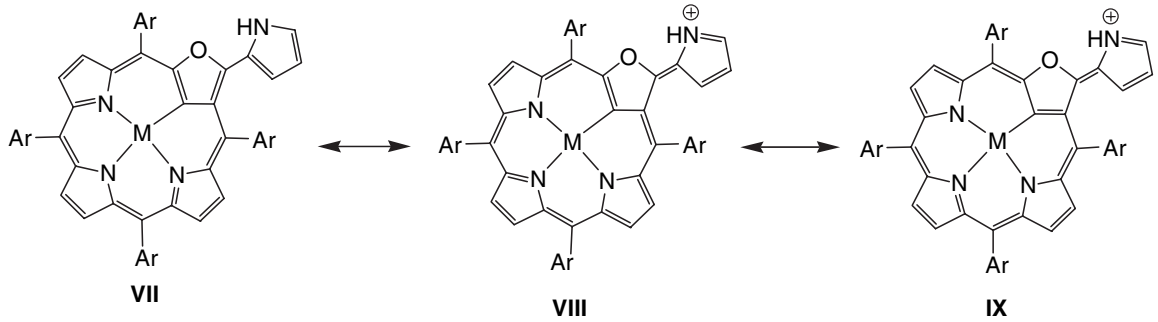

Chart 16. Proposed canonical structures for metal complexes of **207**.

Table 6
^{1}H NMR chemical shifts of appended pyrrole moiety of **207** and its metal complexes

Compound	Appended pyrrole protons (ppm)			
	3′	4′	5′	NH
Pyrrole	6.22	6.22	6.68	
207	5.54	5.82	6.33	7.26
207a	6.34	6.17	6.76	8.10
207b	6.36	6.20	6.79	8.16
207d	6.60	6.40	7.27	9.81

for the contribution of different canonical structures for metal complexes on **207** was clearly evident from ^{1}H as well as ^{13}C NMR chemical shift values of the appended pyrrole moiety. The ^{1}H NMR chemical shifts of the appended pyrrole moiety of **207** and its metal complexes shown in Table 6 indicated that there was a gradual increase in the chemical shift values of appended pyrrole moiety in the series **207**, **207a**, **207b** and **207d**. The largest shift value observed for **207d** was due to the effective conjugation between the macrocycle and the appended pyrrole moiety [170].

The structures of **207a** and **207c** were determined by X-ray crystallography [170]. In **207a**, the macrocycle was only slightly distorted from planarity (Fig. 24) and the dihedral angle between the macrocycle and the appended pyrrole planes reflects the biphenyl-like arrangement with the NH group pointing out towards the adjacent phenyl ring on the C5 position. The Ni–N distances in **207a** were comparable to those of other diamagnetic Ni(II) porphyrins and Ni–N bond length was similar to other Ni(II) carbaporphyrinoids where the trigonal carbon atom coordinated to the metal ions. The C_α–C_β and C_β–C_β bond lengths were changed in **207a** compared to free furan indicating that π-delocalization through the furan ring was altered. The bond length changes in the furan ring of **207a** were in between the range of furan ring which was built into non-aromatic and aromatic macrocycles and supporting the view that the canonical structure **VII** is the dominant form for this macrocycle. The crystal structure solved for **207c** [170] showed that it exhibited only slight distortion from planarity (Fig. 25). The Ag–N and

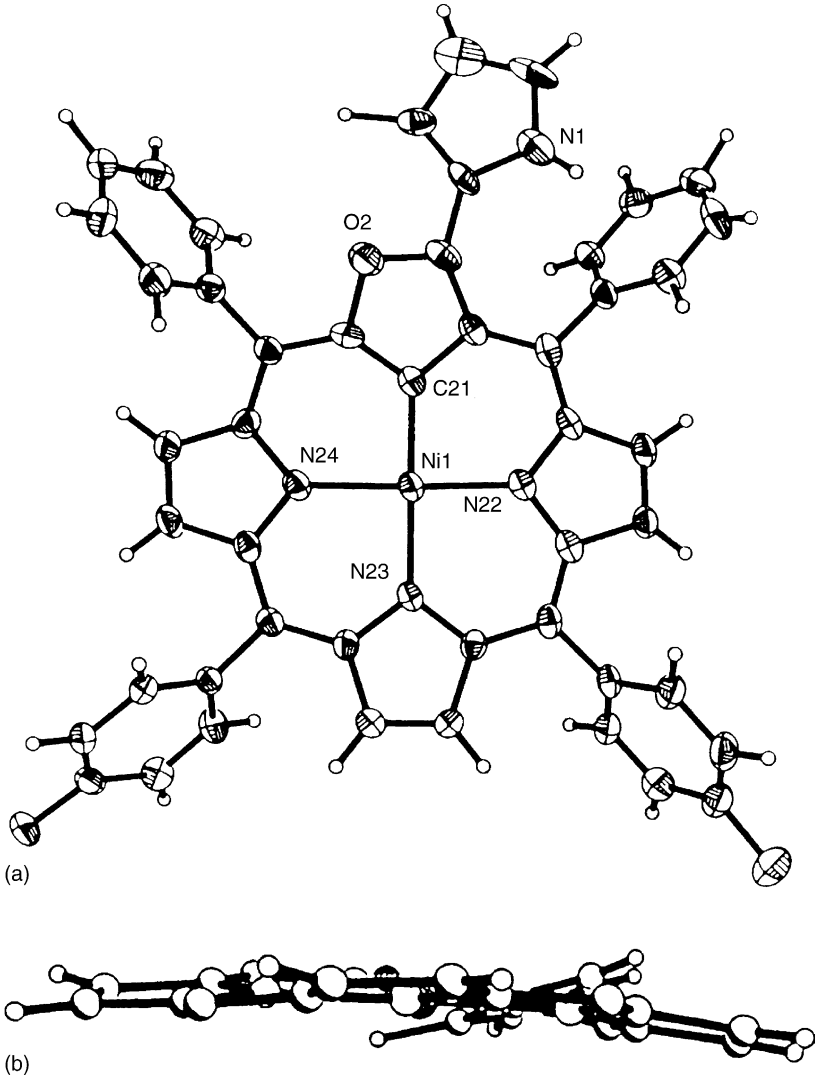

Fig. 24. X-ray structure of **207a**. (a) Top view and (b) side view (reproduced with permission from Ref. [170]).

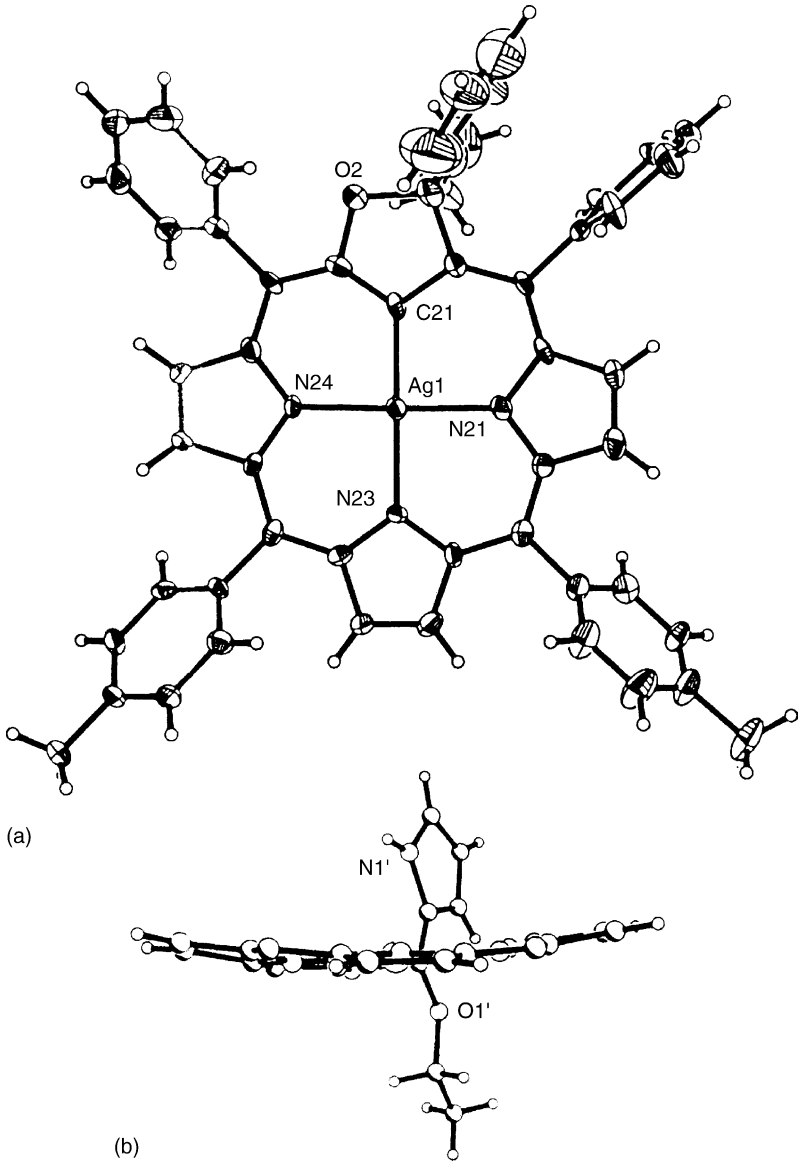

Fig. 25. X-ray structure of **207c**. (a) Top view and (b) side view (reproduced with permission from Ref. [170]).

Ag–C distances in **207c** were comparable to those in other silver(III) carbaporphyrinoids [124].

10. Unusual reactivity of telluraporphyrins

The telluraporphyrins although not very well studied, possess unusual properties and reactivity compared to their lighter chalcogen analogues. Latos-Grażyński et al. [171] first noted the unusual reactivity of 21-telluroporphyrin **5** by treating it with *m*-chloroperoxybenzoic acid. When **5** was treated with excess *m*-chloroperoxybenzoic acid, **2** was formed in good yield. However, when **5** was treated with a limited quantity of oxidant, first the green intermediate species **208** was formed, which on further treatment of additional oxidant gave **2**. The two compounds

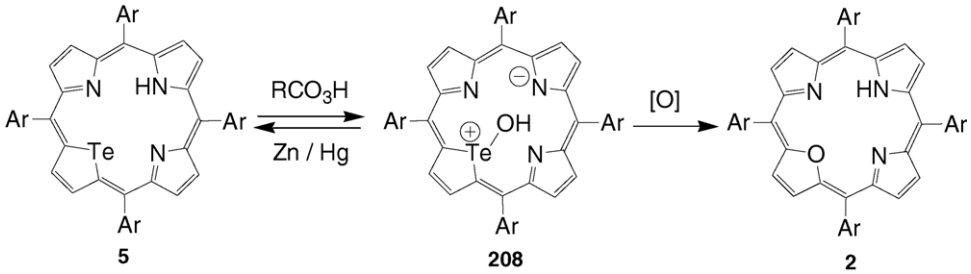

Scheme 39. Unusual reactions of 21-telluraporphyrin.

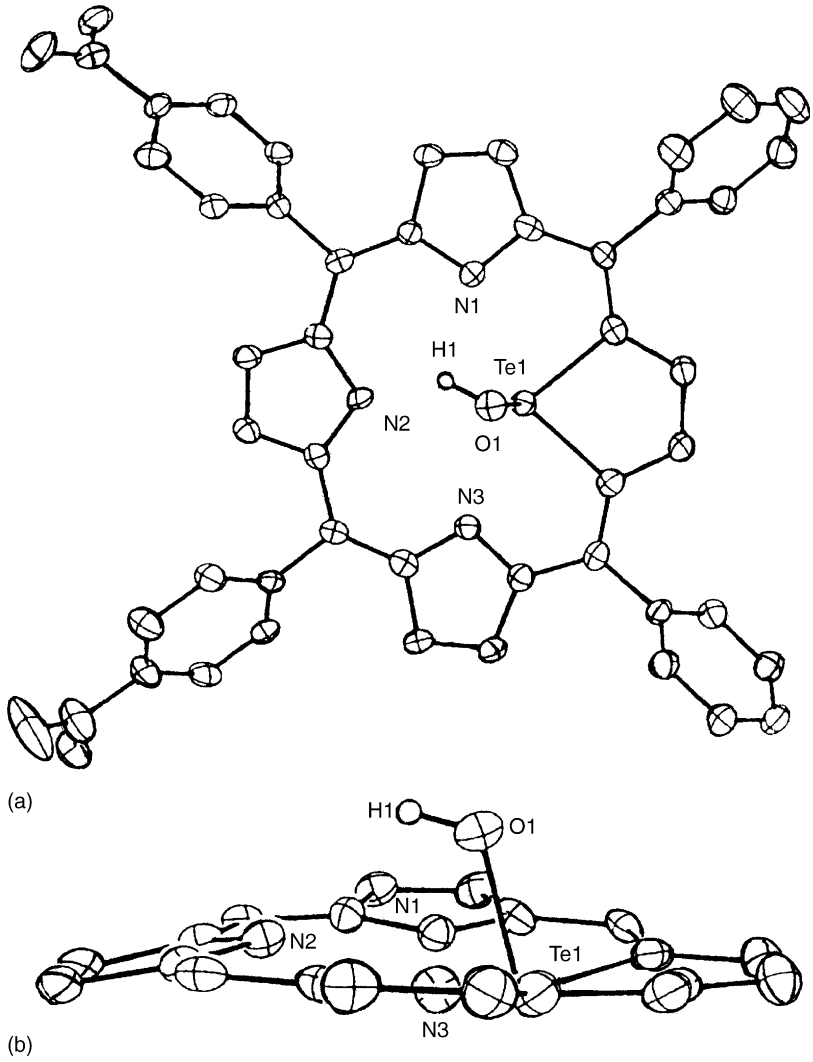

Fig. 26. X-ray structure of **208**. (a) Top view and (b) side view (reproduced with permission from Ref. [171]).

208 and **2** were also formed when **5** was exposed to air [171]. The exposure of **5** to air for few minutes gave **208**, which on prolonged exposure to air converted to **2** (Scheme 39). **208** can be reduced back to **5** by treating it with either zinc-amalgam or sodium dithionate [171]. The **208** was isolated and characterized by X-ray diffraction analysis. The structure of **208** [171] indicated that it was forming a zwitterions by transferring the hydrogen atom of the *trans* pyrrole nitrogen to the oxygen atom with a hydroxyl group attached to the tellurium atom (Fig. 26). The hydroxyl group attached to the tellurium atom interacted with *trans* pyrrole ring via a weak hydrogen bond resulting in bending the *trans* pyrrole ring upward towards the hydroxyl group.

Recently, Detty and co-workers [172] solved the crystal structure of **5c** and isolated the tautomeric form of 21-telluraporphyrin in which the H-atom resides on a pyrrole N that was *cis* to the tellurophene ring. The structure of **5c** was only slightly distorted from planarity as noted previously for the other 21-telluraporphyrin **5b** in which pyrrole ring bearing H-atom was *trans* to the tellurophene ring (Fig. 27). They also noticed that in **5c**, the Te atom interacted with the H-atom of N3 through hydrogen bonding with a Te1···HN3 distance of 1.827 Å. The Te atom also interacted strongly with N1 on the second *cis* pyrrole ring with a Te1···N1 distance of 2.558 Å. The Te1···N2 distance (3.173 Å) was nearly identical to that of **5b** [172].

The reactivity of **5c** was further explored by first oxidizing the **5c** with air or chemically to **208** which was then treated with HCl for several seconds and afforded **209** (Scheme 40) [172]. The X-ray structure of **209** (Fig. 28) indicated that the porphyrin macrocycle was non-planar unlike the planar structure observed for **5c** [172]. In **209**, the Te atom was in the +4 oxidation state with two Cl atoms attached in the axial positions to Te in the center of a trigonal bipyramid (Fig. 28). The Cl–Te–Cl bond angle of 168.65° reflected the stereochemically active lone pair of electrons on Te1 in the equatorial plane of the trigonal bipyramid. The Te–Cl bonds are not equal in length, with the Te–Cl2 bond (2.58 A) more elongated than Te–Cl1 bond (2.49 Å). The tellurophene ring was distorted from planarity with Te1 displaced from the plane of the four carbon atoms by 0.281 Å towards the

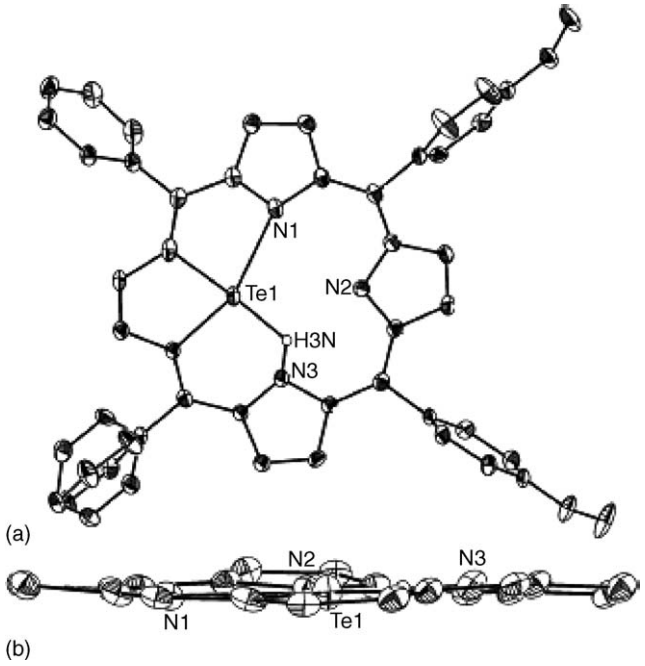

Fig. 27. X-ray structure of **5c**. (a) Top view and (b) side view (reproduced with permission from Ref. [172]).

axial Cl2 (Fig. 28). The N2 atom has a flattened trigonal bipyramidal configuration. The Cl1 atom formed a strong hydrogen bond to HN2 with a Cl···HN2 distance of 2.349 Å. Both Te1 and N2 were tipped out of plane in opposite directions and N1···N3 distance (4.625 Å) was also elongated to accommodate the larger Te atom [172].

Detty and co-workers recently investigated the spectroscopic, electrochemical and catalytic properties of 21-telluraporphyrin **5a** and 21-tellurio-23-thiaporphyrin **11** [172,173]. The ^{125}Te NMR spectrum of **5a** showed a signal at δ 823.6, which was considerably downfield shifted in **11** (δ 1039). This was attributed to the more electronegative nature of sulfur in **11**, which pulled the electron density from tellurium and deshielded the tellurium atom. Similarly, the signal was downfield shifted in 21-telluroporphyrin telluroxide **208** to δ 1046.3 which was also due to the more electron deficient Te(IV) center bearing an electron withdrawing O-atom. Interestingly, the ^{125}Te NMR signal in 21,21-dichloro-21-telluraporphyrin **209** was observed at δ 793.9. The upfield shift of ^{125}Te NMR chemical shift in **209**

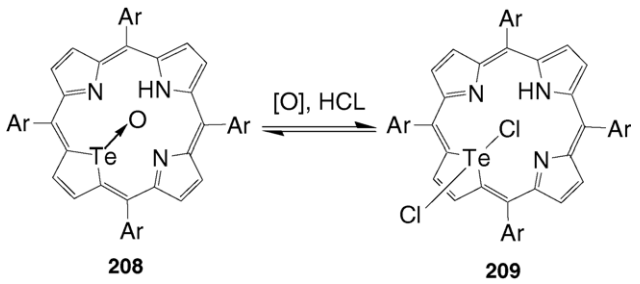

Scheme 40. Synthesis of dichloro derivative of 21-telluraporphyrin **209**.

was attributed to the diamagnetic ring current from an annulene type contribution to the overall electronic structure of **209**. The electrochemical studies indicated that **5a** and **11** were more easily oxidizable compared to the other hetero analogues, which is inconsistent with the facile oxidation of 21-telluraporphyrins when exposed to air. Detty and co-workers also tested the **5c** and **11** as catalysts [174] for the activation of H_2O_2 in the bromination of 4-pentenoic acid and 1,3,5-trimethoxy benzene with H_2O_2 and NaBr and noted high turn over numbers for these bromination reactions.

The high reactivity of 21-telluraporphyrins was further utilized recently by Latos-Grażyński and co-workers to synthesize a novel molecule 21-vacataporphyrin **210** [175]. The **210** was a hybrid of annulene and porphyrin and has a vacant space instead of a heteroatom bridge. **210** was synthesized in 55% yield by reacting **5b** with HCl at refluxing temperature (Scheme 41). The 21-vacataporphyrin **210** was nearly planar as confirmed by X-ray analysis (Fig. 29) and possessed similar spectroscopic properties to that of porphyrin **1**. The **210** has three nitrogen atoms and CH groups favorably prearranged for coordination to a metal ion although the metal coordination properties have not yet been reported.

Latos-Grażyński and co-workers [176] synthesized 21,23-ditelluraporphyrin with a flipped tellurophene ring **211** in 11% yield by following standard synthetic methodology used for 21,23-diheteroporphyrins (Scheme 42). The **211** was the first example of the inverted structure of the 18-π-electron porphyrin-like frame with four five-membered rings linked by four methane carbon atoms. The X-ray structure solved for **211** (Fig. 30) showed a remarkable distortion of the porphyrin, which was attributed to the size of the tellurium atoms [176]. One of the tellurophene moieties (Te23) was coplanar with the two adjacent pyrrole rings while the second tellurophene ring (Te21) was directed away from the center of the macrocycle (Fig. 30). The degree of distortion was reflected by a dihedral angle between the plane of the *meso*-carbon atoms and the tellurophene plane of 123.0(2)°. The electronic spectrum of **211** did not show a strong Soret band but showed three major bands of comparable intensities at 348, 464 and 668 nm. However, the protonated form **211** showed the presence of Soret like band at 490 nm and a less intense band at 767 nm, which was attributed to the more aromatic nature of the protonated form compared with the neutral species.

In ^{1}H NMR, the tellurophene protons at δ 8.53 and 6.08 ppm, respectively, were due to the regular and flipped tellurophene rings [176]. However, protonation with TFA resulted in a regular structure in which Te21 and Te23 tellurophene atoms were simultaneously directed towards the center of the macrocycle (**X-H**$_2^{2+}$, Chart 17). This was evident in ^{1}H NMR, which showed only one signal at δ 8.03 corresponding to the tellurophene ring protons. Also the NH resonances appeared in high field region (−0.7 ppm) due to the changed ring current effect supported the regular structure [176]. Furthermore, based on the NMR studies at different temperatures, the molecule **211** appears to interchange between two energetically and structurally identical flipped forms **XI** and **XII** (Chart 17).

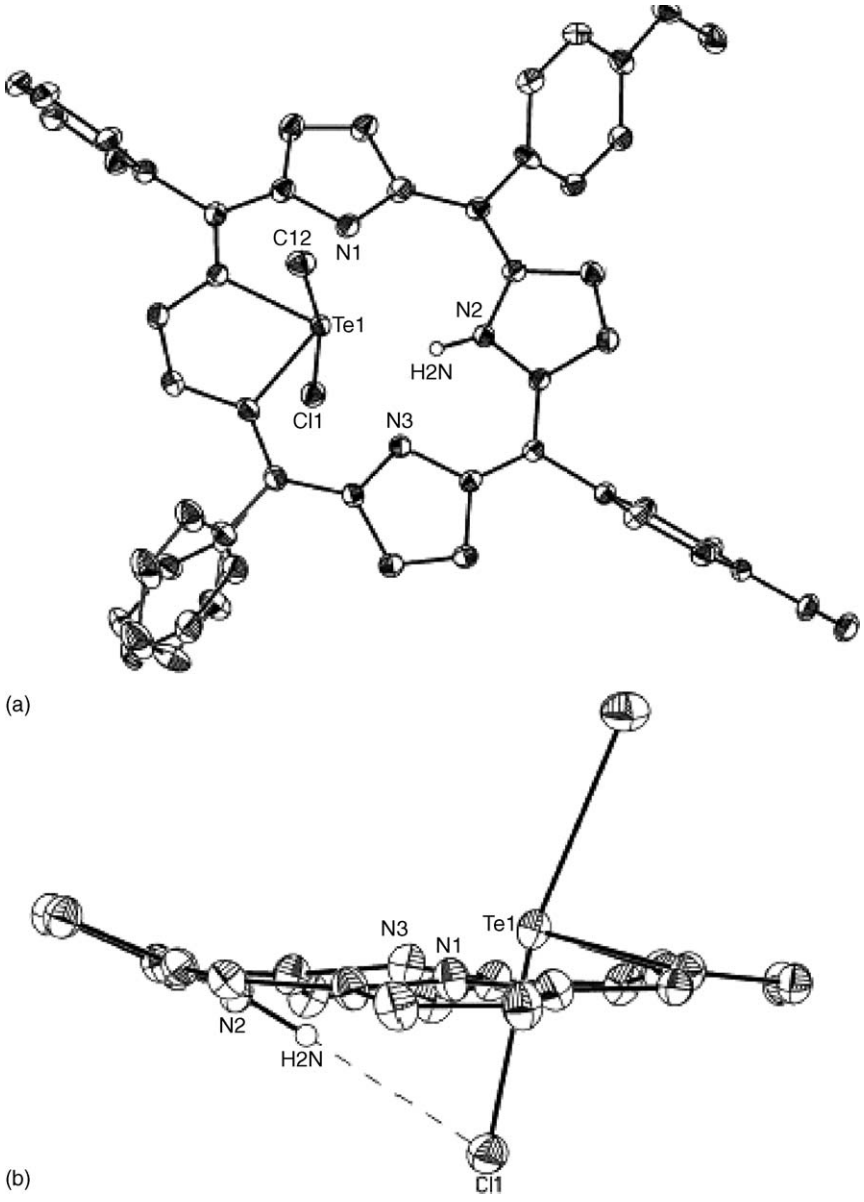

Fig. 28. X-ray structure of **209**. (a) Top view and (b) side view (reproduced with permission from Ref. [171]).

11. Water-soluble heteroporphyrins

Water-soluble porphyrins are important materials with significant applications in many applied fields including biology and medicine [177]. Specifically, the water-soluble porphyrins are potential photo sensitizers for photodynamic therapy (PDT) of cancer in which light and endogenous oxygen, facilitated by a photo sensitizer, on irradiation produces a cascade of biochemical events that inactivate cancer cells [177]. Water-soluble porphyrins with an N_4 core, such as 5,10,15,20-tetrakis(4-sulfonatophenyl)porphyrin (TPPS) have been studied extensively as sensitizers for PDT and have shown promising results. However, the N_4 water-soluble porphyrins besides exhibiting neurotoxicity, also absorbs weakly near the 630 nm region where light has greater penetration into the tissue. The presently available porphyrin PDT drug, Photofrin, also absorbs weakly in the same region and hence is not an ideal drug [177]. Thus, the water-soluble heteroatom substituted porphyrins, which absorbs in longer wavelength region (650–700 nm) can be explored as photo sensitizers for PDT.

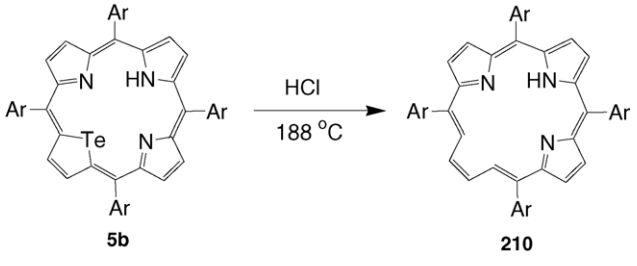

Scheme 41. Synthesis of 21-vacataporphyrin **210**.

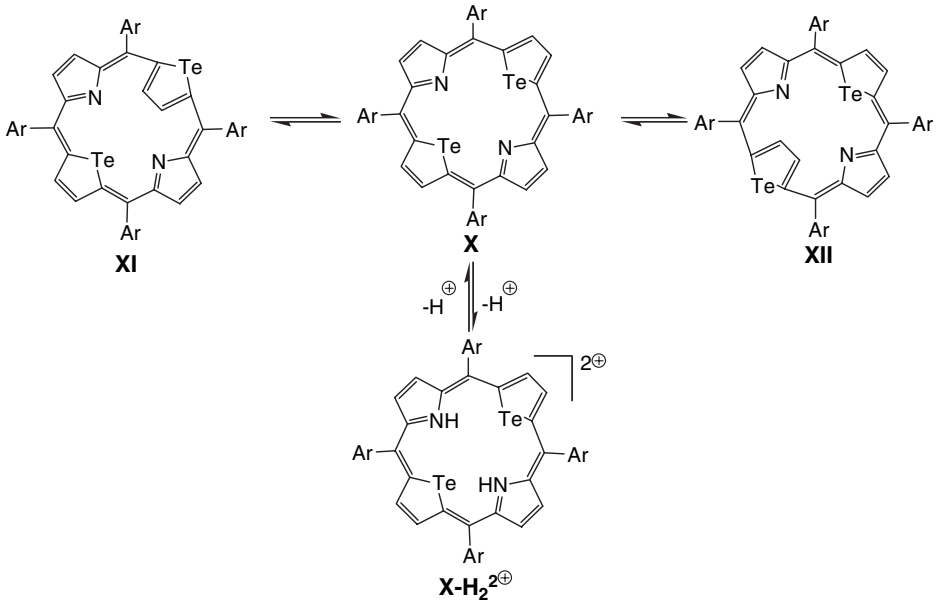

Chart 17. Canonical forms of **211**.

Chandrashekar and co-workers [178,179] synthesized the first anionic water-soluble tetrasulfonated 21-thiaporphyrin **212** and 21,23-dithiaporphyrin **213** by sulfonation of porphyrins with chlorosulfonic acid under mild reaction conditions. Comparison of the spectroscopic and electrochemical properties of **212** and **213** with regular anionic water-soluble porphyrins showed the expected bathochromic shifts of the absorption bands, and red shifts of the fluorescence bands with reduced quantum yields. Oxidation and reduction were harder and easier, respectively. The Cu(II) and Ni(II) derivatives of **212** were prepared and the electrochemical studies indicated the reduction

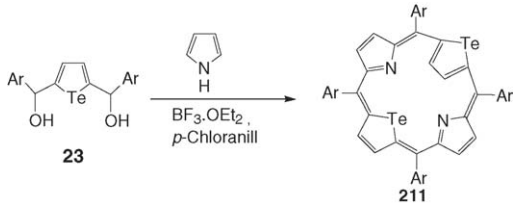

Scheme 42. Synthesis of confused telluroporphyrin **211**.

of the metal center. The aggregation properties of **212** and **213** were similar to regular anionic water-soluble porphyrins [179]. Latos-Grażyński and co-workers [180,181] have used similar reaction conditions and prepared the disulfonated water-soluble

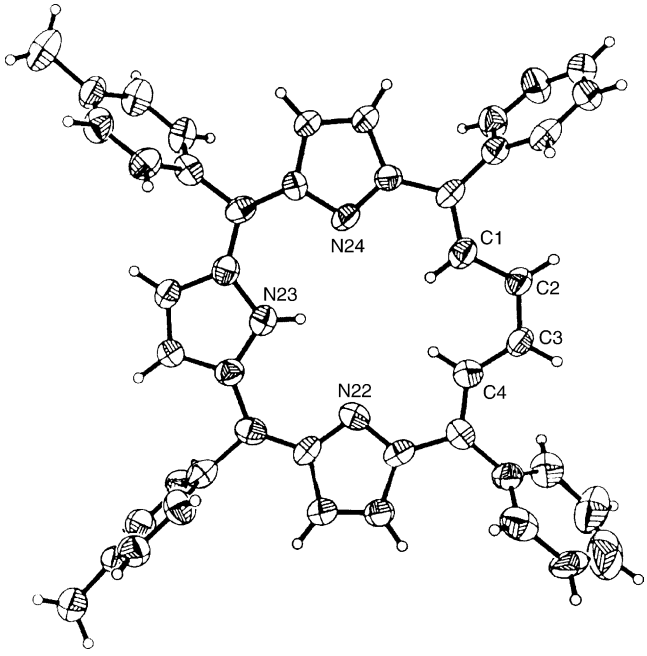

Fig. 29. X-ray structure of **210**, top view (reproduced with permission from Ref. [175]).

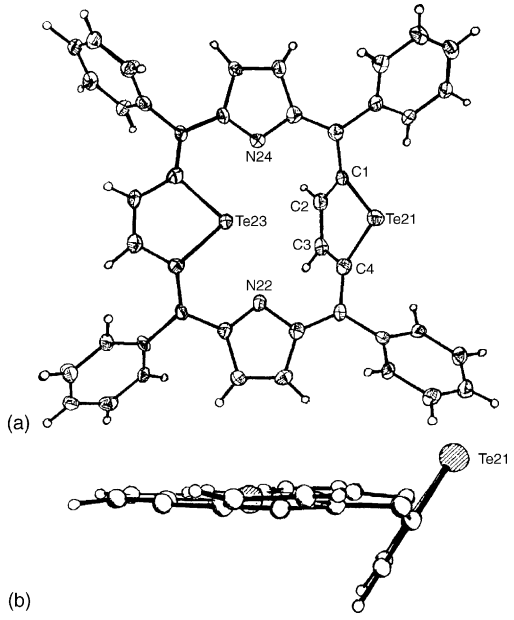

Fig. 30. X-ray structure of **211**. (a) Top view and (b) side view (reproduced with permission from Ref. [176]).

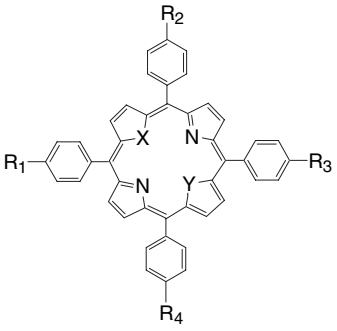

$R_1 = R_2 = R_3 = R_4 = SO_3Na$; X = S , Y = NH : **212**

$R_1 = R_2 = R_3 = R_4 = SO_3Na$; X = Y = S : **213**

$R_1 = R_2 = R_3 = R_4 = SO_3Na$; X = Y = Se : **214**

$R_1 = R_2 = F$, $R_3 = R_4 = SO_3Na$; X = S , Y = NH : **215**

$R_1 = R_2 = F$, $R_3 = R_4 = SO_3Na$; X = Y = S : **216**

$R_1 = R_2 = F$, $R_3 = R_4 = SO_3Na$; X = Y = Se : **217**

$R_1 = R_2 = F$, $R_3 = R_4 = SO_3Na$; X = S , Y = Se : **218**

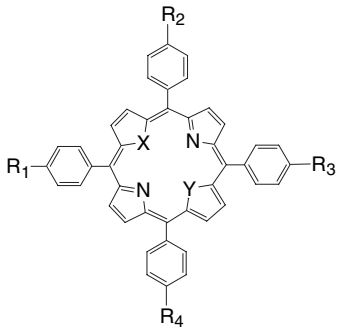

$R_1 = OCH_2CO_2Na$, $R_2 = R_3 = R_4 = H$; X = Y = S : **219**

$R_1 = R_2 = OCH_2CO_2Na$, $R_3 = R_4 = H$; X = Y = S : **220**

$R_1 = R_2 = R_3 = OCH_2CO_2Na$, $R_4 = H$; X = Y = S : **221**

$R_1 = R_2 = R_3 = R_4 = OCH_2CO_2Na$; X = Y = S : **222**

$R_1 = R_2 = H$, $R_3 = R_4 = OCH_2CO_2Na$; X = Y = Se : **223**

Chart 18. Anionic water-soluble heteroporphyrins.

21-selenaporphyrin in which the sulfonated groups were at *o*-position (the structure is not shown in Chart 18).

Detty and co-workers [182,183] recently synthesized the tetrasulfonated water-soluble 21-thiaporphyrin **212**, 21,23-dithiaporphyrin **213** and 21,23-diselenaporphyrin **214** as tetra-sodium salts by sulfonation of the corresponding porphyrin by treatment with sulfuric acid followed by treatment with NaOH. They have also synthesized a series of disulfonated derivatives of heteroporphyrins **215**–**218** under similar reaction conditions. Detty and co-workers further synthesized a series of water-soluble heteroporphyrins bearing 1–4 carboxylic acid groups **219**–**223** by saponification of the corresponding esters [184]. The sulfonated and carboxylated heteroporphyrins were evaluated in vitro as photo sensitizers for photodynamic therapy and some showed promising results.

We synthesized [57,60] a series of the first cationic water-soluble 21-thiaporphyrins (**224a**–**c** and **226a**–**c**) and 21-oxaporphyrins (**225a**–**c** and **227a**–**b**) containing two and three

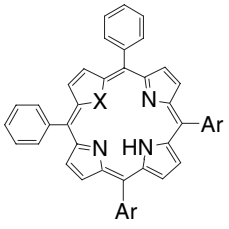

Ar = 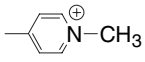 ; X = S , Y = NH : **224a**

Ar = 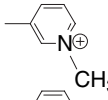 ; X = S , Y = NH : **224b**

Ar = 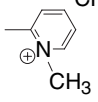 ; X = S , Y = NH : **224c**

Ar = 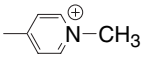 ; X = O, Y = NH : **225a**

Ar = 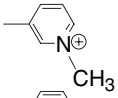 ; X = O , Y = NH : **225b**

Ar = 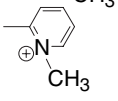 ; X = O , Y = NH : **225c**

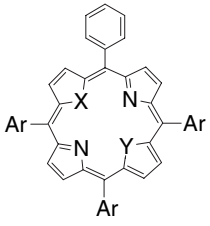

Ar = 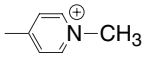 ; X = S , Y = NH : **226a**

Ar = 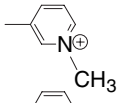 ; X = S , Y = NH : **226b**

Ar = 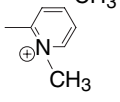 ; X = S , Y = NH : **226c**

Ar = 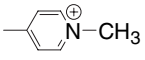 ; X = O, Y = NH : **227a**

Ar = 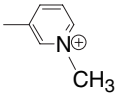 ; X = O , Y = NH : **227b**

Chart 19. Cationic water-soluble heteroporphyrins.

N-methylpyridiniumyl ions at *meso*-positions by methylation of the corresponding *meso*-pyridyl porphyrins with 500-fold excess of CH_3I in CH_2Cl_2 at refluxing temperature overnight (Chart 19). The absorption and fluorescence bands of these cationic water-soluble heteroporphyrins as expected were red shifted compared to tetrakis(*N*-methylpyridiniumyl)porphyrin because of the presence of the heteroatom in the core [60]. However, these compounds have not been tested for any applications.

12. Conclusions

The present review reflects that even though the monoheteroporphyrins and diheteroporphyrins have been known for almost three and half decades, there have been significant developments in synthetic heteroporphyrin chemistry over the past 5–6 years. Up until 1998, very few new heteroporphyin derivatives were known and most of the research till then was focused on syntheses and structures of metal complexes of simple to make heteroporphyrin ligands and stabilization of metals in unusual oxidation states. In the last few years, heteroporphyrin chemistry has advanced rapidly and almost every hetero analogue(s) of porphyrins and their derivatives, such as chlorins, corroles, carbaporphyrins, confused porphyrins have been synthesized and studied for their potential use for various applications as a substitute for regular porphyrins. The most important synthetic developments in heteroporphyrin chemistry during the 1999–2005 period are: (1) new and modified synthetic routes to prepare heteroporphyins, (2) first metal complex of 21,23-dithiaporphyrin, (3) covalent and non-covalent unsymmetrical porphyrin dimers and higher arrays, (4) β-pyrrole and β-thiophene substituted thiaporphyrins, (5) *meso*-unsubstituted porphyrins and their functionalization and *meso*-substituted porphyrins having thienyl, furyl and sterically crowded dendrons, (6) chlorins and bacteriochlorins, tetrabenzoporphyrins, (7) carbaporphyrins and their organometallic complexes, (8) N-confused as well as heteroatom confused porphyrins, (9) corroles and their metal complexes and (10) water-soluble porphyrins. Thus, these novel heteroanalogues of porphyrins set the stage for further research for new methods and new heteroporphyrin systems. In terms of future efforts, we expect the synthesis of many other heteroporphyins with cores having various heteroatom combinations and also large complex systems, such as a porphyrin arrays containing four or more different porphyrin cores connected via covalently or non-covalently, to be studied for their potential applications in molecular electronics and other related applied fields. More synthetic heteroporphyrin chemistry will be carried out in the coming years to develop all the possibilities of this fascinating family of molecules.

Acknowledgements

M.R. thanks CSIR and DST, Govt. of India for financial support and I.G. thanks CSIR for SRF fellowship. Our contributions in this area of research would not have been possible without the hard work of our co-workers whose names appear in the references.

References

[1] J.S. Lindsey, in: K.M. Kadish, K.M. Smith, R. Guilard (Eds.), The Porphyrin Handbook, Academic Press, San Diego, 2000.
[2] L. Latos-Grażyński, in: K.M. Kadish, K.M. Smith, R. Guilard (Eds.), The Porphyrin Handbook, vol. 2, Academic Press, New York, 2000, p. 361.
[3] P.J. Chmielewski, M. Grzeszczuk, L. Latos-Grażyński, J. Lisowski, Inorg. Chem. 28 (1989) 3546.
[4] L. Latos-Grażyński, J. Lisowski, M.M. Olmstead, A.L. Balch, Inorg. Chem. 28 (1989) 3328.
[5] L. Latos-Grażyński, J. Lisowski, M.M. Olmstead, A.L. Balch, Inorg. Chem. 28 (1989) 4065.
[6] J. Lisowski, M. Grzeszczuk, L. Latos-Grażyński, Inorg. Chim. Acta 161 (1989) 153.
[7] R.P. Pandian, T.K. Chandrashekar, Inorg. Chem. 33 (1994) 3317.
[8] R.P. Pandian, T.K. Chandrashekar, J. Chem. Soc. Dalton Trans. (1994) 119.
[9] P.J. Chmielewski, L. Latos-Grażyński, M.M. Olmstead, A.L. Balch, Chem. Eur. J. 3 (1997) 268.
[10] P.J. Chmielewski, L. Latos-Grażyński, Inorg. Chem. 37 (1998) 4179.
[11] B. Sridevi, S.J. Narayanan, A. Srinivasan, T.K. Chandrashekar, J. Subramanian, J. Chem. Soc. Dalton Trans. (1998) 1979.
[12] M.J. Broadhurst, R. Grigg, A.W. Johnson, J. Chem. Soc. C (1969) 3681.
[13] M.J. Broadhurst, R. Grigg, A.W. Johnson, J. Chem. Soc. D (1969) 1480.
[14] M.J. Broadhurst, R. Grigg, A.W. Johnson, J. Chem. Soc. D (1970) 807.
[15] M.J. Broadhurst, R. Grigg, J. Chem. Soc. C (1971) 3681.
[16] L. Latos-Grażyński, J. Lisowski, M.M. Olmstead, A.L. Balch, J. Am. Chem. Soc. 109 (1987) 4428.
[17] L. Latos-Grażyński, J. Lisowski, M.M. Olmstead, A.L. Balch, J. Am. Chem. Soc. 109 (1987) 319.
[18] L. Latos-Grażyński, J. Lisowski, M.M. Olmstead, A.L. Balch, Inorg. Chem. 28 (1989) 1183.
[19] L. Latos-Grażyński, J. Lisowski, P.J. Chmielewski, M. Grzeszczuk, M.M. Olmstead, A.L. Balch, Inorg. Chem. 33 (1994) 192.
[20] L. Latos-Grażyński, E. Pacholska, P.J. Chmielewski, M.M. Olmstead, A.L. Balch, Inorg. Chem. 35 (1996) 566.
[21] Z. Gross, I. Saltsman, R.P. Pandian, C. Barzilay, Tetrahedron Lett. 38 (1997) 2383.
[22] L. Latos-Grażyński, P.J. Chmielewski, New J. Chem. 21 (1997) 691.
[23] P.J. Chmielewski, L. Latos-Grażyński, Inorg. Chem. 31 (1992) 5231.
[24] E. Pacholska, P.J. Chmielewski, L. Latos-Grażyński, Inorg. Chim. Acta 273 (1998) 184.
[25] T.K. Chandrashekar, S. Venkatraman, Acc. Chem. Res. 36 (2003) 676.
[26] J.L. Sessler, D. Seidel, Angew. Chem. Int. Ed. 42 (2003) 5134.
[27] A. Ulman, J. Manassen, J. Am. Chem. Soc. 97 (1975) 6540.
[28] A. Ulman, J. Manassen, F. Frolow, D. Rabinovich, Tetrahedron Lett. (1978) 167.
[29] A. Ulman, J. Manassen, F. Frolow, D. Rabinovich, Tetrahedron Lett. (1978) 1885.
[30] A. Ulman, J. Manassen, J. Chem. Soc. Perkin I (1979) 1066.
[31] P.-Y. Heo, K. Shin, C.-H. Lee, Tetrahedron Lett. 37 (1996) 197.
[32] P.-Y. Heo, K. Shin, C.-H. Lee, Bull. Korean Chem. Soc. 17 (1996) 515.
[33] C.-H. Lee, J.-Y. Park, H.-J. Kim, Bull. Korean Chem. Soc. 21 (2000) 97.
[34] A. Srinivasan, B. Sridevi, M.V. Reddy, S.J. Narayanan, T.K. Chandrashekar, Tetrahedron Lett. 38 (1997) 4149.
[35] B. Sridevi, S.J. Narayanan, A. Srinivasan, M.V. Reddy, T.K. Chandrashekar, J. Porphyrins Phthalocyanines 2 (1998) 69.
[36] A.D. Adler, F.R. Longo, J.D. Finarelli, J. Goldmacher, J. Assour, L. Korsakoff, J. Org. Chem. 32 (1967) 476.
[37] J.S. Lindsey, I.C. Schreiman, H.C. Hsu, P.C. Kearney, A.M. Marguerettaz, J. Org. Chem. 52 (1987) 827.

[38] I. Gupta, N. Agarwal, M. Ravikanth, Eur. J. Org. Chem. (2004) 1693.
[39] I. Gupta, M. Ravikanth, J. Org. Chem. 69 (2004) 6796.
[40] W.-S. Cho, C.-H. Lee, Bull. Korean Chem. Soc. 19 (1998) 314.
[41] C.-H. Lee, W.-S. Cho, Tetrahedron Lett. 40 (1999) 8879.
[42] A. Ulman, J. Manassen, F. Frolow, D. Rabinovich, J. Am. Chem. Soc. 101 (1979) 7055.
[43] R.J. Abraham, P. Leonard, A. Ulman, Org. Magn. Reson. 22 (1984) 561.
[44] L. Hill, M. Gouterman, A. Ulman, Inorg. Chem. 21 (1982) 1450.
[45] R.P. Pandian, D. Reddy, N. Chidambaram, T.K. Chandrashekar, Proc. Indian Acad. Sci. 102 (1990) 307.
[46] R.P. Pandian, T.K. Chandrashekar, G.S.S. Saini, A.L. Verma, J. Chem. Soc. Faraday Trans. 89 (1993) 677.
[47] A. Ulman, J. Manassen, F. Frolow, D. Rabinovich, Inorg. Chem. 20 (1981) 1987.
[48] C.-H. Hung, C.-K. Ou, G.-H. Lee, S.-M. Peng, Inorg. Chem. 40 (2001) 6845.
[49] A. Gebauer, J.A.R. Schmidt, J. Arnold, Inorg. Chem. 39 (2000) 3424.
[50] J.-Y. Tung, B.-C. Liao Elango, J.-H. Chen, H.-Y. Hsieh, F.-L. Liao, S.-L. Wang, L.-P. Hwang, Inorg. Chem. Commun. 5 (2002) 150.
[51] M. Pawlicki, L. Latos-Grażyński, Inorg. Chem. 41 (2002) 5866.
[52] M. Pawlicki, L. Latos-Grażyński, Inorg. Chem. 43 (2004) 5564.
[53] W.S. Cho, H.J. Kim, B.J. Littler, M.A. Miller, C.-H. Lee, J.S. Lindsey, J. Org. Chem. 64 (1999) 7890.
[54] M. Ravikanth, Tetrahedron Lett. 41 (2000) 3709.
[55] D. Kumaresan, N. Agarawal, M. Ravikanth, J. Chem. Soc. Perkin Trans. I (2001) 1644.
[56] D. Kumaresan, I. Gupta, M. Ravikanth, Tetrahedron Lett. 42 (2001) 8547.
[57] D. Kumaresan, S. Santra, M. Ravikanth, Syn. Lett. (2001) 1635.
[58] D. Kumaresan, N. Agarwal, I. Gupta, M. Ravikanth, Tetrahedron 58 (2002) 5347.
[59] A. Berlicka, E. Pacholoska, L. Latos-Grażyński, J. Porphyrins Phthalocyanines 7 (2003) 8.
[60] S. Santra, D. Kumaresan, N. Agarwal, M. Ravikanth, Tetrahedron 58 (2003) 5347.
[61] S. Punidha, M. Ravikanth, Tetrahedron 60 (2004) 8437.
[62] S. Punidha, N. Agarwal, M. Ravikanth, Eur. J. Org. Chem. (2005) 2500.
[63] M. Ravikanth, N. Agarwal, D. Kumaresan, Chem. Lett. (2000) 836.
[64] D. Kumaresan, Ph.D. Thesis, I.I.T. Bombay, 2004.
[65] R.W. Wagner, T.E. Johnson, F. Li, J.S. Lindsey, J. Org. Chem. 60 (1995) 5266.
[66] D. Kumaresan, A. Datta, M. Ravikanth, Chem. Phys. Lett. 395 (2004) 87.
[67] F. Li, S.I. Yang, Y. Ciringh, J. Seth, C.H. Martin III, D.L. Singh, D. Kim, R.R. Birge, D.F. Bocian, D. Holten, J.S. Lindsey, J. Am. Chem. Soc. 120 (1998) 10001.
[68] M. Ravikanth, unpublished results.
[69] M. Ravikanth, T.K. Chandrashekar, Struct. Bond. 82 (1995) 105.
[70] J.A. Shelnutt, X.-Z. Song, J.-G. Ma, S.-L. Jia, W. Jentzen, C.J. Medforth, Chem. Soc. Rev. 27 (1998) 31.
[71] P.E. Elllis, J.E. Lyons, Coord. Chem. Rev. 105 (1990) 181.
[72] M.W. Grinstaff, M.G. Hill, J.A. Labinger, H.B. Gray, Science 264 (1994) 1311.
[73] K. Ozette, P. Luduc, M. Palacio, J.F. Bartoli, K.M. Barkigia, J. Fajer, J.F. Battioni, D. Mansuy, J. Am. Chem. Soc. 119 (1997) 6442.
[74] M. Ravikanth, Chem. Lett. (2000) 480.
[75] N. Agarwal, S.P. Mishra, A. Kumar, C.-H. Hung, M. Ravikanth, J. Chem. Soc. Chem. Commun. (2002) 2642.
[76] N. Agarwal, S.P. Mishra, A. Kumar, M. Ravikanth, Chem. Lett. 32 (2003) 744.
[77] N. Agarwal, S.P. Mishra, C.-H. Hung, A. Kumar, M. Ravikanth, Bull. Chem. Soc. Jpn. 77 (2004) 1173.
[78] N. Agarwal, M. Ravikanth, Tetrahedron 60 (2004) 4739.
[79] N. Agarwal, C.-H. Hung, M. Ravikanth, Tetrahedron 60 (2004) 10671.
[80] L. Latos-Grażyński, J. Lisowski, L. Szterenberg, M.M. Olmstead, A.L. Balch, J. Org. Chem. 56 (1991) 4043.
[81] H. Segawa, F.-P. Wu, N. Nakayama, S. Sagisaka, N. Higuchi, M. Fujitsuka, T. Shimidzu, Synth. Met. 71 (1995) 2151.
[82] M.S. Vollmer, F. Wurthner, F. Effenberger, P. Emele, D.U. Meyer, T. Stumpfig, H. Port, H.C. Wolf, Chem. Eur. J. 4 (1998) 260.
[83] P. Bhavana, P. Bhyrappa, Acta Crystallogr., Sect. C 57 (2001) 252.
[84] P. Bhavana, P. Bhyrappa, Chem. Phys. Lett. 349 (2001) 399.
[85] D.-F. Shi, R.T. Wheelhouse, Tetrahedron Lett. 43 (2002) 9341.
[86] I. Gupta, M. Ravikanth, Tetrahedron Lett. 43 (2002) 9453.
[87] I. Gupta, M. Ravikanth, Tetrahedron 59 (2003) 6131.
[88] I. Gupta, C.-H. Hung, M. Ravikanth, Eur. J. Org. Chem. (2003) 4392.
[89] I. Gupta, M. Ravikanth, J. Chem. Sci. 117 (2005) 161.
[90] I. Gupta, M. Ravikanth, J. Photochem. Photobiol. A Chem., in press.
[91] N. Tomioka, D. Takasu, T. Takahasi, T. Aida, Angew. Chem. Int. Ed. Engl. 37 (1998) 1531.
[92] P.J. Dandliker, P. Diederich, M. Gross, C.B. Knobler, A. Louati, E.M. Sanford, Angew. Chem. Int. Ed. Engl. 33 (1994) 1739.
[93] P. Bhyrappa, G. Vaijayanthimala, K.S. Suslick, J. Am. Chem. Soc. 121 (1999) 262.
[94] S.C. Zimmerman, F. Zeng, Science 271 (1996) 1095.
[95] A.W. Bosman, H.M. Janssen, E.W. Meijer, Chem. Rev. 99 (1999) 1665.
[96] D. Kumaresan, M. Ravikanth, Chem. Lett. (2003) 1120.
[97] N. Agarwal, Ph.D. Thesis, I.I.T. Bombay, 2004.
[98] N. Agarwal, C.-H. Hung, M. Ravikanth, Eur. J. Org. Chem. (2003) 3730.
[99] S. Punidha, N. Agarwal, R. Burai, M. Ravikanth, Eur. J. Org. Chem. (2004) 2223.
[100] D.P. Arnold, Y. Sakata, K.L. Sugiura, E.I. Worthinton, J. Chem. Soc. Chem. Commun. (1998) 2331.
[101] W.W. Kalisch, M.O. Senge, Angew. Chem. Int. Ed. Engl. 37 (1998) 1107.
[102] R. Paolesse, in: K.M. Kadish, K.M. Smith, R. Guilard (Eds.), The Porphyrin Handbook, vol. 2, Academic Press, San Diego, CA, 2000, p. 201.
[103] D.T. Gryko, Eur. J. Org. Chem. (2002) 1735 (and references cited therein).
[104] A.W. Johnson, I.T. Kay, Proc. Chem. Soc. (1961) 168.
[105] A.W. Johnson, I.T. Kay, R. Rodrigo, J. Chem. Soc. (1963) 2336.
[106] M.J. Broadhurst, R. Grigg, A.W. Johnson, J. Chem. Soc. Perkin Trans. 1 (1972) 1124.
[107] M.J. Broadhurst, R. Grigg, A.W. Johnson, J. Chem. Soc. Chem. Commun. (1969) 23.
[108] S.J. Narayanan, B. Sridevi, T.K. Chandrashekar, U. Englich, K.R. Senge, Org. Lett. 1 (1999) 587.
[109] B. Sridevi, S.J. Narayanan, T.K. Chandrashekar, U. English, K.R. Senge, Chem. Eur. J. 6 (2000) 2554.
[110] J. Sankar, V.G. Anand, S. Venkataraman, H. Rath, T.K. Chandrashekar, Org. Lett. 4 (2002) 4233.
[111] J. Sankar, H. Rath, V. Prabhuraja, T.K. Chandrashekar, J.J. Vittal, J. Org. Chem. 69 (2004) 5135.
[112] S. Venkataraman, R. Kumar, J. Sankar, T.K. Chandrashekar, K. Sendhil, C. Vijayan, A. Kelling, M.O. Senge, Chem. Eur. J. 10 (2004) 1423.
[113] W.-S. Cho, C.-H. Lee, Tetrahedron Lett. 41 (2000) 697.
[114] C.-H. Lee, W.-S. Cho, J.-W. Ka, H.-J. Kim, P.H. Lee, Bull. Korean Chem. Soc. 21 (2000) 429.
[115] M. Pawlicki, L. Latos-Grażyński, L. Szterenberg, J. Org. Chem. 67 (2002) 5644.
[116] T.D. Lash, Angew. Chem. Int. Ed. Engl. 34 (1995) 2533.
[117] T.D. Lash, S.T. Chaney, Chem. Eur. J. 2 (1996) 944.
[118] T.D. Lash, S.T. Chaney, Angew. Chem. Int. Ed. Engl. 36 (1997) 839.
[119] T.D. Lash, M.J. Hayes, Angew. Chem. Int. Ed. Engl. 36 (1997) 840.
[120] T.D. Lash, S.T. Chaney, D.T. Richter, J. Org. Chem. 63 (1998) 9076.
[121] M. Stepien, L. Latos-Grażyński, T.D. Lash, L. Szterenberg, Inorg. Chem. 40 (2001) 6892.
[122] D.T. Richter, T.D. Lash, Tetrahedron 57 (2001) 3659.
[123] S.R. Graham, G.M. Ferrence, T.D. Lash, J. Chem. Soc. Chem. Commun. (2002) 894.
[124] M.A. Muckey, L.F. Szczepura, G.M. Ferrence, T.D. Lash, Inorg. Chem. 41 (2002) 4840.

[125] T.D. Lash, M.J. Hayes, J.D. Spence, M.A. Muckey, G.M. Ferrence, L.F. Szczepura, J. Org. Chem. 67 (2002) 4860.
[126] T.D. Lash, D.A. Colby, S.R. Graham, G.M. Ferrence, L.F. Szczepura, Inorg. Chem. 42 (2003) 7326.
[127] D. Liu, T.D. Lash, J. Org. Chem. 68 (2003) 1755.
[128] T.D. Lash, J.M. Rasmussen, K.M. Bergman, D.A. Colby, Org. Lett. 6 (2004) 549.
[129] T.D. Lash, D.A. Colby, L.F. Szczepura, Inorg. Chem. 43 (2004) 5258.
[130] T.D. Lash, in: K.M. Kadish, K.M. Smith, R. Guilard (Eds.), The Porphyrin Handbook, vol. 2, Academic Press, New York, 2002, p. 125.
[131] S.R. Graham, D.A. Colby, T.D. Lash, Angew. Chem. Int. Ed. Engl. 41 (2002) 1371.
[132] T.D. Lash, D.A. Colby, S.R. Graham, S.T. Chaney, J. Org. Chem. 69 (2004) 8851.
[133] T.D. Lash, J. Chem. Soc. Chem. Commun. (1998) 1683.
[134] S. Venkataraman, V.G. Anand, V. Prabhuraja, H. Rath, J. Sankar, T.K. Chandrashekar, W. Teng, K. Ruhlandt, J. Chem. Soc. Chem. Commun. (2002) 1660.
[135] S. Venkataraman, V.G. Anand, S.K. Pushpan, J. Sankar, T.K. Chandrashekar, J. Chem. Soc. Chem. Commun. (2002) 462.
[136] D. Liu, T.D. Lash, J. Chem. Soc. Chem. Commun. (2002) 2426.
[137] D. Liu, G.M. Ferrence, T.D. Lash, J. Org. Chem. 69 (2004) 6079.
[138] K. Miyabe, T.D. Lash, J. Chem. Soc. Chem. Commun. (2004) 178.
[139] Y. Shimizu, Z. Shen, T. Okijima, H. Uno, N. Ono, J. Chem. Soc. Chem. Commun. (2004) 374.
[140] K.K. Lara, C.R. Rinaldo, C. Bruckner, Tatrahedron Lett. 44 (2003) 7793.
[141] H. Furuta, T. Asano, T. Ogawa, J. Am. Chem. Soc. 116 (1994) 767.
[142] P.J. Chmielewski, L. Latos-Grażyński, K. Rachlewicz, T. Glowink, Angew. Chem. Int. Ed. Engl. 33 (1994) 779.
[143] P.J. Chmielewski, L. Latos-Grażyński, T. Glowiak, J. Am. Chem. Soc. 118 (1996) 5690.
[144] P.J. Chmielewski, L. Latos-Grażyński, Inorg. Chem. 39 (2000) 5639.
[145] H. Furuta, T. Ogawa, Y. Uwatoko, K. Araki, Inorg. Chem. 38 (1999) 2676.
[146] T. Ogawa, H. Furuta, A. Morino, M. Takahashi, H. Uno, J. Organomet. Chem. 611 (2000) 551.
[147] P.J. Chmielewski, L. Latos-Grażyński, I. Schmidt, Inorg. Chem. 39 (2000) 5475.
[148] W.-C. Chen, C.-H. Hung, Inorg. Chem. 40 (2001) 5070.
[149] A. Srinivasan, H. Furuta, A. Osuka, J. Chem. Soc. Chem. Commun. (2001) 1666.
[150] H. Furuta, T. Ishizuka, A. Osuka, J. Am. Chem. Soc. 124 (2002) 5622.
[151] D.S. Bhole, W.-C. Chen, C.-H. Hung, Inorg. Chem. 41 (2002) 3334.
[152] J.D. Harvey, C.J. Ziegler, J. Chem. Soc. Chem. Commun. (2002) 1942.
[153] C.-H. Hung, W.-C. Chen, G.-H. Lee, S.-M. Peng, J. Chem. Soc. Chem. Commun. (2002) 1516.
[154] J.D. Harvey, C.J. Ziegler, Coord. Chem. Rev. 247 (2003) 1 (and references cited therein).
[155] H. Furuta, T. Ishizuka, A. Osuka, T. Ogawa, J. Am. Chem. Soc. 121 (1999) 2945.
[156] H. Furuta, T. Ishizuka, A. Osuka, T. Ogawa, J. Am. Chem. Soc. 122 (2000) 5748.
[157] H. Furuta, H. Maeda, A. Osuka, J. Am. Chem. Soc. 122 (2000) 803.
[158] H. Furuta, H. Maeda, A. Osuka, M. Yasutake, T. Shinmyozu, Y. Ishikawa, J. Chem. Soc. Chem. Commun. (2000) 1143.
[159] K. Araki, H. Winnishofer, H.E. Toma, H. Maeda, A. Osuka, H. Furuta, Inorg. Chem. 40 (2001) 2020.
[160] H. Furuta, H. Maeda, A. Osuka, J. Chem. Soc. Chem. Commun. (2002) 1795 (and references cited therein).
[161] C.-H. Lee, H.-J. Kim, Tetrahedron Lett. 38 (1997) 3935.
[162] C.-H. Lee, H.-J. Kim, D.-W. Yoon, Bull. Korean Chem. Soc. 20 (1999) 276.
[163] D.-W. Yoon, C.-H. Lee, Bull. Korean Chem. Soc. 21 (2000) 618.
[164] S.K. Pushpan, A. Srinivasan, V.R.C. Anand, T.K. Chandrashekar, A. Subramanian, R. Roy, K.-I. Sugiura, Y. Sakata, J. Org. Chem. 66 (2001) 153.
[165] E. Pacholska, L. Latos-Grażyński, L. Szterenberg, Z. Ciunik, J. Org. Chem. 65 (2000) 8188.
[166] N. Sprutta, L. Latos-Grażyński, Org. Lett. 3 (2001) 1933.
[167] Y. Joo, K.K. Baeck, C.-H. Lee, J. Phys. Chem. A 106 (2002) 1035.
[168] N. Sprutta, L. Latos-Grażyński, Tetrahedron Lett. 40 (1999) 8457.
[169] L. Szterrenberg, N. Sprutta, L. Latos-Grażyński, J. Inclusion Phenom. 41 (2001) 209.
[170] M. Pawlicki, L. Latos-Grażyński, Chem. Eur. J. 9 (2003) 4650.
[171] L. Latos-Grażyński, E. Pacholska, P.J. Chmielewski, M.M. Olmstead, A.L. Balch, Angew. Chem. Int. Ed. Engl. 34 (1995) 2252.
[172] M. Abe, M.R. Detty, O.O. Gerlits, D.K. Sukumaran, Organometallics 23 (2004) 4513.
[173] M. Abe, D.G. Hilmey, C.E. Stilts, D.K. Sukumaran, M.R. Detty, Organometallics 21 (2002) 2986.
[174] M. Abe, Y. You, M.R. Detty, Organometallics 21 (2002) 4546.
[175] E. Pacholska, L. Latos-Grażyński, Z. Ciunik, Chem. Eur. J. 8 (2002) 5403.
[176] E. Pacholska, L. Latos-Grażyński, Z. Ciunik, Angew. Chem. Int. Ed. 40 (2001) 4466.
[177] R. Bonnett, Chem. Soc. Rev. 24 (1995) 19 (and references cited therein).
[178] R.P. Pandian, D. Reddy, N. Chidambaram, T.K. Chandrashekar, Proc. Indian Acad. Sci. 102 (1990) 307.
[179] R.P. Pandian, T.K. Chandrashekar, J. Chem. Soc. Dalton Trans. (1993) 119.
[180] P. Ziolkowski, J. Milach, K. Symonowicz, P.J. Chmielewski, L. Latos-Grażyński, E. Marcinkowska, Tumori 81 (1995) 364.
[181] E. Marcinkowska, P. Ziolkowski, E. Pacholska, L. Latos-Grażyński, Cz. Radzikowski, P.J. Chmielewski, Anticancer Res. 17 (1997) 3313.
[182] C.E. Stilts, M.I. Nelen, D.G. Hilmey, S.R. Davies, S.O. Gollnick, A.R. Oseroff, S.L. Gibson, R. Hiff, M.R. Detty, J. Med. Chem. 43 (2000) 2403.
[183] D.G. Hilmey, M. Abe, M.I. Nelen, C.E. Stilts, G.A. Baker, S.N. Baker, F.V. Bright, S.R. Davies, S.O. Gollnick, A.R. Oseroff, S.L. Gibson, R. Hilf, M.R. Detty, J. Med. Chem. 45 (2002) 449.
[184] Y. You, S.L. Gibson, R. Hilf, S.R. Davies, A.R. Oseroff, I. Roy, T.Y. Ohulchanskyy, E.J. Bergey, M.R. Detty, J. Med. Chem. 46 (2003) 3734.